

Joint Relay and Jammer Selection Improves the Physical Layer Security in the Face of CSI Feedback Delays

Lei Wang, *Student Member, IEEE*, Yueming Cai, *Senior Member, IEEE*, Yulong Zou, *Senior Member, IEEE*, Weiwei Yang, *Member, IEEE*, and Lajos Hanzo, *Fellow, IEEE*

Abstract—We enhance the physical layer security (PLS) of amplify-and-forward (AF) relaying networks with the aid of joint relay and jammer selection (JRJS), despite the deleterious effect of channel state information (CSI) feedback delays. Furthermore, we conceive a new outage-based characterization approach for the JRJS scheme. The traditional best relay selection (TBRS) is also considered as a benchmark. We first derive closed-form expressions of both the connection outage probability (COP) and the secrecy outage probability (SOP) for both the TBRS and JRJS schemes. Then, a reliable and secure connection probability (RSCP) is defined and analyzed for characterizing the effect of the correlation between the COP and the SOP introduced by the corporate source-relay link. The reliability-security ratio (RSR) is introduced for characterizing the relationship between the reliability and the security through asymptotic analysis. Moreover, the concept of effective secrecy throughput is defined as the product of the secrecy rate and of the RSCP for the sake of characterizing the overall efficiency of the system, as determined by the transmit SNR, the secrecy codeword rate, and the power sharing ratio between the relay and the jammer. The impact of the direct source-eavesdropper link and additional performance comparisons with respect to other related selection schemes are also included. Our numerical results show that the JRJS scheme outperforms the TBRS method both in terms of the RSCP and in terms of its effective secrecy throughput, but it is more sensitive to the feedback delays. Increasing the transmit signal-to-noise ratio (SNR) will not always improve the overall throughput. Moreover, the RSR results demonstrate that, upon reducing the CSI feedback delays, the reliability improves more substantially than the security degrades, implying an overall improvement in terms of the security-reliability tradeoff. Additionally, the secrecy throughput loss due to the second-hop feedback delay is more pronounced than that due to the first-hop one.

Index Terms—Effective secrecy throughput, feedback delay, physical layer security (PLS), relay and jammer selection, reliability and security.

I. INTRODUCTION

WIRELESS communications systems are particularly vulnerable to security attacks because of the inherent openness of the transmission medium. Traditionally, the information privacy of wireless networks has been focused on the higher layers of the protocol stack employing cryptographically secure schemes. However, these methods typically assume a limited computing power for the eavesdroppers and exhibit inherent vulnerabilities in terms of the inevitable secret key distribution and management [1]. In recent years, physical layer security (PLS) has emerged as a promising technique of improving the confidentiality wireless communications, which exploits the time-varying properties of fading channels, instead of relying on conventional cryptosystems. The pivotal idea of PLS solutions is to exploit the dynamically fluctuating random nature of radio channels for maximizing the uncertainty concerning the source messages at the eavesdropper [2], [3].

To achieve this target, several PLS-enhancement approaches have been proposed in the literature, including secrecy-enhancing channel coding [4], secure on-off transmission designs [5], secrecy-improving beamforming (BF)/precoding, and artificial-noise-aided techniques relying on multiple antennas [6], as well as secure relay-assisted transmission techniques [7]. Specifically, apart from improving the reliability and coverage of wireless transmissions, user cooperation also has a great potential in terms of enhancing the wireless security against eavesdropping attacks. There has been a growing interest in improving the security of cooperative networks at the physical layer [8]–[14]. To explore the spatial diversity potential of the relaying networks and to boost the secrecy capacity (the difference between the channel capacity of the legitimate main link and that of the eavesdropping link), most of the existing work has been focused on secrecy-enhancing BF [8], [9], as well as on intelligent relay node/jammer node (RN/JN) selection, etc. Notably, given the availability of multiple relays, appropriately designed RN/JN selection is capable of achieving a significant security improvement for cooperative networks, which is emerging as a promising research topic. In particular, Zou *et al.* investigated both amplify-and-forward (AF)- and decode-and-forward (DF)-based optimal relay selection conceived for

Manuscript received October 2, 2014; revised February 25, 2015 and July 27, 2015; accepted September 8, 2015. This work was supported in part by the National Natural Science Foundation of China under Grant 61371122, Grant 61471393, and Grant 61501512 and in part by the Natural Science Foundation of Jiangsu Province under Grant BK20150718 and Grant BK20150040. The review of this paper was coordinated by Prof. M. C. Gursoy.

L. Wang, Y. Cai, and W. Yang are with the College of Communications Engineering, PLA University of Science and Technology, Nanjing 210007, China (e-mail: csu-wl@163.com; caiym@vip.sina.com; yww_1010@aliyun.com).

Y. Zou is with the School of Telecommunications and Information Engineering, Nanjing University of Posts and Telecommunications, Nanjing 210003, China (e-mail: yulong.zou@njupt.edu.cn).

L. Hanzo is with the Department of Electronics and Computer Science, University of Southampton, Southampton SO17 1BJ, U.K. (e-mail: lh@ecs.soton.ac.uk).

Color versions of one or more of the figures in this paper are available online at <http://ieeexplore.ieee.org>.

Digital Object Identifier 10.1109/TVT.2015.2478029

83 enhancing the PLS in cooperative wireless networks [10], [11],
 84 where the global channel state information (CSI) of both the
 85 main link and the eavesdropping link was assumed to be avail-
 86 able. Similarly, jamming techniques, which impose artificial
 87 interference on the eavesdropper, have also attracted substantial
 88 attention [12]–[14]. More specifically, several sophisticated
 89 joint relay and jammer selection (JRJS) schemes were proposed
 90 in [12], where the beneficially selected relay increases the reli-
 91 ability of the main link, whereas the carefully selected jammer
 92 imposes interference on the eavesdropper and simultaneously
 93 protects the legitimate destination from interference. In [13]
 94 and [14], cooperative jamming has been studied in the context
 95 of bidirectional scenarios, and efficient RN/JN selection criteria
 96 have been developed for achieving improved secrecy rates with
 97 the aid of multiple relays. Furthermore, more effective relaying
 98 and jamming schemes, when taking the information leakage
 99 of the source–eavesdropper link into consideration, have been
 100 presented lately in [15] and [16].

101 Nevertheless, an idealized assumption of the previously re-
 102 ported research on PLS is the availability of perfect channel
 103 state information (CSI), which is regarded as a stumbling block
 104 in the way of invoking practical secrecy-enhancing Wyner
 105 coding, on–off design, BF/precoding, and RN/JN selection.
 106 However, this idealized simplifying assumption is not realistic,
 107 since practical channel estimation imposes CSI imperfections,
 108 which are aggravated by the feedback delay, limited-rate feed-
 109 back, and channel estimation errors (CEEs) [17]. Generally, the
 110 related research has been focused on the issues of robust secure
 111 BF design from an average secrecy-rate-based optimization
 112 perspective for point-to-point multiantenna aided channels and
 113 relay channels [18], [19] supporting delay-tolerant systems.
 114 For systems imposing stringent delay constraints, particularly
 115 in imperfect CSI scenarios, perfect secrecy cannot always be
 116 achieved. Hence, the secrecy-outage-based characterization of
 117 systems is more appropriate, which provides a probabilistic
 118 performance measure of secure communication. The concept
 119 of secrecy outage was adopted in [20] for characterizing the
 120 probability of having both reliable and secure transmission,
 121 which, however, is inapplicable for the imperfect CSI case and
 122 fails to distinguish a connection outage from the secrecy outage.
 123 In [21], an alternative secrecy outage formulation is proposed
 124 for characterizing the attainable security level and provided
 125 a general framework for designing transmission schemes that
 126 meet specific target security requirements. To quantify both the
 127 reliability and security performance at both the legitimate and
 128 eavesdropper nodes separately, two types of outages, namely,
 129 the connection outage probability (COP) and the secrecy outage
 130 probability (SOP) are introduced. Then, considering the impact
 131 of time delay caused by the antenna selection process at the
 132 legitimate receiver, Hu *et al.* [22] proposed a new secure
 133 transmission scheme in the multiinput multioutput multieaves-
 134 dropper wiretap channel. Much recently, considering the out-
 135 dated CSI from the legitimate receiver, a new secure on–off
 136 transmission scheme was proposed for enhancing the secrecy
 137 throughput in [23].

138 Moreover, prior studies of the outage-based secure trans-
 139 mission design are limited to single-antenna-assisted single-
 140 hop systems and have not been considered for cooperative

relaying systems. Hence, the issues of secure transmissions 141
 over cooperative relaying channels expressed in terms of the 142
 SOP, COP, and secrecy throughput constitute an open problem. 143
 On the other hand, apart from CEE, the CSI feedback delay 144
 results in critical challenges for the PLS of cooperative relaying 145
 systems, particularly when considering the specifics of RN/JN 146
 selection. In [15], the effects of outdated CSI knowledge con- 147
 cerning the legitimate links on the ergodic secrecy rate achieved 148
 by the proposed secure transmission strategy in the context 149
 of DF relaying is investigated. The impact of CSI feedback 150
 delay on the secure relay and jammer selection conceived for 151
 DF relaying was investigated in [24], albeit only in terms 152
 of the SOP. In our previous study [25], we considered the 153
 secure transmission design and the secrecy performance of an 154
 opportunistic DF system relying on outdated CSI, where only a 155
 single relay is invoked. Additionally, during the revision of this 156
 work, we investigated the security performance for outdated AF 157
 relay selection in [26]. Therefore, in this treatise, we extend 158
 our investigations to the PLS of multiple AF relaying assisted 159
 networks relying on RN/JN selection. 160

Explicitly, we focus our attention on the outage-based char- 161
 acterization of secure transmissions in cooperative relay-aided 162
 networks relying on realistic CSI feedback delay. To exploit the 163
 multirelay induced diversity gain and the associated jamming 164
 capabilities, joint AF relay node and jammer node selection 165
 is employed by the relay–destination link. We assume that, in 166
 line with the practical reality, the instantaneous eavesdropper’s 167
 CSI is unavailable at the legitimate transmitter and that the 168
 RN/JN selections are performed based on the outdated CSI of 169
 the main links. Two types of cooperative strategies are invoked 170
 by our cooperative network operating under secrecy constraints, 171
 namely, the traditional best relay selection (TBRS) strategy and 172
 the JRJS strategy. Specifically, the main contributions of this 173
 paper can be summarized as follows. 174

- We develop an outage-based characterization for quan- 175
 tifying both the reliability and security performance of 176
 a two-hop AF relaying system. Specifically, in contrast 177
 to [21] and [22], we propose the novel definition of 178
 the reliable and secure connection probability (RSCP). 179
 Explicitly, closed-form expressions of the COP, the SOP, 180
 and the RSCP are derived for both the TBRS and for our 181
 JRJS strategies. Numerical results demonstrate that the 182
 JRJS scheme outperforms the TBRS scheme in terms of 183
 its RSCP. 184
- We also introduce the reliability–security ratio (RSR) 185
 for characterizing their direct relationship by a single 186
 parameter through the asymptotic analysis of the COP and 187
 the SOP in the high-SNR regime. We derive the RSR for 188
 both the TBRS and JRJS strategies for investigating the 189
 effect of secrecy codeword rate setting, as well as that 190
 of the feedback delay and that of the power sharing ratio 191
 between the relay and the jammer on the RSR. 192
- We then modify the definition of effective secrecy 193
 throughput by multiplying the secrecy rate with the RSCP, 194
 which results in an optimization problem of the trans- 195
 mit signal-to-noise ratio (SNR), secrecy codeword rate, 196
 and power sharing between the relay and the jammer. 197
 198

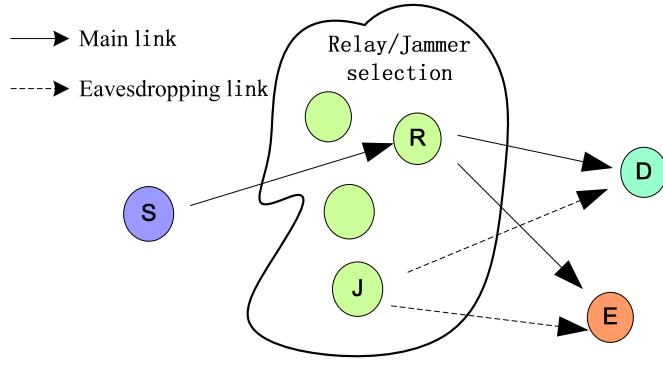


Fig. 1. Cooperative relaying network assisted by multiple relays in the presence of an eavesdropper.

199 It is shown that, compared with the TBRs strategy,
 200 JRJS achieves a significantly higher effective secrecy
 201 throughput, and the corresponding throughput loss is
 202 more sensitive to feedback delays. The impact of the direct
 203 source–eavesdropper link and additional throughput
 204 performance comparisons with respect to other related
 205 selection schemes are further discussed.

206 The remainder of this paper is organized as follows.
 207 Section II introduces our system model and describes both
 208 the TBRs and our JRJS strategies. In Sections III and IV,
 209 we present the mathematical framework of our performance
 210 analysis both for the TBRs strategy and for the JRJS strategy,
 211 respectively, including the COP, the SOP, the RSCP, the RSR,
 212 and the effective secrecy throughput. Our numerical results
 213 and discussions are provided in Section V. Finally, Section VI
 214 presents our concluding remarks.

215 II. SYSTEM MODEL

216 A. System Description

217 Consider a cooperative relaying network consisting of a
 218 source S , a destination D , K_r relays R_k , $k = 1, \dots, K_r$, and
 219 an eavesdropper E , as shown in Fig. 1, where all nodes are
 220 equipped with a single transmit antenna (TA), except for the
 221 source, which has N_t TAs. The cooperative relay architecture
 222 in Fig. 1 is generally applicable to diverse practical wireless
 223 systems in the presence of an eavesdropper, including the
 224 family of wireless sensor networks (WSNs), mobile ad hoc
 225 networks (MANETs), and the long-term evolution advanced
 226 cellular systems [11].

227 To exploit the diversity potential of multiple relay nodes over
 228 independently fading channels, AF relay/jammer selection is
 229 employed. All relays operate in the half-duplex AF mode, and
 230 data transmission is performed in two phases. More particu-
 231 larly, during the broadcast phase, the source node transmits its
 232 signal to a selected relay with the aid of BF, which is invoked
 233 for forwarding the signal received from S to D . An inherent
 234 assumption is that the transmit BF weights are based on the
 235 CSI estimates quantified and fed back by the selected relay.
 236 During the cooperative phase, a pair of appropriately selected
 237 relays transmit toward D and E , respectively. A conventional

relay (denoted by R^*) forwards the source’s message to the
 238 destination. Another relay (denoted by J^*) operates in the
 239 “jammer mode” and imposes intentional interference upon E in
 240 order to confuse it. However, D is unable to mitigate the artificial
 241 interference emanating from the jammer node J^* due to its
 242 critical secrecy constraints [12]. It should be noted that both
 243 the process of RN/JN selection and the feedback of the transmit
 244 BF weights from R^* to S may impose a time lag between the
 245 data transmission and the channel estimation. These time delays
 246 are denoted by $T_{d_{SR}}$ and $T_{d_{RD}}$, respectively. Furthermore, we
 247 assume that the BF and RN/JN selection process is based
 248 on the perfectly estimated but outdated CSI. We employ the
 249 first-order autoregressive outdated CSI model of [20], while
 250 relying on the correlation coefficients of $\rho_{SR} = J_0(2\pi f_d T_{d_{SR}})$
 251 and $\rho_{RD} = J_0(2\pi f_d T_{d_{RD}})$ for the two hops, where $J_0(\cdot)$ is
 252 the zero-order Bessel function of the first kind, and f_d is the
 253 Doppler frequency.
 254

A slow flat block Rayleigh fading environment is assumed,
 255 where the channel remains static for the coherence interval (one
 256 slot) and changes independently in different coherence inter-
 257 vals, as denoted by $h_{i,j} \sim \mathcal{CN}(0, \sigma_{i,j}^2)$, $i, j \in \{S, R, J, D, E\}$.
 258 The direct communication links are assumed to be unavailable
 259 due to the presence of obstructions between S and D , as well
 260 as the eavesdropper.¹ This assumption follows the rationale of
 261 [12] and has been routinely exploited in previous literature (see
 262 [27] and [28] and the references therein), where the source
 263 and relays belong to the same cluster, whereas the destination
 264 and the eavesdropper are located in another. More specifically,
 265 this assumption is particularly valid in networks with broadcast
 266 and unicast transmission, where each terminal is a legitimate
 267 receiver for one signal and acts as an eavesdropper for some
 268 other signal. Therefore, the security concerns are only related
 269 to the cooperative relay-aided channel. Furthermore, additive
 270 white Gaussian noise (AWGN) is assumed with zero mean
 271 and unit variance N_0 . Let P_i be the transmit power of node
 272 i , and the instantaneous SNR of the $i \rightarrow j$ link is given by
 273 $\gamma_{i,j} = P_i |h_{i,j}|^2 / N_0$.
 274

We employ the constant-rate Wyner coding scheme for con-
 275 structing wiretap codes of [2] to meet the PLS requirements
 276 due to the fact that the accurate global CSI is not available.
 277 Let $\mathcal{C}(R_0, R_s, N)$ denote the set of all possible Wyner codes
 278 of length N , where R_0 is the codeword transmission rate, and
 279 R_s is the confidential information rate ($R_0 > R_s$). The positive
 280 rate difference $R_e = R_0 - R_s$ is the cost of providing secrecy
 281 against the eavesdropper. A confidential message is encoded
 282 into a codeword at S and then transmitted to D .
 283

284 B. Secure Transmission

In the broadcast phase, S transmits its BF signal $s(t)$ to the
 285 selected relay R^* , where the relay selection is performed
 286 before data transmission commences, and the selection cri-
 287 terion will be detailed later in the context of the cooper-
 288 ative phase. The transmit BF vector $\mathbf{w}(t|T_d)$ is calculated
 289 using the perfectly estimated but outdated CSI given by
 290

¹The case when the $S \rightarrow E$ link is introduced will be investigated separately in Section VI.

291 $\mathbf{w}(t|T_{d_{SR}}) = \mathbf{h}_{SR^*}^H(t - T_d)/|\mathbf{h}_{SR^*}(t - T_{d_{SR}})|$ [29], where we
 292 have $\mathbf{h}_{SR^*}(t) = [h_{SR^*,1}(t), \dots, h_{SR^*,N_t}(t)]^T$, and the signal
 293 received by the relay R^* can be written as

$$y_{R^*}(t) = \sqrt{P_s} \mathbf{w}(t|T_d) \mathbf{h}_{SR^*}(t) s(t) + n_{SR^*}(t) \quad (1)$$

294 where $n_{SR^*}(t)$ is the AWGN at the relay. Then, we can
 295 define the received SNR at the relay node as $\gamma_{SR} =$
 296 $P_S |\mathbf{w}(t|T_{d_{SR}}) \mathbf{h}_{SR^*}(t)|^2 / N_0$.

297 In the cooperative phase, we consider two RN/JN selection
 298 schemes performed by D : relay selection without jamming
 299 and JRJS.

300 1) *Traditional Best Relay Selection*: The first category of so-
 301 lutions does not involve a jamming process, and therefore, only
 302 a conventional relay accesses the channel during the second
 303 phase of the protocol. The relay selection process is performed
 304 based on the highest instantaneous SNR of the second hop,
 305 which is formulated as

$$R^* = \arg \max_{R_k \in \mathcal{R}} \left\{ \frac{\tilde{\gamma}_{R_k D}}{\mathbb{E}[\gamma_{R_k E}]} = \frac{P_R |\tilde{h}_{R_k D}(t - T_d)|^2}{N_0 \mathbb{E}[\gamma_{R_k E}]} \right\} \quad (2)$$

306 where $\tilde{\gamma}_{R_k D}$ is the instantaneous SNR in the relay selection
 307 process, and $\mathbb{E}[\gamma_{R_k E}]$ denotes the average SNR at E . We can
 308 model $\gamma_{R_k D}$ and $\tilde{\gamma}_{R_k D}$ as two gamma distributed random
 309 variables having the correlation factor of ρ_{RD}^2 .

310 During the second phase, the received signal $y_{R^*}(t)$
 311 is multiplied by a time-variant AF-relay gain G and
 312 retransmitted to D , where we have $G =$
 313 $\sqrt{P_R / (P_S |\mathbf{w}_{\text{opt}}(t|T_{d_{SR}}) \mathbf{h}_{SR^*}(t)|^2 + N_0)}$. After further math-
 314 ematical manipulations, the mutual information (MI) between
 315 S and D , as well as the eavesdropper, can be written as

$$I_D^{\text{TBRS}} = \frac{1}{2} \log(1 + \gamma_D^{\text{TBRS}}) = \frac{1}{2} \log \left(1 + \frac{\gamma_{SR} \gamma_{R^* D}}{\gamma_{SR} + \gamma_{R^* D} + 1} \right) \quad (3)$$

$$I_E^{\text{TBRS}} = \frac{1}{2} \log(1 + \gamma_E^{\text{TBRS}}) = \frac{1}{2} \log \left(1 + \frac{\gamma_{SR} \gamma_{R^* E}}{\gamma_{SR} + \gamma_{R^* E} + 1} \right). \quad (4)$$

316 2) *Joint Relay and Jammer Selection*: Similarly, consider-
 317 ing the unavailability of the instantaneous CSI regarding the
 318 eavesdropper, we adopt a suboptimal RN/JN selection metric
 319 conditioned on the outdated CSI as

$$R^* = \arg \max_{R_k \in \mathcal{R}} \left\{ \frac{\tilde{\gamma}_{R_k D}}{\mathbb{E}[\gamma_{R_k E}]} \right\} \quad (5)$$

$$J^* = \arg \min_{R_k \in \mathcal{R} - R^*} \left\{ \frac{\tilde{\gamma}_{R_k D}}{\mathbb{E}[\gamma_{R_k E}]} \right\}$$

320 where J^* is selected for minimizing the interference imposed
 321 on D .

322 It should be noted that, to have the same transmit power as
 323 that of the TBRS case, we assume that $P_{R^*} + P_{J^*} = P_R$ for
 324 our JRJS strategy and introduce $\lambda = P_{R^*} / (P_{R^*} + P_{J^*})$ as the

ratio of the relay's transmit power to the total power required
 by the active relay and jammer. 326

In the cooperative phase, R^* will also amplify the received
 signal $y_{R^*}(t)$ by G and forward it to D . At the same time, the
 jammer J^* will generate intentional interference to confuse E ,
 which will also cause interference at D . Consequently, the MI
 between the terminals is given by 331

$$I_D^{\text{JRJS}} = \frac{1}{2} \log(1 + \gamma_D^{\text{JRJS}}) = \frac{1}{2} \log \left(1 + \frac{\gamma_{SR} \frac{\gamma_{R^* D}}{\gamma_{J^* D} + 1}}{\gamma_{SR} + \frac{\gamma_{R^* D}}{\gamma_{J^* D} + 1} + 1} \right) \quad (6)$$

$$I_E^{\text{JRJS}} = \frac{1}{2} \log(1 + \gamma_E^{\text{JRJS}}) = \frac{1}{2} \log \left(1 + \frac{\gamma_{SR} \frac{\gamma_{RE}}{\gamma_{JE} + 1}}{\gamma_{SR} + \frac{\gamma_{RE}}{\gamma_{JE} + 1} + 1} \right). \quad (7)$$

Remark 1: Generally, the optimal RN/JN selection scheme
 should take into account the global SNR knowledge set
 $\{\gamma_{SR}, \gamma_{RD}, \gamma_{RE}\}$. However, given the potentially excessive
 implementational complexity overhead of the optimal selection
 schemes and the unavailability of the global CSI, we employ
 suboptimal selection schemes as in [12].² Furthermore, it is
 commonly assumed that the average SNR of the eavesdropper
 is available at the transmitter, which seems, somehow, not
 reasonable. However, as stated in most of the literature, such as
 [12]–[22], [24]–[28], and [30], provided that the eavesdropper
 belongs to the network, which is also the case in our paper,
 the related assumption might still be deemed reasonably. Addi-
 tionally, as in [8], [11], [12], and [24], for mathematical conve-
 nience, we assume that the relaying channels are independent
 and identically distributed and that we have $\mathbb{E}[\gamma_{SR_k}] = \bar{\gamma}_{SR}$,
 $\mathbb{E}[\gamma_{R_k D}] = \bar{\gamma}_{RD}$, and $\mathbb{E}[\gamma_{R_k E}] = \bar{\gamma}_{RE}$. The distances between
 the relays are assumed to be much smaller than the distances
 between relays and source/destination/eavesdropper; hence, the
 corresponding path losses among the different relays are ap-
 proximately the same. This assumption is reasonable both for
 WSNs and for MANETs associated with a symmetric clustered
 relay configuration, and it may be also satisfied as valid by
 classic cellular systems in a statistical sense [11]. 354

III. SECURE TRANSMISSION WITHOUT JAMMING 355

Here, we endeavor to characterize both the reliability and
 security performance comprehensively of the TBRS scheme.
 We first derive closed-form expressions for both the COP and
 the SOP. Then, the RSR is introduced through the asymptotic
 analysis of the COP and the SOP. Furthermore, we propose
 the novel definition of the RSCP and the effective secrecy
 throughput. 362

²To further alleviate the cooperation-related overhead, the selection criterion is based on the $R \rightarrow D$ link, since the second hop plays a dominant role in determining the received SNR, because the first hop corresponds to a multiple-input-single-output channel with the aid of multiple antennas, and hence, it is more likely to be better than the second hop. The optimal selection based on both hops is beyond the scope of this work.

363 A. COP and SOP

364 When the perfect instantaneous CSI of the eavesdropper's
 365 channel and even the legitimate users' channel is unavailable,
 366 alternative definitions of the outage probability may be adopted
 367 for the statistical characterization of the attainable secrecy
 368 performance, particularly for delay-limited applications. Based
 369 on [31, Def. 2], perfect secrecy cannot be achieved, when we
 370 have $R_e < I_E$, where I_E denotes the MI between the source
 371 and the eavesdropper. Encountering this event is termed as a
 372 secrecy outage. Furthermore, the destination is unable to flaw-
 373 lessly decode the received codewords when $R_0 > I_D$, which is
 374 termed as a connection outage. The grade of reliability and the
 375 grade of security maintained by a transmission scheme may be
 376 then quantified by the COP and the SOP, respectively.

377 We continue by presenting our preliminary results versus the
 378 point-to-point SNRs. Let us denote the cumulative distribution
 379 function (CDF) and the probability density function (PDF) of a
 380 random variable X by $F_X(x)$ and $f_X(x)$, respectively. On one
 381 hand, the PDF of γ_{SR} using [29, eq. (15)] is given by

$$f_{\gamma_{SR}}(x) = \sum_{n=0}^{N_t-1} \binom{N_t-1}{n} \frac{\rho_{SR}^{2(N_t-1-n)} (\bar{\gamma}_{SR} (1 - \rho_{SR}^2))^n}{\bar{\gamma}_{SR}^{N_t} (N_t - 1 - n)!} \times x^{N_t-1-n} e^{-\frac{x}{\bar{\gamma}_{SR}}} \quad (8)$$

382 whereas its CDF is given by

$$F_{\gamma_{SR}}(x) = 1 - \sum_{n=0}^{N_t-1} \sum_{m=0}^{N_t-1-n} \binom{N_t-1}{n} \times \frac{\rho_{SR}^{2(N_t-1-n)} (1 - \rho_{SR}^2)^n}{m! \bar{\gamma}_{SR}^m} x^m e^{-\frac{x}{\bar{\gamma}_{SR}}}. \quad (9)$$

383 On the other hand, for the instantaneous SNR of the $R \rightarrow$
 384 D hop, according to the principles of concomitants or induced
 385 order statistics, the CDF of γ_{R^*D} can be derived as in [32]

$$F_{\gamma_{R^*D}}(y) = K_r \sum_{k=0}^{K_r-1} (-1)^k \binom{K_r-1}{k} \frac{1 - e^{-\frac{-(k+1)y}{k(1-\rho_{RD}^2)+1} \bar{\gamma}_{RD}}}{k+1}. \quad (10)$$

386 Thus, the COP of the TBRS strategy is given by

$$P_{co}^{\text{TBRS}}(R_0) = \Pr [I_D^{\text{TBRS}} < R_0] = F_{\gamma_D^{\text{TBRS}}}(\gamma_{th}^D) \quad (11)$$

387 where we have $\gamma_{th}^D = 2^{2R_0} - 1$, and the CDF of γ_D^{TBRS} can be
 388 calculated as

$$F_{\gamma_D^{\text{TBRS}}}(x) = 1 - \int_0^\infty \left[1 - F_{\gamma_{R^*D}}\left(\frac{xz + x(x+1)}{z}\right) \right] f_{\gamma_{SR^*}}(z+x) dz. \quad (12)$$

389 Consequently, by substituting (8) and (10) into (12) and using
 390 [33, eq. (3.471.9)], we arrive at a closed-form expression for

$F_{\gamma_D^{\text{TBRS}}}(x)$ as

391

$$F_{\gamma_D^{\text{TBRS}}}(x) = 1 - 2 \sum_{n=0}^{N_t-1} \sum_{k=0}^{K_r-1} \sum_{m=0}^{N_t-1-n} (-1)^k K_r \binom{N_t-1}{n} \times \binom{K_r-1}{k} \binom{N_t-1-n}{m} \times \frac{\rho_{SR}^{2(N_t-1-n)} (1 - \rho_{SR}^2)^n x^{N_t-1-n-m}}{(N_t-1-n)! (k+1) \bar{\gamma}_{SR}^{N_t-n}} \times \left[\frac{\bar{\gamma}_{SR} x(x+1)}{\omega_k \bar{\gamma}_{RD}} \right]^{\frac{m+1}{2}} \times e^{-\left(\frac{\bar{\gamma}_{SR} + \omega_k \bar{\gamma}_{RD}}{\omega_k \bar{\gamma}_{SR} \bar{\gamma}_{RD}}\right) x} K_{m+1} \left(2 \sqrt{\frac{x(x+1)}{\omega_k \bar{\gamma}_{SR} \bar{\gamma}_{RD}}} \right) \quad (13)$$

where we have $\omega_k = (k(1 - \rho_{RD}^2) + 1)/(k+1)$. Then, by
 substituting $x = \gamma_{th}^D$ into (13), we obtain P_{co}^{TBRS} .

393 Furthermore, the SOP of the TBRS strategy may be expressed as 394

$$P_{so}^{\text{TBRS}}(R_0, R_s) = \Pr [J_E^{\text{TBRS}} > R_0 - R_s] = 1 - F_{\gamma_E^{\text{TBRS}}}(\gamma_{th}^E) \quad (14)$$

where we have $\gamma_{th}^E = 2^{2(R_0 - R_s)} - 1$. Similarly, we may calcu-
 late the CDF of γ_E^{TBRS} in (14) as 396

$$F_{\gamma_E^{\text{TBRS}}}(x) = 1 - 2 \sum_{n=0}^{N_t-1} \sum_{m=0}^{N_t-1-n} \binom{N_t-1}{n} \binom{N_t-1-n}{m} \times \frac{\rho_{SR}^{2(N_t-1-n)} (1 - \rho_{SR}^2)^n x^{N_t-1-n-m}}{(N_t-1-n)! \bar{\gamma}_{SR}^{N_t-n}} \times \left[\frac{\bar{\gamma}_{SR} x(x+1)}{\bar{\gamma}_{RE}} \right]^{\frac{m+1}{2}} \times e^{-\left(\frac{\bar{\gamma}_{SR} + \bar{\gamma}_{RE}}{\bar{\gamma}_{SR} \bar{\gamma}_{RE}}\right) x} K_{m+1} \left(2 \sqrt{\frac{x(x+1)}{\bar{\gamma}_{SR} \bar{\gamma}_{RE}}} \right). \quad (15)$$

Then, by substituting $x = \gamma_{th}^E$ into (15), we can derive P_{so}^{TBRS} .

397 The COP and the SOP in (11) and (14) characterize the at-
 398 tainable reliability and security performance, respectively, and
 399 can be regarded as the detailed requirements of accurate system
 400 design. From the definition of COP and SOP, it is clear that
 401 the reliability of the main link can be improved by increasing
 402 the transmit SNR (or decreasing its data rate) to reduce the
 403 COP, which unfortunately increases the risk of eavesdropping.
 404 Thus, a tradeoff between reliability and security may be struck,
 405 despite the fact that closed-form expressions cannot be obtained
 406 as in [11]. Furthermore, we denote the minimal reliability and
 407 security requirements by ν and δ , where the feasible range of
 408 the reliability constraint is $0 < \nu < 1$. Bearing in mind that
 409 the COP is a monotonously increasing function of R_0 , the
 410 corresponding threshold of the codeword transmission rate is
 411 $R_0^{th} = \arg\{P_{co}^{\text{TBRS}}(R_0) = \nu\}$, which leads to a lower bound of
 412 the SOP, when we have $(R_0 - R_s) \rightarrow R_0^{th}$. Thus, the feasible
 413 range of δ is $P_{so}^{\text{TBRS}}(R_0^{th}, 0) < \delta < 1$. The preceding analysis
 414 indicates that, given a reliability constraint ν , the lower bound
 415 of the security constraint is determined. 416

417 B. Reliability–Security Ratio

418 Here, we will focus our attention on the asymptotic analysis
419 of the COP and the SOP in the high-SNR regime. Then, inspired
420 by [25], we introduce the concept of the RSR for characterizing
421 the direct relationship between reliability and security.

422 *Proposition 1:* Based on the asymptotic probabilities of P_{co}
423 and P_{so} at high SNRs,³ the RSR is defined as

$$P_{co}(R_0) = \Lambda [1 - P_{so}(R_0, R_s)] \quad (16)$$

424 where $\Lambda = \lim_{\eta \rightarrow \infty} P_{co}/(1 - P_{so})$, which represents the im-
425 provement in COP upon decreasing the SOP. More specifically,
426 since the reduction of the SOP/COP must be followed by an
427 improvement of COP/SOP, a lower Λ implies that, when the
428 security is reduced, the reliability is improved, and *vice versa*.
429 Thus, for the TBRS scheme studied earlier, the RSR is derived
430 as (17), shown at the bottom of the page.

431 *Proof:* The proof is given in Appendix B.

432 *Remark 2:* It can be seen from the preceding expression
433 that the factor Λ is independent of the transmit SNR, but
434 directly depends on the channel gains, the rate pair (R_0, R_s) ,
435 and the number of TAs and relays. For a given R_s , reducing
436 R_0 to enhance the reliability may erode the security, because
437 $(R_0 - R_s)$ is also reduced. Conversely, increasing R_0 provides
438 more redundancy for protecting the security of the information,
439 but simultaneously, the reliability is reduced. Hence, the RSR
440 analysis underlines an important point of view concerning how
441 to balance the reliability versus security tradeoff by adjusting
442 (R_0, R_s) . Furthermore, as long as a CSI feedback delay exists,
443 the RSR has an intimate relationship with ρ_{SR} and ρ_{RD} . It is
444 clear that the value of Λ^{TBRS} decreases as ρ_{RD} increases, which
445 is due to the fact that the relay selection process only improves
446 the reliability of the legitimate user. On the other hand, since
447 we always have the conclusion that $\sum_{k=0}^{K_r-1} (-1)^k \binom{K_r-1}{k} (K_r/k - 1) < 1$, when σ_{RD}^2 and σ_{RE}^2 are comparable,
449 Λ^{TBRS} will be reduced as ρ_{SR} increases. This observation
450 implies that, although both P_{co} and $(1 - P_{so})$ are reduced
451 when the first-hop CSI becomes better, the improvement of

the reliability is more substantial than the security loss, as ρ_{SR}
increases.

C. Effective Secrecy Throughput

It should be noted that the COP and SOP metrics ignore the
correlation between these two outage events. More specifically,
in contrast to the point-to-point transmission case, since the
 $S \rightarrow R$ link's SNR included in the MI expressions of (3) and
(4), the secrecy outage and the connection outage are definitely
not independent of each other. Therefore, it might be of limited
benefit in evaluating the reliability or the security separately.
We note furthermore that, although another metric referred to
as the secrecy throughput was introduced as the product of the
successful decoding probability and of the secrecy rate [21],
[22], this definition ignores the fact that a reliable transmission
may be insecure, and the SOP is not taken into consideration.
Hence, this metric is unable to holistically characterize the
efficiency of our scheme, while capable of achieving both re-
liable and secure transmission. Therefore, here, we redefine the
effective secrecy throughput as the probability of a successful
transmission (reliable and secure) multiplied by the secrecy
rate, namely, as $\varsigma = R_s P_{R\&S}$, where the RSCP is defined as

$$P_{R\&S} = \Pr\{I_D > R_0, I_E < R_0 - R_s\}. \quad (18)$$

Upon substituting the expressions of I_D and I_E in (3) and (4)
into (18), we can rewrite $P_{R\&S}$ for the TBRS strategy in (19),
shown at the bottom of the page.

Finally, using the corresponding CDFs and PDFs of (8)–(10)
from our previous analysis, we can obtain $P_{R\&S}^{\text{TBRS}}$ in (20),
shown at the bottom of the next page, as well as the secrecy
throughput.

Furthermore, considering the asymptotic result for RSCP at
high SNRs in (20) by applying the approximation $K_v(x) \approx$
 $(v-1)!/2(x/2)^v$ and closing the highest terms of η after
invoking the McLaurin series representation for the exponential
function, the asymptotic effective secrecy throughput can be
approximated as

Remark 3: Given the definition of COP, SOP, and the secrecy
throughput result of (21), shown at the bottom of the next page,
it can be shown that, for a fixed R_s , if R_0 is too small, although

³Assume equal power allocation between S and the relay, yielding $P_S = P_R = P$, and define $\eta = P/N_0$ as the transmit SNR [24].

$$\Lambda^{\text{TBRS}} = \frac{\left[(1 - \rho_{SR}^2)^{N_t-1} + \sum_{k=0}^{K_r-1} (-1)^k \binom{K_r-1}{k} \frac{K_r \sigma_{SR}^2}{[k(1 - \rho_{RD}^2) + 1] \sigma_{RD}^2} \right] (2^{2R_0} - 1)}{\left[N_t (1 - \rho_{SR}^2)^{N_t-1} + \sigma_{SR}^2 / \sigma_{RE}^2 \right] (2^{2(R_0 - R_s)} - 1)} \quad (17)$$

$$\begin{aligned} P_{R\&S}^{\text{TBRS}} &= \Pr \left\{ \left\{ \gamma_{SR} > \gamma_{th}^D, \gamma_{R^*D} > \frac{\gamma_{th}^D \gamma_{SR} + \gamma_{SR}}{\gamma_{SR} - \gamma_{th}^D} \right\} \cap \left[\left\{ \gamma_{SR} > \gamma_{th}^E, \gamma_{R^*E} < \frac{\gamma_{th}^E \gamma_{SR} + \gamma_{SR}}{\gamma_{SR} - \gamma_{th}^E} \right\} \cup \left\{ \gamma_{SR} < \gamma_{th}^E \right\} \right] \right\} \\ &= \Pr \left\{ \gamma_{SR} > \gamma_{th}^D, \gamma_{R^*D} > \gamma_{th}^D + \frac{\gamma_{th}^D (\gamma_{th}^D + 1)}{\gamma_{SR} - \gamma_{th}^D}, \gamma_{R^*E} < \gamma_{th}^E + \frac{\gamma_{th}^E (\gamma_{th}^E + 1)}{\gamma_{SR} - \gamma_{th}^E} \right\} \end{aligned} \quad (19)$$

489 P_{RS} may be high (i.e., close to 1), the value of ς remains small.
 490 By contrast, if R_0 is too large, the value of P_{co} is close to 1,
 491 and therefore, ς will also become small. This observation is
 492 also suitable for R_s . Thus, as pointed out in the RSR analysis,
 493 it is elusive to improve both the reliability and the security
 494 simultaneously, but both of them are equally crucial in terms
 495 of the effective secrecy throughput, which depends on the rate
 496 pair (R_0, R_s) .

497 Additionally, (21) also reveals that increasing the SNR would
 498 drastically reduce the effective secrecy throughput. For high
 499 transmit SNRs, a high reliability can indeed be perfectly guar-
 500 anteed, but at the same time, the grade of the security is severely
 501 degraded. However, the probability of a reliable and simultane-
 502 ously secure transmission will tend toward zero. Hence, we may
 503 conclude that there exists an optimal SNR, which achieves the
 504 maximal secrecy throughput.

505 In conclusion, adopting the appropriate code rate pair and
 506 transmit SNR is crucial for achieving the maximum effective
 507 secrecy throughput, which can be formulated as

$$\begin{aligned} \max_{R_0, R_s, \eta} \quad & \varsigma(R_0, R_s) = R_s P_{R\&S}^{\text{TBRS}} \\ \text{s.t.} \quad & P_{co} \leq \nu, P_{so} \leq \delta, 0 < R_s < R_0 \end{aligned} \quad (22)$$

508 where ν and δ denote the system's reliability and security
 509 requirements. Unfortunately, it is quite a challenge to find
 510 the closed-form optimal solution to this problem due to the
 511 complexity of the expressions. Although suboptimal solutions
 512 can be found numerically (with the aid of gradient-based search
 513 techniques), the secrecy throughput optimization problem and
 514 the corresponding complexity analysis and performance com-
 515 parisons are beyond the scope of this work.

516 IV. SECURE TRANSMISSION WITH JAMMING

517 Here, we consider the extension of the aforementioned relay
 518 selection approaches to systems additionally invoking relay-

aided jamming. JRJS is based on the outdated but perfectly 519
 estimated CSI, and the details have been presented in Section II. 520
 We would also like to investigate the security performance 521
 from an outage-based perspective. The COP, SOP, RSCP, and 522
 effective secrecy throughput will be included. 523

A. COP and SOP 524

It is plausible that the main differences between the JRJS and 525
 TBRS schemes are determined by the instantaneous SNR of the 526
 $R \rightarrow D$ hop, where, now, a jammer is included. Based on our 527
 preliminary results detailed for the point-to-point SNRs in (8) 528
 and (10), we now focus our attention on the statistical analysis 529
 of the SNR, including J^* . As stated for the JRJS scheme in 530
 Section II, J^* corresponds to the lowest $\tilde{\gamma}_{R_k D}$ and is selected 531
 from the set $\{\mathcal{R} - R^*\}$. Recalling that R^* is the best relay 532
 of the second hop, we have $\tilde{\gamma}_{J^* D} = \min_{R_k \in \mathcal{R} - R^*} \{\tilde{\gamma}_{R_k D}\} \triangleq$ 533
 $\min_{R_k \in \mathcal{R}} \{\tilde{\gamma}_{R_k D}\}$ for $K_r > 1$. Using the induced order statis- 534
 tics, the corresponding CDF of $\gamma_{R^* D}$ is presented in (10), 535
 whereas the PDF of $\gamma_{J^* D}$ can be formulated as 536

$$f_{\gamma_{J^* D}}(x) = \frac{K_r \exp\left(\frac{-K_r x}{[(K_r - 1)(1 - \rho_{RD}^2) + 1]\tilde{\gamma}_{JD}}\right)}{[(K_r - 1)(1 - \rho_{RD}^2) + 1]\tilde{\gamma}_{JD}}. \quad (23)$$

Although the relay and jammer selection processes are not 537
 entirely disjoint, we may exploit the assumption that $\gamma_{R^* D}$ and 538
 $\gamma_{J^* D}$ are independent of each other, which is valid when the 539
 number of relays is sufficiently high, as justified in [24]. Let us 540
 define the signal-to-interference-plus-noise ratio of the second 541
 hop as $\xi_D = \gamma_{R^* D} / (\gamma_{J^* D} + 1)$, using (10) and (23), whose 542
 CDF can be formulated as 543

$$F_{\xi_D}(x) = 1 - K_r \sum_{k=0}^{K_r-1} (-1)^k \binom{K_r-1}{k} \frac{\varphi_k e^{\frac{-x}{\tilde{\gamma}_{RD}\omega_k}}}{(k+1)(x+\varphi_k)} \quad (24)$$

where we have $\varphi_k = \lambda K_r \omega_k / [(K_r - 1)(1 - \rho_{RD}^2) + 1](1 - \lambda)$. 544

$$\begin{aligned} P_{R\&S}^{\text{TBRS}} &= \int_{\gamma_{th}^D}^{\infty} \left[1 - F_{\gamma_{R^* D}} \left(\gamma_{th}^D + \frac{\gamma_{th}^D (\gamma_{th}^D + 1)}{x - \gamma_{th}^D} \right) \right] F_{\gamma_{R^* E}} \left(\gamma_{th}^E + \frac{\gamma_{th}^E (\gamma_{th}^E + 1)}{x - \gamma_{th}^E} \right) f_{\gamma_{SR^*}}(x) dx \\ &\approx 2 \sum_{n=0}^{N_t-1} \sum_{k=0}^{K_r-1} \sum_{m=0}^{N_t-1-n} (-1)^k \binom{K_r-1}{k} \binom{N_t-1}{n} \binom{N_t-1-n}{m} \frac{K_r \rho_{SR}^{2(N_t-1-n)} (1 - \rho_{SR}^2)^n (\gamma_{th}^D)^{N_t-1-n-m}}{(N_t-1-n)!(k+1)\tilde{\gamma}_{SR}^{N_t-n-(m+1)/2}} \\ &\quad \times \exp \left[- \left(\frac{\gamma_{th}^D}{\tilde{\gamma}_{SR}} + \frac{\gamma_{th}^D}{\omega_k \tilde{\gamma}_{RD}} \right) \right] \left[\left(\frac{\gamma_{th}^D (\gamma_{th}^D + 1)}{\omega_k \tilde{\gamma}_{RD}} \right)^{\frac{m+1}{2}} K_{m+1} \left(2 \sqrt{\frac{\gamma_{th}^D (\gamma_{th}^D + 1)}{\omega_k \tilde{\gamma}_{SR} \tilde{\gamma}_{RD}}} \right) \right. \\ &\quad \left. - \exp \left(\frac{-\gamma_{th}^E}{\tilde{\gamma}_{RE}} \right) \left(\frac{\gamma_{th}^D (\gamma_{th}^D + 1)}{\omega_k \tilde{\gamma}_{RD}} + \frac{\gamma_{th}^E (\gamma_{th}^E + 1)}{\tilde{\gamma}_{RE} + \gamma_{th}^D - \gamma_{th}^E} \right)^{\frac{m+1}{2}} K_{m+1} \left(2 \sqrt{\frac{\gamma_{th}^D (\gamma_{th}^D + 1)}{\omega_k \tilde{\gamma}_{SR} \tilde{\gamma}_{RD}} + \frac{\gamma_{th}^E (\gamma_{th}^E + 1)}{\tilde{\gamma}_{SR} (\tilde{\gamma}_{RE} + \gamma_{th}^D - \gamma_{th}^E)}} \right) \right] \end{aligned} \quad (20)$$

$$\zeta^{\text{TBRS}}(R_0, R_s, \eta) = R_s \left\{ 1 - \left[\frac{N_t (1 - \rho_{SR}^2)^{N_t-1}}{\sigma_{SR}^2} + \sum_{k=0}^{K_r-1} \frac{K_r (-1)^k}{[k(1 - \rho_{RD}^2) + 1] \sigma_{RD}^2} \binom{K_r-1}{k} \right] \times \frac{2^{2R_0} - 1}{\eta} \right\} \frac{2^{2(R_0 - R_s)} - 1}{\sigma_{RE}^2 \eta} \quad (21)$$

545 As far as the eavesdropper is concerned, γ_{R^*E} and γ_{J^*E}
546 are independent and exponentially distributed. Furthermore, for
547 $\xi_E = \gamma_{R^*E}/(\gamma_{J^*E} + 1)$, we have

$$F_{\xi_E}(x) = 1 - \frac{\phi}{x + \phi} e^{-\frac{x}{\phi}} \quad (25)$$

548 where $\phi = \lambda/(1 - \lambda)$. According to the definition of COP and
549 SOP in Section III-A, we can obtain the following closed-form
550 approximations of the COP and the SOP.⁴

551 *Lemma 1:* The COP and the SOP of the JRJS strategy
552 associated with feedback delays are approximated by

$$\begin{aligned} P_{\text{co}}^{\text{JRJS}}(R_0) &\approx 1 - \sum_{n=0}^{N_t-1} \sum_{k=0}^{K_r-1} \sum_{m=0}^{N_t-1-n} \binom{N_t-1}{n} \\ &\times \binom{K_r-1}{k} \binom{N_t-1-n}{m} \\ &\times \frac{(-1)^k (K_r+1) \rho_{SR}^{2(N_t-1-n)} (1 - \rho_{SR}^2)^n}{(N_t-1-n)! (k+1) \bar{\gamma}_{SR}^{N_t-n}} \\ &\times \frac{\Gamma(m+2) \hat{\phi}_k (\gamma_{th}^D)^{N_t-n} (\gamma_{th}^D + 1)^{m+1}}{(\gamma_{th}^D + \hat{\phi}_k)^{m+2}} \\ &\times \exp \left[-\frac{\gamma_{th}^D (\hat{\phi}_k - 1)}{\bar{\gamma}_{SR} (\gamma_{th}^D + \hat{\phi}_k)} \right] \\ &\times \Gamma \left(-m-1, \frac{\gamma_{th}^D (\gamma_{th}^D + 1)}{\bar{\gamma}_{SR} (\gamma_{th}^D + \hat{\phi}_k)} \right) \end{aligned} \quad (26)$$

553 where $\hat{\phi}_k = K_r \lambda \omega_k \eta \sigma_{RD}^2 / [(K_r - 1)(1 - \rho_{RD}^2) + 1](1 -$
554 $\lambda) \eta \sigma_{RD}^2 + K_r)$, and

$$\begin{aligned} P_{\text{so}}^{\text{JRJS}}(R_0, R_s) &\approx \sum_{n=0}^{N_t-1} \sum_{m=0}^{N_t-1-n} \binom{N_t-1}{n} \\ &\times \frac{\rho_{SR}^{2(N_t-1-n)} (1 - \rho_{SR}^2)^n}{m! \bar{\gamma}_{SR}^m} \\ &\times \frac{(2\gamma_{th}^E)^m \phi}{(2\gamma_{th}^E + \phi)} \exp \left[-\left(\frac{2\gamma_{th}^E}{\bar{\gamma}_{SR}} + \frac{2\gamma_{th}^E}{\bar{\gamma}_{RE}} \right) \right]. \end{aligned} \quad (27)$$

555 *Proof:* The proof is given in Appendix B.

556 The feasible range of the reliability constraint is similar to
557 that of the TBRS strategy, and hence, it is omitted here.

558 B. Reliability–Security Ratio

559 *Lemma 2:* Recalling the definition in Section III, the RSR
560 for the JRJS strategy may be expressed in (28), shown at the
561 bottom of the page.

⁴When we have $\lambda \rightarrow 1$, (24) will degenerate into the TBRS case seen in (10). The performance analysis of the JRJS will be presented separately in the following, since several approximations have to be included.

562 It can be seen from the previous expression that, in contrast
563 to the analysis of the TBRS strategy operating without jam-
564 ming, for a fixed SNR threshold, the CDF of the second-hop
565 SNR will converge to a nonzero limit. We also find that this
566 limit is determined by the power sharing ratio between the
567 relay and the jammer. Furthermore, according to the analy-
568 sis of the TBRS strategy, for $\eta \rightarrow \infty$, we have $F_{\gamma_{SR^*}}(x) \rightarrow$
569 0. Thus, by exploiting the tight upper bound that $\gamma_D^{\text{TBRS}} \leq$
570 $\min\{\gamma_{SR}, \gamma_{R^*D}\}$ and $\gamma_E^{\text{TBRS}} \leq \min\{\gamma_{SR}, \gamma_{R^*E}\}$, we have
571 $P_{\text{co}}^{\text{JRJS}, \infty} \rightarrow F_{\gamma_{\xi_D}}(\gamma_{th}^D)$ and $1 - P_{\text{so}}^{\text{JRJS}, \infty} \rightarrow F_{\gamma_{\xi_E}}(\gamma_{th}^E)$. Finally,
572 substituting the corresponding results into (16), we arrive at the
573 RSR of the JRJS strategy.

Remark 4: It can be seen from the RSR expression of (28)
574 again that the rate-pair setting (R_0, R_s) has an inconsistent
575 influence on the RSR, and hence, we have to carefully adjust R_0
576 and R_s to balance the reliability versus security performance.
577 Let us now focus our attention on the differences between the
578 JRJS scheme and the TBRS arrangement.

579 First, we may find that the power sharing ratio λ between
580 the relay and the jammer plays a very important role. The
581 optimization of λ will be investigated from an effective secrecy
582 throughput optimization point of view in the following.

583 Second, it is plausible that, in contrast to the behavior of the
584 TBRS strategy, Λ^{JRJS} of (28) is only related to the delay of the
585 second hop, but it is still a monotonically decreasing function of
586 ρ_{RD} . This implies that the improvement of the channel quality
587 of the JRJS will achieve a more pronounced COP improvement
588 than the associated SOP improvement. Furthermore, recalling
589 that the RSR is considered in the high-SNR region, it has no
590 dependence on the first hop quality. This is due to the fact that
591 if the first-hop channel quality is sufficiently high for ensuring
592 a successful transmission, the asymptotic CDFs of ξ_D and ξ_E
593 in (29) and (30) associated with $\eta \rightarrow \infty$ will converge to a
594 nonzero limit at high SNRs, which ultimately dominates the
595 COP and the SOP.

597 C. Effective Secrecy Throughput

598 Before proceeding to the effective secrecy throughput analy-
599 sis, we also have to investigate the RSCP.

600 *Lemma 3:* The RSCP of our JRJS strategy may be approxi-
601 mated as in (31), shown at the bottom of the next page, where
602 we have $\theta_{1,k} = (\gamma_{th}^D (\gamma_{th}^D + 1)) / (\gamma_{th}^D + \hat{\phi}_k)$, $\theta_2 = \gamma_{th}^D - \gamma_{th}^E +$
603 $(\gamma_{th}^E (\gamma_{th}^E + 1)) / (\gamma_{th}^E + \hat{\phi})$, and $\hat{\phi} = \lambda \eta \sigma_{RE}^2 / ((1 - \lambda) \eta \sigma_{RE}^2 + 1)$.

604 *Proof:* The proof is given in Appendix C.

605 Apart from the rate pair (R_0, R_s) , the aforementioned $P_{R\&S}^{\text{JRJS}}$
606 of (31) is also a function of the power sharing ratio λ between
607 the selected relay and the jammer.

608 Given the complexity of the RSCP expression, it is quite
609 a challenge to find a closed-form result for maximizing the

$$\Lambda^{\text{JRJS}} = \frac{(2^{2R_0} - 1)}{(2^{2(R_0 - R_s)} - 1)} \sum_{k=0}^{K_r-1} \binom{K_r-1}{k} \frac{(-1)^k K_r [(K_r - 1)(1 - \rho_{RD}^2) + 1] [(\lambda^{-1} - 1)(2^{2(R_0 - R_s)} - 1) + 1]}{[(K_r - 1)(1 - \rho_{RD}^2) + 1] (k+1)(\lambda^{-1} - 1)(2^{2R_0} - 1) + K_r [k(1 - \rho_{RD}^2) + 1]} \quad (28)$$

610 effective secrecy throughput that $\max_{0 < \lambda < 1} \varsigma = R_s P_{R\&S}^{\text{JRJS}}$. Al-
 611 ternatively, we can focus on the asymptotic analysis in the high-
 612 SNR region and try to find a general closed-form solution for λ .
 613 Specifically, when we have $\eta \rightarrow \infty$, $P_{R\&S}^{\text{JRJS}}$ will be dominated
 614 by the channel quality of the second hop; hence, we have

$$P_{R\&S}^{\text{JRJS},\infty}(R_0, R_s, \lambda) \approx \Pr \{ \xi_D > \gamma_{th}^D, \xi_E < \gamma_{th}^E \} \\ = [1 - F_{\xi_D}(\gamma_{th}^D)] F_{\xi_E}(\gamma_{th}^E) \quad (32)$$

615 where the approximation is based on the fact that, in contrast to
 616 both $F_{\xi_D}(\gamma_{th}^D)$ and $F_{\xi_E}(\gamma_{th}^E)$, which converge to a nonzero limit
 617 regardless of η , the first hop's $F_{\gamma_{SR}}(x)$ will tend to zero, and
 618 hence, it can be neglected. Substituting the asymptotic results
 619 of (29) and (30) into (33), we can obtain $P_{R\&S}^{\text{JRJS},\infty}$. In contrast to
 620 the TBRS case operating without jamming, as the SNR tends to
 621 ∞ , the RSCP will tend to a nonzero value and, upon increasing
 622 the transmit SNR beyond a certain limit, will no longer increase
 623 the effective secrecy throughput.

624 Then, based on (32), we arrive at the approximated optimal
 625 value λ_{opt} , which is the solution of the following equation:

$$\frac{\partial P_{R\&S}^{\text{JRJS},\infty}(R_0, R_s, \lambda)}{\partial \lambda} = 0. \quad (33)$$

626 Then, by exploiting the approximation of $[k(1 - \rho_{RD}^2) + 1]/$
 627 $(k + 1) \approx 1 - \rho_{RD}^2$ in (29) for a large ρ_{RD} (practically, the CSI
 628 delay is small, and $\rho_{RD} \rightarrow 1$), we have

$$\lambda_{\text{subopt}} = \frac{\sqrt{[(K_r - 1)(1 - \rho_{RD}^2) + 1] \gamma_{th}}}{\sqrt{[(K_r - 1)(1 - \rho_{RD}^2) + 1] \gamma_{th} + \sqrt{K_r(1 - \rho_{RD}^2)}}} \quad (34)$$

629 where $\gamma_{th} = (2^{2R_0} - 1)(2^{2(R_0 - R_s)} - 1)$. It is clear that this
 630 value is determined by the number of relays and (R_0, R_s) .

631 V. NUMERICAL RESULTS

632 Both our numerical and Monte Carlo simulation results are
 633 presented here for verifying the theoretical PLS performance
 634 analysis of the multiple-relay-aided network under CSI feed-

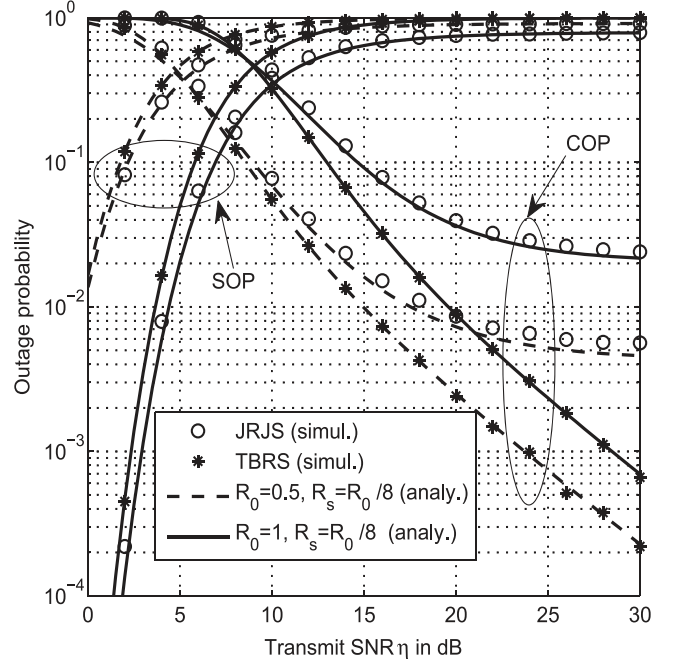


Fig. 2. COP and SOP versus transmit SNR for the TBRS and JRJS strategies in conjunction with different rate pairs, for $N_t = K_r = 3$, $f_d T_d = 0.1$, and $\lambda = 1/10$.

back delays. Explicitly, the COP, SOP, RSCP, and RSR are 635
 validated for both the TBRS and JRJS strategies. Furthermore, 636
 the effects of feedback delays and system parameters (including 637
 the transmission rate pair (R_0, R_s) and the power sharing ratio 638
 λ between the relay and the jammer) on the achievable effective 639
 secrecy throughput are evaluated. The Rayleigh fading model 640
 is employed for characterizing all communication links in our 641
 system. Additionally, we set the total power to $P = 1$ and 642
 $\sigma_{SR}^2 = \sigma_{RD}^2 = \sigma_{RE}^2 = 1$, and used $T_{dSR} = T_{dRD} = T_d$. 643

Fig. 2 plots the COP and the SOP versus the transmit SNR for 644
 both the TBRS and JRJS strategies in conjunction with different 645
 rate pairs. The analytical lines are plotted by using (11) and (14) 646
 for the TBRS strategy and by using (26) and (27) for the JRJS 647

$$P_{R\&S}^{\text{JRJS}}(R_0, R_s, \lambda) \approx \sum_{n=0}^{N_t-1} \sum_{k=0}^{K_r-1} \sum_{m=0}^{N_t-1-n} (-1)^k \binom{N_t-1}{n} \binom{K_r-1}{k} \binom{N_t-1-n}{m} \\ \times \frac{K_r \rho_{SR}^{2(N_t-1-n)} (1 - \rho_{SR}^2)^n \hat{\varphi}_k(\gamma_{th}^D)^{N_t-1-n-m}}{(N_t-1-n)!(k+1) \bar{\gamma}_{SR}^{N_t-n} (\gamma_{th}^D + \hat{\varphi}_k) e^{\frac{\gamma_{th}^D}{\bar{\gamma}_{SR}} + \frac{\gamma_{th}^D}{\bar{\gamma}_{RD} \omega_k}}} \\ \times \left\{ \theta_{1,k}^{m+1} e^{\frac{\theta_1}{\bar{\gamma}_{SR}}} \Gamma(m+2) \Gamma\left(-m-1, \frac{\theta_{1,k}}{\bar{\gamma}_{SR}}\right) - \frac{\hat{\phi} e^{-\gamma_{th}^E / \bar{\gamma}_{RE}}}{(\gamma_{th}^E + \phi) (\theta_{1,k} - \theta_2)} \Gamma(m+3) \right. \\ \times \left[\theta_2^{m+2} e^{\frac{\theta_2}{\bar{\gamma}_{SR}}} \Gamma\left(-m-2, \frac{\theta_2}{\bar{\gamma}_{SR}}\right) - \theta_{1,k}^{m+2} e^{\frac{\theta_1}{\bar{\gamma}_{SR}}} \Gamma\left(-m-2, \frac{\theta_{1,k}}{\bar{\gamma}_{SR}}\right) \right] + \Gamma(m+2) (\gamma_{th}^D - \gamma_{th}^E) \\ \left. \times \left[\theta_2^{m+1} e^{\frac{\theta_2}{\bar{\gamma}_{SR}}} \Gamma\left(-m-1, \frac{\theta_2}{\bar{\gamma}_{SR}}\right) - \theta_{1,k}^{m+1} e^{\frac{\theta_1}{\bar{\gamma}_{SR}}} \Gamma\left(-m-1, \frac{\theta_{1,k}}{\bar{\gamma}_{SR}}\right) \right] \right\} \quad (31)$$

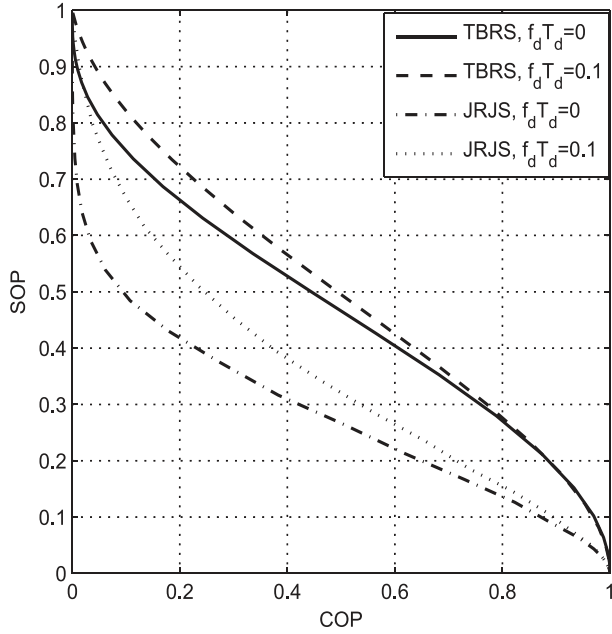


Fig. 3. SOP versus COP for the TBRS and JRJS strategies with different feedback delays for $N_t = K_r = 3$, $R_s = R_0/8$, and $\lambda = 1/10$.

648 case, respectively. It can be clearly seen from the figure that the
649 analytical and simulated outage probability curves match well,
650 which confirms the accuracy of the mathematical analysis. As
651 expected, compared with the TBRS strategy, the SOP of the
652 JRJS strategy is much better, whereas the COP is worse. We
653 can also find that both the COP and the SOP will converge to an
654 outage floor at high SNRs for the JRJS strategy. The reason for
655 this is that the jammer also imposes interference on the destina-
656 tion and the interference inflicted increases with the SNR. Thus,
657 the designers have to take into account the tradeoff between
658 the reliability and the security and the interference imposed on
659 D , particularly when considering the JRJS strategy. Moreover,
660 we can observe in Fig. 2 that increasing the transmission rate
661 decreases the COP and increases the SOP.

662 Fig. 3 further characterizes the SOP versus COP for both the
663 TBRS and JRJS strategies based on the numerical results in
664 Fig. 2, which shows the tradeoff between the reliability and the
665 security. It can be seen from the figure that the SOP decreases as
666 the COP increases, and for a specific COP, the SOP of the JRJS
667 scheme is strictly lower than that of TBRS. This confirms that
668 the JRJS scheme performs better than the conventional TBRS
669 scheme. Furthermore, the CSI feedback delay will also degrade
670 the system tradeoff performance.

671 Fig. 4 illustrates the RSCP versus transmit SNR for the
672 TBRS strategy in the context of different network configura-
673 tions, including different rate pairs, different number of relays,
674 and both perfect and outdated CSI feedback scenarios. The
675 analytical lines are plotted by using the approximation in (20).
676 We may conclude from the figure that the rate-pair setting
677 (R_0, R_s) determines both the reliability and security transmis-
678 sion performance. These curves also show that the RSCP is a
679 concave function of the transmit SNR, whereas the continued
680 boosting of the SNR would only decrease the probability of
681 a successful transmission. We can observe from Fig. 4 that,

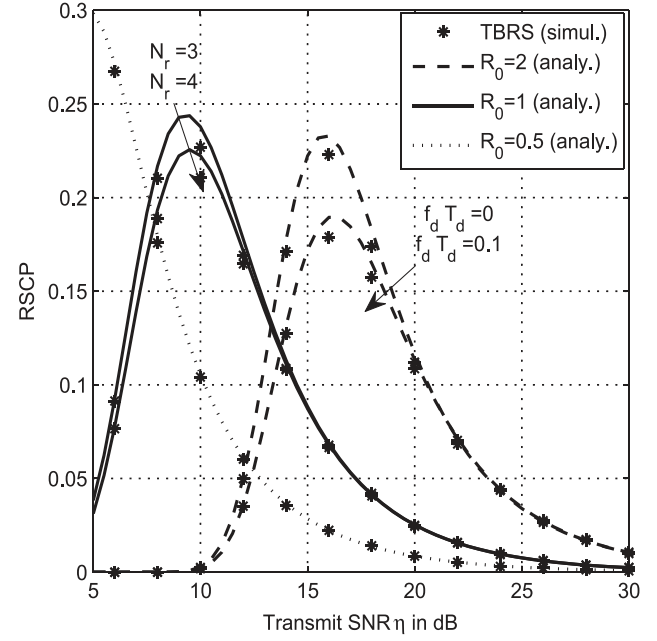


Fig. 4. RSCP versus transmit SNR for the TBRS strategy with different rate pairs for $N_t = K_r = 3$, $f_d T_d = 0.1$.

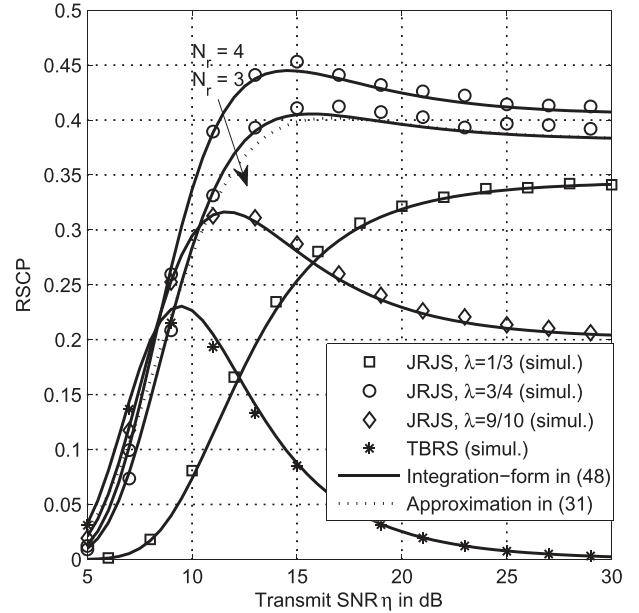


Fig. 5. RSCP versus transmit SNR for the JRJS strategy for different power sharing ratios λ and for $N_t = K_r = 3$, $f_d T_d = 0.1$, and $R_0 = 1$, $R_s = R_0/8$.

for a high transmit SNR, total reliability can be guaranteed,
682 whereas the associated grade of security is severely eroded.
683 Furthermore, increasing the number of relays and decreasing
684 the feedback delay will improve both the reliability and security
685 performance. 686

The RSCP of the JRJS strategy is presented in Fig. 5 for
687 different power sharing ratios between relaying and jamming.
688 Both the integration form (45) and the approximated closed
689 form in (31) match well with the Monte Carlo simulations.
690 The performance of the TBRS strategy is also included for
691 comparison. The JRJS scheme outperforms the TBRS operating
692

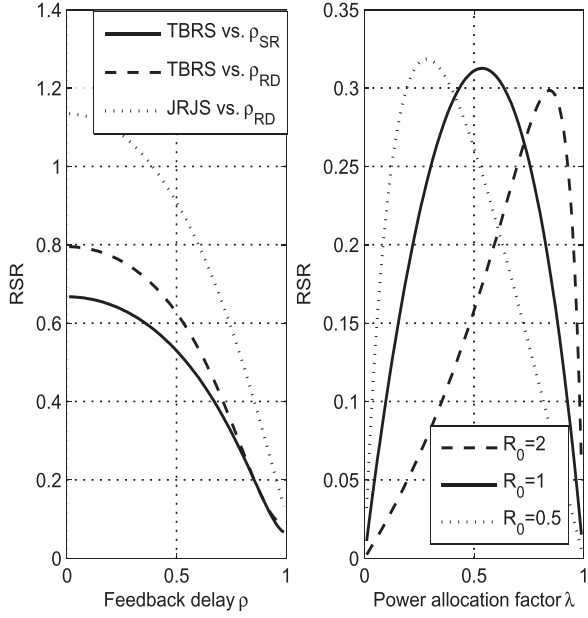


Fig. 6. RSR versus feedback delay coefficient ($R_0 = 1$, $R_s = R_0/8$, $\lambda = 3/4$) and power sharing ratio λ ($R_s = R_0/8$, $\rho_{SR} = \rho_{RD} = 0.9$) for the TBRS and JRJS strategies, with $N_t = K_r = 3$.

693 without jamming under the scenario considered when encoun-
 694 tering comparable relay–destination and relay–eavesdropper
 695 channels. For some extreme configurations (when the relay–
 696 eavesdropper links are comparatively weak), this statement
 697 may not hold, but this scenario is beyond the scope of this
 698 paper. The maximum RSCP appears at about $\eta = 15$ dB
 699 for the JRJS strategy using $\lambda = 3/4$, whereas it is $\eta = 10$ dB
 700 for the TBRS strategy. Furthermore, as expected, increasing the
 701 number of available relays and jamming nodes will always be
 702 able to improve the reliability and security performance. How-
 703 ever, the continued boosting of the jammer’s power (decreasing
 704 λ) will not always improve the overall performance, because
 705 the interference improves initially the security, but then, it starts
 706 to reduce the reliability as λ decreases. This further motivates
 707 the designer to carefully take into account the power sharing
 708 between relaying and jamming. The effect of the rate-pair
 709 setting on the security and reliability of the JRJS strategy is
 710 neglected here, which follows a similar trend to that of the
 711 TBRS strategy.

712 Fig. 6 characterizes the RSR versus feedback delay and
 713 power sharing ratio for both TBRS and JRJS, in which the
 714 RSR curves are plotted by using (17) and (28), respectively.
 715 The first illustration shows that the RSR decreases as the delay
 716 coefficients (ρ_{SR} and ρ_{RD}), which confirms that the im-
 717 provement of reliability becomes more pronounced than the
 718 reduction of the security as the feedback delay decreases.
 719 This observation implies an improvement in terms of the
 720 security–reliability tradeoff. In addition, the RSR versus ρ_{RD}
 721 is larger than that of ρ_{SR} , which indicates that the impact of the
 722 second-hop CSI feedback delay is more prominent. The other
 723 illustration in the right demonstrates that the RSR is a concave
 724 function of the power sharing ratio, which reflects the tradeoff
 725 between the reliability and the security struck by adjusting λ .

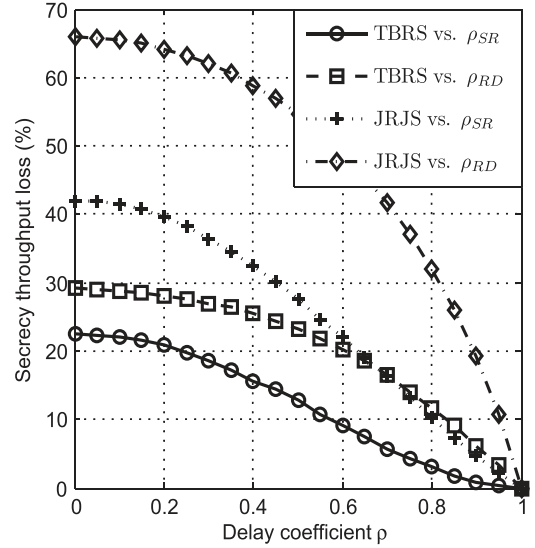


Fig. 7. Percentage secrecy throughput loss versus delay coefficients with $N_t = K_r = 3$, $R_0 = 1$, $R_s = R_0/8$, $\lambda = 3/4$, and $\eta = 10$ dB.

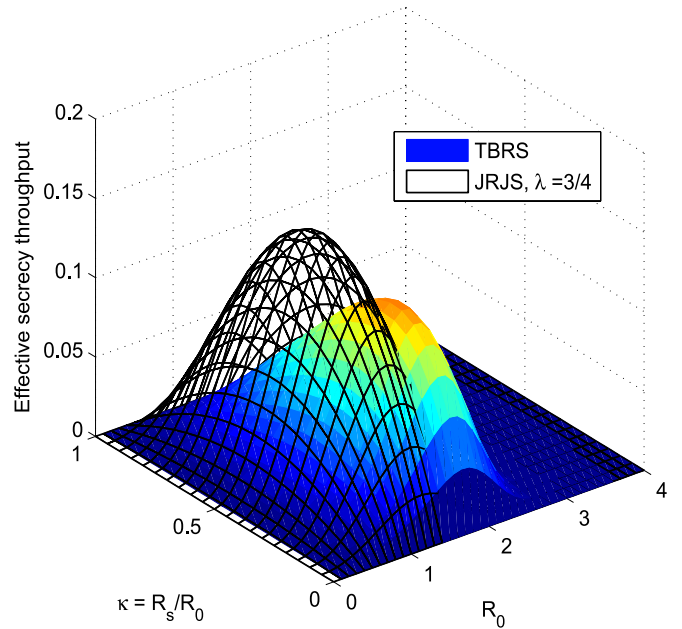


Fig. 8. Secrecy throughput versus R_0 and $\kappa = R_s/R_0$ for both the TBRS and JRJS strategies with $N_t = K_r = 3$, $f_d T_d = 0.1$, and $\eta = 15$ dB.

To further evaluate the effect of feedback delays on the
 726 secrecy performance, Fig. 7 plots the resultant percentage of 727
 728 secrecy throughput loss versus the delay, which is defined as

$$\text{Loss} = \frac{S_{\text{no-delay}} - S_{\text{delay}}}{S_{\text{no-delay}}}. \quad (35)$$

It can be seen from the figure that, compared with the TBRS
 729 scheme, JRJS is more sensitive to the feedback delays. Further-
 730 more, recalling that increasing the delay coefficient ρ_{SR} of the
 731 first hop improves the reliability, but at the same time also helps
 732 the eavesdropper, it is not surprising that the secrecy throughput
 733 loss due to the second-hop feedback delay is more pronounced. 734

Fig. 8 illustrates the achievable effective secrecy throughput
 735 for both the TBRS and JRJS strategies versus the codeword 736

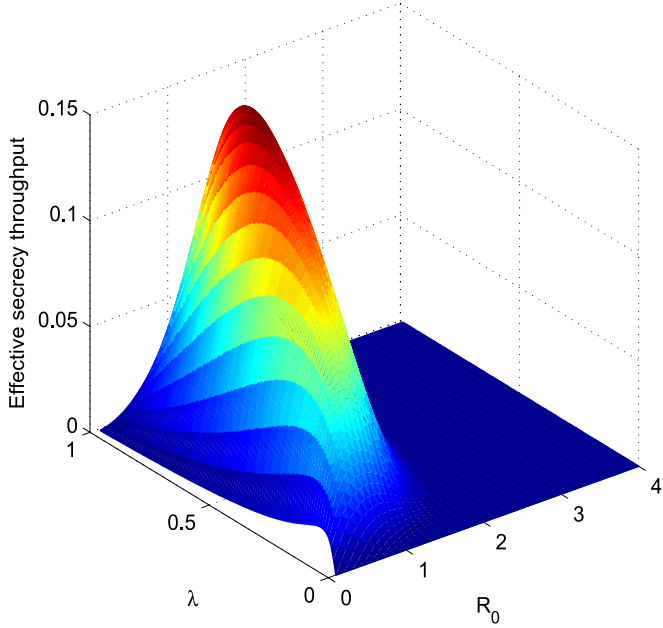


Fig. 9. Secrecy throughput versus R_0 and λ for the JRJS strategy with $N_t = K_r = 3$, $f_d T_d = 0.1$, $\eta = 15$ dB, and $R_s/R_0 = 1/8$.

737 transmission rate R_0 and the secrecy code ratio $\kappa = R_s/R_0$
 738 with no outage constraints ($v = \delta = 1$). The values of the
 739 effective secrecy throughput are plotted by using $\zeta = R_s P_{R\&S}$.
 740 We can observe in Fig. 8 that, subject to a fixed code rate
 741 ratio κ , the effective secrecy throughput increases to a peak
 742 value as R_0 reaches its optimal value and then decreases. This
 743 phenomenon can be explained as follows. At a low transmission
 744 rate, although the COP increases with R_0 , which has a negative
 745 effect on the effective secrecy throughput, both the secrecy
 746 rate and the SOP performance will benefit. However, after
 747 reaching the optimal R_0 , the effective secrecy throughput drops
 748 since the main link cannot afford a reliable transmission, and
 749 the resultant COP increase becomes dominant. On the other
 750 hand, subject to a fixed R_0 (which results in a constant COP),
 751 the effective secrecy throughput is also a concave function
 752 of κ , and increasing the code rate ratio ultimately results
 753 in an increased secrecy information rate at the cost of an
 754 increased SOP.

755 The achievable effective secrecy throughput for the JRJS
 756 strategy is also presented in Fig. 8, and similar conclusions and
 757 trends can be observed to that of the TBRS case. Additionally,
 758 the comparison of the two strategies indicates that the JRJS
 759 scheme attains a higher effective secrecy throughput than the
 760 TBRS scheme operating without jamming, even if no power
 761 sharing optimization has been employed.

762 Fig. 9 further illustrates the impact of power sharing between
 763 the relay and the jammer on the achievable effective secrecy
 764 throughput of the JRJS strategy versus R_0 in the absence of
 765 outage constraints. Given a fixed code rate pair (R_0, R_s) , the
 766 effective secrecy throughput follows the trend of the RSCP,
 767 which is a concave function of λ , as shown in Fig. 6. The
 768 interference introduced by the jammer initially improves both
 769 the reliability and the security as λ increases, but this trend is
 770 reversed beyond a certain point.

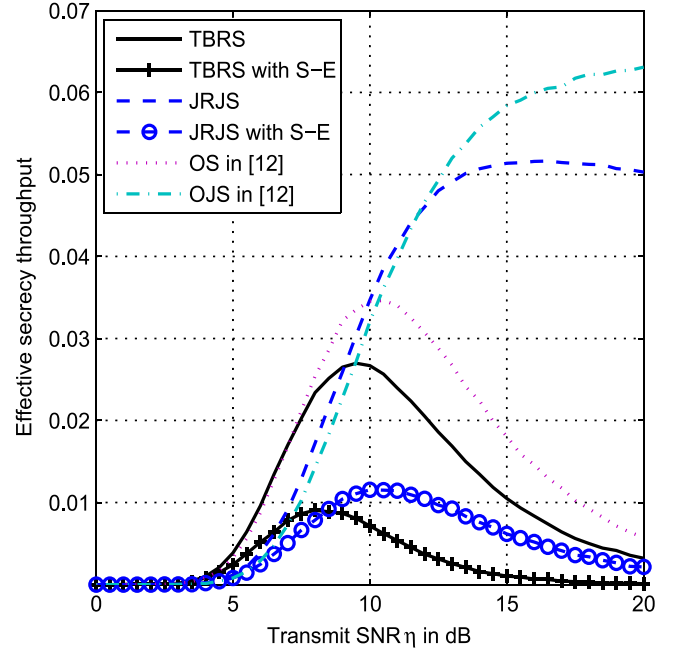


Fig. 10. Comparisons for different strategies with and without the S-E link, for $N_t = K_r = 3$, $R_0 = 1$, $R_s = R_0/8$, $f_d T_d = 0.1$, and $\lambda = 3/4$.

VI. DISCUSSION

771

A. Impact of the S-E Link

772

We note that the introduction of the S-E link, i.e., the
 773 information leakage in the first phase, is very critical to the
 774 security. There are also some research studies focusing on
 775 the corresponding secure transmission design and performance
 776 evaluation for cooperative networks with the S-E link, such
 777 as [15] and [16]. Here, we assume that the eavesdropper can
 778 receive information directly from the source in the first phase.
 779 Thus, following the steps in the prior sections, for the TBRS
 780 and JRJS schemes, it is clear that the SNR experienced at the
 781 eavesdropper should be rewritten as

$$\tilde{\gamma}_E^\tau = \gamma_{SE} + \gamma_E^\tau \quad (36)$$

where $\gamma_{SE} = P_s |\mathbf{w}_{\text{opt}}(t|T_{dSR}) \mathbf{h}_{SE}(t)|^2 / N_0$ follows the ex-
 783 ponential distribution with the average value $\bar{\gamma}_{SE}$, $\tau =$
 784 $\{\text{TBRS, JRJS}\}$, and γ_E^τ has been defined in (4) and (7).
 785

Then, the corresponding SOP, RSCP, and effective secrecy
 786 throughput have to be reconsidered. Unfortunately, to the best
 787 of our knowledge, it is a mathematically intractable problem
 788 to obtain closed-form results for the related performance eval-
 789 uations. Therefore, we resorted to numerical simulations for
 790 further investigating the impact of the S-E link. Fig. 10 com-
 791 pares the effective secrecy throughput of the TBRS and JRJS
 792 schemes both with and without considering the direct S-E
 793 link. It becomes clear that the information leakage in the first
 794 phase will lead to a severe security performance degradation,
 795 particularly for the JRJS scheme, which will no longer be
 796 capable of maintaining a steady throughput at high SNRs. The
 797 reason for this trend is that increasing the transmit SNR will
 798 help the eavesdropper in the presence of the direct S-E link.
 799

800 B. Comparisons

801 Here, based on the outdated CSI assumption, we provide per-
802 formance comparisons with a range of other schemes advocated
803 in [12] with the aid of the proposed outage-based characteriza-
804 tion. Fig. 10 also incorporates our effective secrecy throughput
805 performance comparison, where the optimal selection (OS)
806 regime and the optimal selection combined with jamming (OSJ)
807 were proposed in [12]. They are formulated as

$$808 \text{ OS : } R^* = \arg \max_{R_k \in \mathcal{R}} \left\{ \frac{\tilde{\gamma}_{R_k D}}{\tilde{\gamma}_{R_k E}} \right\} \quad (37)$$

$$809 \text{ OSJ : } \left\{ \begin{array}{l} R^* = \arg \max_{R_k \in \mathcal{R}} \left\{ \frac{\tilde{\gamma}_{R_k D}}{\tilde{\gamma}_{R_k E}} \right\} \\ J^* = \arg \min_{R_k \in \mathcal{R} - R^*} \left\{ \frac{\tilde{\gamma}_{R_k D}}{\tilde{\gamma}_{R_k E}} \right\} \end{array} \right\} \quad (38)$$

810 where $\tilde{\gamma}_{R_k E}$ is the delayed version of the instantaneous CSI of
811 the R–E link. It should be noted that this constitutes an entirely
812 new performance characterization of these schemes from the
813 perspective of the effective secrecy throughput. It is shown in
814 Fig. 1 that the selection combined with jamming outperforms
815 the corresponding nonjamming techniques at high SNRs, albeit
816 this trend may no longer prevail at low SNRs. In comparison,
817 compared with those selections relying on the average SNRs of
818 the R–E link, the optimal selections relying on the idealized
819 simplifying assumptions of having global CSI (OS and OSJ
820 schemes) knowledge can only achieve throughput gains at high
821 SNRs due to the inevitable feedback delay.

822

VII. CONCLUSION

823 An outage-based characterization of cooperative relay net-
824 works has been provided in the face of CSI feedback delays.
825 Two types of relaying strategies were considered, namely, the
826 TBRs strategy and the JRJS strategy. Closed-form expressions
827 of the COP, the SOP, and the RSCP, as well as of the RSR,
828 were derived. The RSR results demonstrated that the reliability
829 is improved more substantially than the security performance
830 when the CSI feedback delays are reduced. Furthermore, we
831 presented a modified effective secrecy throughput definition
832 and demonstrated that the JRJS strategy achieves a significant
833 effective secrecy throughput gain over the TBRs strategy. The
834 transmit SNR, the secrecy codeword rate setting, and the power
835 sharing ratio between the relay and jammer nodes play impor-
836 tant roles in striking a balance between the reliability and the
837 security in terms of the secrecy throughput. The impact of the
838 direct S–E link and the performance comparisons with other
839 selection schemes were also included. Additionally, our results
840 demonstrate that JRJS is more sensitive to the feedback delays
841 and that the secrecy throughput loss due to the second-hop
842 feedback delay is more pronounced than that due to the first-
843 hop one.

844

APPENDIX A

845

PROOF OF PROPOSITION 1

846 To simplify the asymptotic performance analysis, (3) can be
847 expressed in a more mathematically tractable form by the com-
848 monly used tight upper bound of $\gamma_D^{\text{TBRs}} \leq \min\{\gamma_{SR}, \gamma_{R^*D}\}$

and $\gamma_E^{\text{TBRs}} \leq \min\{\gamma_{SR}, \gamma_{R^*E}\}$. When we have $\eta \rightarrow \infty$, based
849 on the CDFs in (9) and (10) and closing the smallest order terms
850 of x/η , we have

$$851 F_{\gamma_{SR}}(x) \rightarrow 1 - \left[\sum_{n=0}^{N_t-1} \binom{N_t-1}{n} \rho_{SR}^{2(N_t-1-n)} (1 - \rho_{SR}^2)^n \right. \\ 852 + \sum_{n=0}^{N_t-2} \binom{N_t-1}{n} \times \rho_{SR}^{2(N_t-1-n)} \\ 853 \left. \times (1 - \rho_{SR}^2)^n \frac{x}{\tilde{\gamma}_{SR}} + \mathcal{O}\left(\frac{x}{\tilde{\gamma}_{SR}}\right) \right] \\ 854 \times \left[1 - \frac{x}{\tilde{\gamma}_{SR}} + \mathcal{O}\left(\frac{x}{\tilde{\gamma}_{SR}}\right) \right] \\ 855 = 1 - \left[1 + (1 - (1 - \rho_{SR}^2)^{N_t-1}) \frac{x}{\tilde{\gamma}_{SR}} + \mathcal{O}\left(\frac{x}{\tilde{\gamma}_{SR}}\right) \right] \\ 856 \times \left[1 - \frac{x}{\tilde{\gamma}_{SR}} + \mathcal{O}\left(\frac{x}{\tilde{\gamma}_{SR}}\right) \right] \\ 857 = (1 - \rho_{SR}^2)^{N_t-1} \frac{x}{\tilde{\gamma}_{SR}} + \mathcal{O}\left(\frac{x}{\tilde{\gamma}_{SR}}\right) \quad (39)$$

858 where $\mathcal{O}(x)$ denotes the high-order infinitely small contribu-
859 tions as a function of x , and

$$860 F_{\gamma_{R^*D}}(x) \rightarrow 1 - \sum_{k=0}^{K_r-1} (-1)^k \frac{K_r}{k+1} \binom{K_r-1}{k} \\ 861 \times \left[1 - \frac{k+1}{k(1 - \rho_{RD}^2) + 1} \frac{x}{\tilde{\gamma}_{RD}} + \mathcal{O}\left(\frac{x}{\tilde{\gamma}_{RD}}\right) \right] \\ 862 = \sum_{k=0}^{K_r-1} (-1)^k \binom{K_r-1}{k} \frac{K_r}{k(1 - \rho_{RD}^2) + 1} \\ 863 \times \frac{x}{\tilde{\gamma}_{RD}} + \mathcal{O}\left(\frac{x}{\tilde{\gamma}_{RD}}\right). \quad (40)$$

864 Then, applying the upper bound of the receiver SNR, we may
865 rewrite the COP and the SOP of the TBRs strategy at high
866 SNRs as

$$867 P_{\text{co}}^{\text{TBRs}, \infty} = 1 - (1 - F_{\gamma_{SR^*}}(\gamma_{th}^D)) (1 - F_{\gamma_{R^*D}}(\gamma_{th}^D)) \\ 868 = \left[\frac{(1 - \rho_{SR}^2)^{N_t-1}}{\sigma_{SR}^2} + \sum_{k=0}^{K_r-1} (-1)^k \right. \\ 869 \left. \times \binom{K_r-1}{k} \frac{K_r}{[k(1 - \rho_{RD}^2) + 1] \sigma_{RD}^2} \right] \frac{2^{2R_0} - 1}{\eta} \quad (41)$$

870 and according to the fact that γ_{R^*E} is exponentially distributed,
871 we have

$$872 1 - P_{\text{so}}^{\text{TBRs}, \infty} = 1 - (1 - F_{\gamma_{SR^*}}(\gamma_{th}^E)) (1 - F_{\gamma_{R^*E}}(\gamma_{th}^E)) \\ 873 = \left[\frac{(1 - \rho_{SR}^2)^{N_t-1}}{\sigma_{SR}^2} + \frac{1}{\sigma_{RE}^2} \right] \frac{2^{2(R_0 - R_s)} - 1}{\eta}. \quad (42)$$

874 Finally, substituting (41) and (42) into the definition of RSR
875 in (16), we can obtain (17). 876

859 APPENDIX B
860 PROOF OF LEMMA 1

861 According to the description of COP and SOP, replacing
862 $F_{\gamma_{R^*D}}(x)$ and $F_{\gamma_{R^*E}}(x)$ by $F_{\xi_D}(x)$ and $F_{\xi_E}(x)$ in (12) and (14)
863 will involve a mathematically intractable integration of the form

$$\Upsilon(a, b, \mu, \nu) = \int_0^{\infty} \frac{z^a}{z+b} \exp\left(-\mu z - \frac{\nu}{z}\right) dz \quad (43)$$

864 which, to the best of our knowledge, does not have a closed-
865 form solution. Alternatively, bearing in mind that the preceding
866 integration has a great matter with ξ_D , we now focus our
867 attention on the approximation of ξ_D . Based on the PDF
868 results in (23), it may be seen that γ_{J^*D} obeys an exponential
869 distribution. Then, we can approximate $\hat{\gamma}_{J^*D} = \gamma_{J^*D} + 1$ by
870 the exponential distribution as well, with an average value
871 of $\mathbb{E}\{\hat{\gamma}_{J^*D}\} = ((K_r - 1)(1 - \rho_{RD}^2) + 1)\bar{\gamma}_{RD} + K_r)/K_r$ by
872 assuming that the AWGN term "1" is part of the stochastic
873 mean terms. The approximation based on this method provides
874 a very accurate analysis, and the accuracy of this method is
875 verified by the numerical results of [34]. Thus, the CDF of
876 $\hat{\xi}_D = \gamma_{R^*D}/\hat{\gamma}_{J^*D}$ can be derived as

$$F_{\hat{\xi}_D}(x) = \sum_{k=0}^{K_r-1} (-1)^k \binom{K_r-1}{k} \frac{K_r}{k+1} \frac{x}{x + \hat{\varphi}_k} \quad (44)$$

877 where $\hat{\varphi}_k = \mathbb{E}\{\gamma_{R^*D}\}/\mathbb{E}\{\hat{\gamma}_{J^*D}\}$.

878 Then, substituting (44) into (11), we have

$$\begin{aligned} & F_{\gamma_{D}^{\text{JRJS}}}(x) \\ & \approx \sum_{n=0}^{N_t-1} \sum_{k=0}^{K_r-1} \sum_{m=0}^{N_t-1-n} \binom{N_t-1}{n} \binom{K_r-1}{k} \binom{N_t-1-n}{m} \\ & \times \frac{(-1)^k K_r \rho_{SR}^{2(N_t-1-n)} (1 - \rho_{SR}^2)^n \varphi_k x^{N_t-1-n-m} e^{-\frac{x}{\bar{\gamma}_{SR}}}}{(N_t-1-n)!(k+1)\bar{\gamma}_{SR}^{N_t-n}(x + \varphi_k)} \\ & \times \int_0^{\infty} \frac{z^{m+1}}{z + \frac{x(x+1)}{x+\varphi_k}} \exp\left(-\frac{z}{\bar{\gamma}_{SR}}\right) dz. \end{aligned} \quad (45)$$

879 Using [33, eq. (3.383.10)], we can obtain the CDF of γ_D^{JRJS} as

$$\begin{aligned} F_{\gamma_D^{\text{JRJS}}}(x) & \approx 1 - \sum_{n=0}^{N_t-1} \sum_{k=0}^{K_r-1} \sum_{m=0}^{N_t-1-n} \binom{N_t-1}{n} \\ & \times \binom{K_r-1}{k} \binom{N_t-1-n}{m} \\ & \times \frac{(-1)^k (K_r+1) \rho_{SR}^{2(N_t-1-n)} (1 - \rho_{SR}^2)^n}{(N_t-1-n)!(k+1)\bar{\gamma}_{SR}^{N_t-n}} \\ & \times \frac{\Gamma(m+2) \hat{\varphi}_k x^{N_t-n} (x+1)^{m+1}}{(x + \hat{\varphi}_k)^{m+2}} \\ & \times \exp\left[-\frac{x(\hat{\varphi}_k - 1)}{\bar{\gamma}_{SR}(x + \hat{\varphi}_k)}\right] \\ & \times \Gamma\left(-m-1, \frac{x(x+1)}{\bar{\gamma}_{SR}(x + \hat{\varphi}_k)}\right). \end{aligned} \quad (46)$$

880 Finally, substituting $x = \gamma_{th}^D$ into (46), we obtain $P_{\text{co}}^{\text{JRJS}}$.

As far as the SOP is considered, we exploit the commonly
used tight upper bound of $\gamma_E^{\text{JRJS}} \geq (1/2) \min\{\gamma_{SR}, \xi_E\}$ to
calculate it, which may be rewritten as

$$\begin{aligned} P_{\text{so}}^{\text{JRJS}} & \approx \Pr\left\{\frac{1}{2} \min\{\gamma_{SR}, \xi_E\} > \gamma_{th}^E\right\} \\ & = [1 - F_{\gamma_{SR}}(2\gamma_{th}^E)] [1 - F_{\xi_E}(2\gamma_{th}^E)]. \end{aligned} \quad (47)$$

Substituting (9) and (25) into (47), we obtain $P_{\text{so}}^{\text{JRJS}}$.

APPENDIX C
PROOF OF LEMMA 3

According to the definition of the RSCP in (18), we can
calculate it by

$$\begin{aligned} P_{RS}^{\text{JRJS}} & = \int_0^{\infty} \left[1 - F_{\xi_D}\left(\gamma_{th}^D + \frac{\gamma_{th}^D(\gamma_{th}^D + 1)}{z}\right)\right] \\ & \times F_{\xi_E}\left(\gamma_{th}^E + \frac{\gamma_{th}^E(\gamma_{th}^E + 1)}{z + \gamma_{th}^D - \gamma_{th}^E}\right) f_{\gamma_{SR^*}}(z + \gamma_{th}^D) dz. \end{aligned} \quad (48)$$

To make the integration mathematically tractable, we invoke
a simple approximation for $F_{\xi_E}(x)$ by treating the AWGN term
"1" in $\xi_E = \gamma_{R^*E}/(\gamma_{J^*E} + 1)$ as part of the stochastic mean
terms. Hence, we have

$$F_{\xi_E}(x) = \frac{x}{x + \hat{\phi}} \quad (49)$$

where $\hat{\phi} = \lambda\eta\sigma_{RE}^2/((1-\lambda)\eta\sigma_{RE}^2 + 1)$.

Then, replacing the corresponding CDFs of the second hop
with $F_{\hat{\xi}_D}(x)$ and $F_{\hat{\xi}_E}(x)$ in (26), the integration can be derived as

$$\begin{aligned} P_{RS}^{\text{JRJS}} & \approx 1 - \sum_{n=0}^{N_t-1} \sum_{k=0}^{K_r-1} \sum_{m=0}^{N_t-1-n} (-1)^k \binom{N_t-1}{n} \\ & \times \binom{K_r-1}{k} \binom{N_t-1-n}{m} \\ & \times \frac{(K_r+1) \rho_{SR}^{2(N_t-1-n)} (1 - \rho_{SR}^2)^n}{(N_t-1-n)!(k+1)\bar{\gamma}_{SR}^{N_t-n}} \\ & \times \frac{\hat{\varphi}_k (\gamma_{th}^D)^{N_t-1-n-m}}{\gamma_{th}^D + \hat{\varphi}_k} \exp\left(-\frac{\gamma_{th}^D}{\bar{\gamma}_{SR}} - \frac{\gamma_{th}^D}{\omega_k \bar{\gamma}_{RD}}\right) \\ & \times \int_0^{\infty} e^{-\frac{z}{\bar{\gamma}_{SR}}} z^{m+1} \left[\frac{1}{z + \theta_{1,k}} - \frac{\hat{\phi} (z + \gamma_{th}^D - \gamma_{th}^E) e^{-\frac{\gamma_{th}^E}{\bar{\gamma}_{RE}}}}{(\gamma_{th}^E + \hat{\phi})(\theta_{1,k} - \theta_2)} \right] \\ & \times \left(\frac{1}{z + \theta_2} - \frac{1}{z + \theta_{1,k}} \right) dz \end{aligned} \quad (50)$$

where $\hat{\varphi}_k$ and $\hat{\phi}$ are introduced by relying on the similar approx-
imation as in Appendix B. Then, using [33, eq. (3.383.10)], we
obtain $P_{R\&S}^{\text{JRJS}}$.

899

REFERENCES

- 900 [1] B. Schneier, "Cryptographic design vulnerabilities," *Computer*, vol. 31,
901 no. 9, pp. 29–33, Sep. 1998.
- 902 [2] A. D. Wyner, "The wire-tap channel," *Bell Syst. Techn. J.*, vol. 54, no. 8,
903 pp. 1355–1387, Oct. 1975.
- 904 [3] I. Csiszar and J. Korner, "Broadcast channels with confidential messages,"
905 *IEEE Trans. Inf. Theory*, vol. IT-24, no. 3, pp. 339–348, May 1978.
- 906 [4] W. K. Harrison, J. Almeida, M. R. Bloch, S. W. McLaughlin, and
907 J. Barros, "Coding for secrecy: An overview of error-control coding techni-
908 ques for physical-layer security," *IEEE Signal Process. Mag.*, vol. 30,
909 no. 5, pp. 41–50, Sep. 2013.
- 910 [5] P. K. Gopala, L. Lai, and H. E. Gamal, "On the secrecy capacity of
911 fading channels," *IEEE Trans. Inf. Theory*, vol. 54, no. 10, pp. 4687–4698,
912 Oct. 2008.
- 913 [6] Y. W. P. Hong, P. C. Lan, and C. C. J. Kuo, "Enhancing physical-layer
914 secrecy in multi-antenna wireless systems: An overview of signal process-
915 ing approaches," *IEEE Signal Process. Mag.*, vol. 30, no. 5, pp. 29–40,
916 Sep. 2013.
- 917 [7] R. Bassily *et al.*, "Cooperative security at the physical layer: A summary
918 of recent advances," *IEEE Signal Process. Mag.*, vol. 30, no. 5, pp. 16–28,
919 Sep. 2013.
- 920 [8] L. Dong, Z. Han, A. P. Petropulu, and H. V. Poor, "Improving wire-
921 less physical layer security via cooperating relays," *IEEE Trans. Signal
922 Process.*, vol. 58, no. 3, pp. 1875–1888, Mar. 2010.
- 923 [9] J. Huang and A. L. Swindlehurst, "Cooperative jamming for secure com-
924 munications in MIMO relay networks," *IEEE Trans. Signal Process.*,
925 vol. 59, no. 10, pp. 4871–4884, Oct. 2011.
- 926 [10] Y. Zou, X. Wang, and W. Shen, "Optimal relay selection for physical-layer
927 security in cooperative wireless networks," *IEEE J. Sel. Areas Commun.*,
928 vol. 31, no. 10, pp. 2099–2111, Oct. 2013.
- 929 [11] Y. Zou, X. Wang, W. Shen, and L. Hanzo, "Security versus reliability
930 analysis of opportunistic relaying," *IEEE Trans. Veh. Technol.*, vol. 63,
931 no. 6, pp. 2653–2661, Jul. 2014.
- 932 [12] I. Krikidis, J. S. Thompson, and S. McLaughlin, "Relay selection
933 for secure cooperative networks with jamming," *IEEE Trans. Wireless
934 Commun.*, vol. 8, no. 10, pp. 5003–5011, Oct. 2009.
- 935 [13] J. Chen, R. Zhang, L. Song, Z. Han, and B. Jiao, "Joint relay and jammer
936 selection for secure two-way relay networks," *IEEE Trans. Inf. Forensic
937 Security*, vol. 7, no. 1, pp. 310–320, Feb. 2012.
- 938 [14] Z. Ding, M. Xu, J. Lu, and F. Liu, "Improving wireless security
939 for bidirectional communication scenarios," *IEEE Trans. Veh. Technol.*,
940 vol. 61, no. 6, pp. 2842–2848, Jul. 2012.
- 941 [15] C. Wang, H. M. Wang, and X. G. Xia, "Hybrid opportunistic relay-
942 ing and jamming with power allocation for secure cooperative net-
943 works," *IEEE Trans. Wireless Commun.*, vol. 14, no. 2, pp. 589–605,
944 Feb. 2015.
- 945 [16] H. Deng, H. M. Wang, W. Guo, and W. Wang, "Secrecy transmission with
946 a helper: To relay or to jam," *IEEE Trans. Inf. Forensic Security*, vol. 10,
947 no. 2, pp. 293–307, Feb. 2015.
- 948 [17] B. He, X. Zhou, and T. D. Abhayapala, "Wireless physical layer secu-
949 rity with imperfect channel state information: A survey," *ZTE Commun.*,
950 vol. 11, no. 3, pp. 11–19, Sep. 2013.
- 951 [18] A. Mukherjee and A. L. Swindlehurst, "Robust beamforming for security
952 in MIMO wiretap channels with imperfect CSI," *IEEE Trans. Signal
953 Process.*, vol. 59, no. 1, pp. 351–361, Jan. 2011.
- 954 [19] J. Zhang and M. C. Gursoy, "Relay beamforming strategies for physical-
955 layer security," in *Proc. CISS*, Princeton, NJ, USA, Mar. 2010, pp. 1–6.
- 956 [20] M. Bloch, J. Barros, M. R. D. Rodrigues, and S. W. McLaughlin, "Wire-
957 less information-theoretic security," *IEEE Trans. Inf. Theory*, vol. 54,
958 no. 6, pp. 2515–2534, Jun. 2008.
- 959 [21] X. Zhou, M. R. McKay, B. Maham, and A. Hjørungnes, "Rethink-
960 ing the secrecy outage formulation: A secure transmission design
961 perspective," *IEEE Commun. Lett.*, vol. 15, no. 3, pp. 302–304,
962 Mar. 2011.
- 963 [22] J. Hu, Y. Cai, N. Yang, and W. Yang, "A new secure transmission scheme
964 with outdated antenna selection," *IEEE Trans. Inf. Forensics Security*,
965 to be published.
- 966 [23] J. Hu, W. Yang, N. Yang, X. Zhou, and Y. Cai, "On-off-based secure trans-
967 mission design with outdated channel state information," *IEEE Trans.
968 Veh. Technol.*, to be published.
- 969 [24] N. E. Wu and H. J. Li, "Effect of feedback delay on secure cooperative
970 networks with joint relay and jammer selection," *IEEE Wireless Commun.
971 Lett.*, vol. 2, no. 4, pp. 415–418, Aug. 2013.
- 972 [25] X. Guan, Y. Cai, and Y. Yang, "Secure transmission design and perfor-
973 mance analysis for cooperation exploring outdated CSI," *IEEE Commun.
974 Lett.*, vol. 18, no. 9, pp. 1637–1640, Sep. 2014.
- [26] L. Wang, S. Xu, W. Yang, W. Yang, and Y. Cai, "Security performance
975 of multiple antennas multiple relaying networks with outdated relay
976 selection," in *Proc. WCSP*, Hefei, China, Oct. 2014, pp. 1–6. 977
- [27] J. Huang and A. L. Swindlehurst, "Buffer-aided relaying for two-hop
978 secure communication," *IEEE Trans. Wireless Commun.*, vol. 14, no. 1,
979 pp. 152–164, Jan. 2015.
- [28] S. I. Kim, I. M. Kim, and J. Heo, "Secure transmission for multiuser relay
980 networks," *IEEE Trans. Wireless Commun.*, vol. 14, no. 7, pp. 3724–3737,
981 Jul. 2015. 982
- [29] Y. Ma, D. Zhang, A. Leith, and Z. Wang, "Error performance of transmit
983 beamforming with delayed and limited feedback," *IEEE Trans. Wireless
984 Commun.*, vol. 8, no. 3, pp. 1164–1170, Mar. 2009. 985
- [30] Z. Rezki, A. Khisti, and M. S. Alouini, "Ergodic secret message capac-
986 ity of the wirechannel with finite-rate feedback," *IEEE Trans. Wireless
987 Commun.*, vol. 13, no. 6, pp. 3364–3379, Jun. 2014. 988
- [31] X. Tang, R. Liu, P. Spasojevic, and H. V. Poor, "On the throughput of
989 secure hybrid-ARQ protocols for Gaussian block-fading channels," *IEEE
990 Trans. Inf. Theory*, vol. 55, no. 4, pp. 1575–1591, Apr. 2009. 991
- [32] H. A. Suraweera, M. Soysa, C. Tellambura, and H. K. Garg, "Performance
992 analysis of partial relay selection with feedback delay," *IEEE Signal
993 Process. Lett.*, vol. 17, no. 6, pp. 531–534, Jun. 2010. 994
- [33] I. S. Gradshteyn and I. M. Ryzhik, *Table of Integrals, Series and Products*,
995 6th ed. San Diego, CA, USA: Academic, 2000. 996
- [34] S. Kim and J. Heo, "Outage probability of interference-limited amplify-
997 and-forward relaying with partial relay selection," in *Proc. IEEE VTC*,
998 Yokohama, Japan, May 2011, pp. 1–5. 999



Lei Wang (S'11) received the B.S. degree in elec- 1001
tronics and information engineering from Central 1002
South University, Changsha, China, in 2004 and 1003
the M.S. degree in communications and informa- 1004
tion systems from PLA University of Science and 1005
Technology, Nanjing, China, in 2011. He is currently 1006
working toward the Ph.D. degree in communications 1007
and information systems with PLA University of 1008
Science and Technology. 1009

His current research interests include cooperative 1010
communications, signal processing in communica- 1011
tions, and physical layer security. 1012



Yueming Cai (M'05–SM'12) received the B.S. 1013
degree in physics from Xiamen University, 1014
Xiamen, China, in 1982 and the M.S. degree in 1015
microelectronics engineering and the Ph.D. degree in 1016
communications and information systems from 1017
Southeast University, Nanjing, China, in 1988 and 1018
1996, respectively. 1019

He is currently with the College of Communica- 1020
tions Engineering, PLA University of Science and 1021
Technology, Nanjing, China. His current research 1022
interests include multiple-input–multiple-output sys- 1023
tems, orthogonal frequency-division multiplexing systems, signal processing in 1024
communications, cooperative communications, and wireless sensor networks. 1025

1026
1027
1028
AQ6 1029
1030
1031
1032
1033
1034
1035
1036

Yulong Zou (SM'13) received the B.Eng. degree in information engineering from Nanjing University of Posts and Telecommunications (NUPT), Nanjing, China, in July 2006; the Ph.D. degree in electrical engineering from Stevens Institute of Technology, Hoboken, NJ, USA, in May 2012; and the Ph.D. degree in signal and information processing from NUPT in July 2012.

He is currently a Professor with NUPT. His research interests span a wide range of topics in wireless communications and signal processing, including cooperative communications, cognitive radio, wireless security, and energy-efficient communications.

Dr. Zou has been a symposium chair, a session chair, and a technical program committee member for several IEEE-sponsored conferences, including the IEEE Wireless Communications and Networking Conference, the IEEE Global Communications Conference, the IEEE International Conference on Communications, the IEEE Vehicular Technology Conference, and the International Conference on Communications in China. He serves on the editorial board of *IEEE Communications Surveys and Tutorials*, *IEEE Communications Letters*, *IET Communications*, and the *EURASIP Journal on Advances in Signal Processing*. He was a received the 2014 IEEE Communications Society Asia-Pacific Best Young Researcher award.

1049
1050
1051
1052
AQ7 1053
1054
1055
1056
1057
1058

Weiwei Yang (S'08–M'12) received the B.S., M.S., and Ph.D. degrees from PLA University of Science and Technology, Nanjing, China, in 2003, 2006, and 2011, respectively.

He is currently with the College of Communications Engineering, PLA University of Science and Technology. His research interests are orthogonal frequency-domain multiplexing systems, signal processing in communications, cooperative communications, cognitive networks, and network security.



Lajos Hanzo (M'91–SM'92–F'04) received the M.S. degree in electronics and the Ph.D. degree from the Technical University of Budapest, Budapest, Hungary, in 1976 and 1983, respectively; the D.Sc. degree from the University of Southampton, Southampton, U.K., in 2004; and the "Doctor Honoris Causa" degree from the Technical University of Budapest in 2009.

During his 38-year career in telecommunications, he has held various research and academic posts in Hungary, Germany, and the U.K. Since 1986, he has

been with the School of Electronics and Computer Science, University of Southampton, where he holds the Chair in Telecommunications. He is currently directing an academic research team, working on a range of research projects in the field of wireless multimedia communications sponsored by industry, the Engineering and Physical Sciences Research Council (EPSRC), the European Research Council's Advanced Fellow Grant, and the Royal Society's Wolfson Research Merit Award. During 2008–2012, he was a Chaired Professor with Tsinghua University, Beijing, China. He is an enthusiastic supporter of industrial and academic liaison and offers a range of industrial courses. He has successfully supervised about 100 Ph.D. students, coauthored 20 John Wiley/IEEE Press books on mobile radio communications totaling in excess of 10 000 pages, and published more than 1400 research entries on IEEE Xplore.

Dr. Hanzo is a Fellow of the Royal Academy of Engineering, the Institution of Engineering and Technology, and the European Association for Signal Processing. He is also a Governor of the IEEE Vehicular Technology Society. During 2008–2012, he was the Editor-in-Chief of IEEE Press. He has served as the Technical Program Committee Chair and the General Chair of IEEE conferences, has presented keynote lectures, and has received a number of distinctions. His published work has more than 20 000 citations. Further information on research in progress and associated publications is available at <http://www-mobile.ecs.soton.ac.uk>.

AUTHOR QUERIES

AUTHOR PLEASE ANSWER ALL QUERIES

AQ1 = RV was expanded as “random variable.” Please check if appropriate. Otherwise, please make the necessary changes.

AQ2 = Equations (29) and (30) are missing in the document. Please check.

AQ3 = Please provide publication update in Ref [22].

AQ4 = Please provide publication update in Ref [23].

AQ5 = Current affiliation of author Yueming Cai was provided as captured from the first footnote. Please check if appropriate. Otherwise, please make the necessary changes.

AQ6 = Please confirm that Dr. Zou has received two Ph.D. degrees.

AQ7 = Current affiliation of author Weiwei Yang was provided as captured from the first footnote. Please check if appropriate. Otherwise, please make the necessary changes.

END OF ALL QUERIES

Joint Relay and Jammer Selection Improves the Physical Layer Security in the Face of CSI Feedback Delays

Lei Wang, *Student Member, IEEE*, Yueming Cai, *Senior Member, IEEE*, Yulong Zou, *Senior Member, IEEE*, Weiwei Yang, *Member, IEEE*, and Lajos Hanzo, *Fellow, IEEE*

Abstract—We enhance the physical layer security (PLS) of amplify-and-forward (AF) relaying networks with the aid of joint relay and jammer selection (JRJS), despite the deleterious effect of channel state information (CSI) feedback delays. Furthermore, we conceive a new outage-based characterization approach for the JRJS scheme. The traditional best relay selection (TBRS) is also considered as a benchmark. We first derive closed-form expressions of both the connection outage probability (COP) and the secrecy outage probability (SOP) for both the TBRS and JRJS schemes. Then, a reliable and secure connection probability (RSCP) is defined and analyzed for characterizing the effect of the correlation between the COP and the SOP introduced by the corporate source-relay link. The reliability-security ratio (RSR) is introduced for characterizing the relationship between the reliability and the security through asymptotic analysis. Moreover, the concept of effective secrecy throughput is defined as the product of the secrecy rate and of the RSCP for the sake of characterizing the overall efficiency of the system, as determined by the transmit SNR, the secrecy codeword rate, and the power sharing ratio between the relay and the jammer. The impact of the direct source-eavesdropper link and additional performance comparisons with respect to other related selection schemes are also included. Our numerical results show that the JRJS scheme outperforms the TBRS method both in terms of the RSCP and in terms of its effective secrecy throughput, but it is more sensitive to the feedback delays. Increasing the transmit signal-to-noise ratio (SNR) will not always improve the overall throughput. Moreover, the RSR results demonstrate that, upon reducing the CSI feedback delays, the reliability improves more substantially than the security degrades, implying an overall improvement in terms of the security-reliability tradeoff. Additionally, the secrecy throughput loss due to the second-hop feedback delay is more pronounced than that due to the first-hop one.

Index Terms—Effective secrecy throughput, feedback delay, physical layer security (PLS), relay and jammer selection, reliability and security.

I. INTRODUCTION

WIRELESS communications systems are particularly vulnerable to security attacks because of the inherent openness of the transmission medium. Traditionally, the information privacy of wireless networks has been focused on the higher layers of the protocol stack employing cryptographically secure schemes. However, these methods typically assume a limited computing power for the eavesdroppers and exhibit inherent vulnerabilities in terms of the inevitable secret key distribution and management [1]. In recent years, physical layer security (PLS) has emerged as a promising technique of improving the confidentiality wireless communications, which exploits the time-varying properties of fading channels, instead of relying on conventional cryptosystems. The pivotal idea of PLS solutions is to exploit the dynamically fluctuating random nature of radio channels for maximizing the uncertainty concerning the source messages at the eavesdropper [2], [3].

To achieve this target, several PLS-enhancement approaches have been proposed in the literature, including secrecy-enhancing channel coding [4], secure on-off transmission designs [5], secrecy-improving beamforming (BF)/precoding, and artificial-noise-aided techniques relying on multiple antennas [6], as well as secure relay-assisted transmission techniques [7]. Specifically, apart from improving the reliability and coverage of wireless transmissions, user cooperation also has a great potential in terms of enhancing the wireless security against eavesdropping attacks. There has been a growing interest in improving the security of cooperative networks at the physical layer [8]–[14]. To explore the spatial diversity potential of the relaying networks and to boost the secrecy capacity (the difference between the channel capacity of the legitimate main link and that of the eavesdropping link), most of the existing work has been focused on secrecy-enhancing BF [8], [9], as well as on intelligent relay node/jammer node (RN/JN) selection, etc. Notably, given the availability of multiple relays, appropriately designed RN/JN selection is capable of achieving a significant security improvement for cooperative networks, which is emerging as a promising research topic. In particular, Zou *et al.* investigated both amplify-and-forward (AF)- and decode-and-forward (DF)-based optimal relay selection conceived for

Manuscript received October 2, 2014; revised February 25, 2015 and July 27, 2015; accepted September 8, 2015. This work was supported in part by the National Natural Science Foundation of China under Grant 61371122, Grant 61471393, and Grant 61501512 and in part by the Natural Science Foundation of Jiangsu Province under Grant BK20150718 and Grant BK20150040. The review of this paper was coordinated by Prof. M. C. Gursoy.

L. Wang, Y. Cai, and W. Yang are with the College of Communications Engineering, PLA University of Science and Technology, Nanjing 210007, China (e-mail: csu-wl@163.com; caiym@vip.sina.com; yww_1010@aliyun.com).

Y. Zou is with the School of Telecommunications and Information Engineering, Nanjing University of Posts and Telecommunications, Nanjing 210003, China (e-mail: yulong.zou@njupt.edu.cn).

L. Hanzo is with the Department of Electronics and Computer Science, University of Southampton, Southampton SO17 1BJ, U.K. (e-mail: lh@ecs.soton.ac.uk).

Color versions of one or more of the figures in this paper are available online at <http://ieeexplore.ieee.org>.

Digital Object Identifier 10.1109/TVT.2015.2478029

83 enhancing the PLS in cooperative wireless networks [10], [11],
 84 where the global channel state information (CSI) of both the
 85 main link and the eavesdropping link was assumed to be avail-
 86 able. Similarly, jamming techniques, which impose artificial
 87 interference on the eavesdropper, have also attracted substantial
 88 attention [12]–[14]. More specifically, several sophisticated
 89 joint relay and jammer selection (JRJS) schemes were proposed
 90 in [12], where the beneficially selected relay increases the reli-
 91 ability of the main link, whereas the carefully selected jammer
 92 imposes interference on the eavesdropper and simultaneously
 93 protects the legitimate destination from interference. In [13]
 94 and [14], cooperative jamming has been studied in the context
 95 of bidirectional scenarios, and efficient RN/JN selection criteria
 96 have been developed for achieving improved secrecy rates with
 97 the aid of multiple relays. Furthermore, more effective relaying
 98 and jamming schemes, when taking the information leakage
 99 of the source–eavesdropper link into consideration, have been
 100 presented lately in [15] and [16].

101 Nevertheless, an idealized assumption of the previously re-
 102 ported research on PLS is the availability of perfect channel
 103 state information (CSI), which is regarded as a stumbling block
 104 in the way of invoking practical secrecy-enhancing Wyner
 105 coding, on–off design, BF/precoding, and RN/JN selection.
 106 However, this idealized simplifying assumption is not realistic,
 107 since practical channel estimation imposes CSI imperfections,
 108 which are aggravated by the feedback delay, limited-rate feed-
 109 back, and channel estimation errors (CEEs) [17]. Generally, the
 110 related research has been focused on the issues of robust secure
 111 BF design from an average secrecy-rate-based optimization
 112 perspective for point-to-point multiantenna aided channels and
 113 relay channels [18], [19] supporting delay-tolerant systems.
 114 For systems imposing stringent delay constraints, particularly
 115 in imperfect CSI scenarios, perfect secrecy cannot always be
 116 achieved. Hence, the secrecy-outage-based characterization of
 117 systems is more appropriate, which provides a probabilistic
 118 performance measure of secure communication. The concept
 119 of secrecy outage was adopted in [20] for characterizing the
 120 probability of having both reliable and secure transmission,
 121 which, however, is inapplicable for the imperfect CSI case and
 122 fails to distinguish a connection outage from the secrecy outage.
 123 In [21], an alternative secrecy outage formulation is proposed
 124 for characterizing the attainable security level and provided
 125 a general framework for designing transmission schemes that
 126 meet specific target security requirements. To quantify both the
 127 reliability and security performance at both the legitimate and
 128 eavesdropper nodes separately, two types of outages, namely,
 129 the connection outage probability (COP) and the secrecy outage
 130 probability (SOP) are introduced. Then, considering the impact
 131 of time delay caused by the antenna selection process at the
 132 legitimate receiver, Hu *et al.* [22] proposed a new secure
 133 transmission scheme in the multiinput multioutput multieaves-
 134 dropper wiretap channel. Much recently, considering the out-
 135 dated CSI from the legitimate receiver, a new secure on–off
 136 transmission scheme was proposed for enhancing the secrecy
 137 throughput in [23].

138 Moreover, prior studies of the outage-based secure trans-
 139 mission design are limited to single-antenna-assisted single-
 140 hop systems and have not been considered for cooperative

relaying systems. Hence, the issues of secure transmissions 141
 over cooperative relaying channels expressed in terms of the 142
 SOP, COP, and secrecy throughput constitute an open problem. 143
 On the other hand, apart from CEE, the CSI feedback delay 144
 results in critical challenges for the PLS of cooperative relaying 145
 systems, particularly when considering the specifics of RN/JN 146
 selection. In [15], the effects of outdated CSI knowledge con- 147
 cerning the legitimate links on the ergodic secrecy rate achieved 148
 by the proposed secure transmission strategy in the context 149
 of DF relaying is investigated. The impact of CSI feedback 150
 delay on the secure relay and jammer selection conceived for 151
 DF relaying was investigated in [24], albeit only in terms 152
 of the SOP. In our previous study [25], we considered the 153
 secure transmission design and the secrecy performance of an 154
 opportunistic DF system relying on outdated CSI, where only a 155
 single relay is invoked. Additionally, during the revision of this 156
 work, we investigated the security performance for outdated AF 157
 relay selection in [26]. Therefore, in this treatise, we extend 158
 our investigations to the PLS of multiple AF relaying assisted 159
 networks relying on RN/JN selection. 160

Explicitly, we focus our attention on the outage-based char- 161
 acterization of secure transmissions in cooperative relay-aided 162
 networks relying on realistic CSI feedback delay. To exploit the 163
 multirelay induced diversity gain and the associated jamming 164
 capabilities, joint AF relay node and jammer node selection 165
 is employed by the relay–destination link. We assume that, in 166
 line with the practical reality, the instantaneous eavesdropper’s 167
 CSI is unavailable at the legitimate transmitter and that the 168
 RN/JN selections are performed based on the outdated CSI of 169
 the main links. Two types of cooperative strategies are invoked 170
 by our cooperative network operating under secrecy constraints, 171
 namely, the traditional best relay selection (TBRS) strategy and 172
 the JRJS strategy. Specifically, the main contributions of this 173
 paper can be summarized as follows. 174

- We develop an outage-based characterization for quan- 175
 tifying both the reliability and security performance of 176
 a two-hop AF relaying system. Specifically, in contrast 177
 to [21] and [22], we propose the novel definition of 178
 the reliable and secure connection probability (RSCP). 179
 Explicitly, closed-form expressions of the COP, the SOP, 180
 and the RSCP are derived for both the TBRS and for our 181
 JRJS strategies. Numerical results demonstrate that the 182
 JRJS scheme outperforms the TBRS scheme in terms of 183
 its RSCP. 184
- We also introduce the reliability–security ratio (RSR) 185
 for characterizing their direct relationship by a single 186
 parameter through the asymptotic analysis of the COP and 187
 the SOP in the high-SNR regime. We derive the RSR for 188
 both the TBRS and JRJS strategies for investigating the 189
 effect of secrecy codeword rate setting, as well as that 190
 of the feedback delay and that of the power sharing ratio 191
 between the relay and the jammer on the RSR. 192
- We then modify the definition of effective secrecy 193
 throughput by multiplying the secrecy rate with the RSCP, 194
 which results in an optimization problem of the trans- 195
 mit signal-to-noise ratio (SNR), secrecy codeword rate, 196
 and power sharing between the relay and the jammer. 197
 198

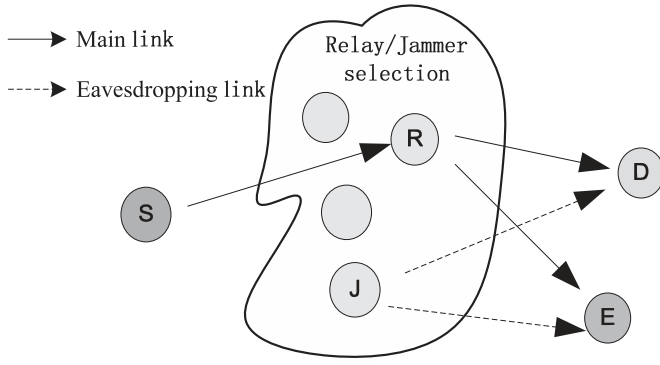


Fig. 1. Cooperative relaying network assisted by multiple relays in the presence of an eavesdropper.

199 It is shown that, compared with the TBRs strategy,
 200 JRJS achieves a significantly higher effective secrecy
 201 throughput, and the corresponding throughput loss is
 202 more sensitive to feedback delays. The impact of the direct
 203 source–eavesdropper link and additional throughput
 204 performance comparisons with respect to other related
 205 selection schemes are further discussed.

206 The remainder of this paper is organized as follows.
 207 Section II introduces our system model and describes both
 208 the TBRs and our JRJS strategies. In Sections III and IV,
 209 we present the mathematical framework of our performance
 210 analysis both for the TBRs strategy and for the JRJS strategy,
 211 respectively, including the COP, the SOP, the RSCP, the RSR,
 212 and the effective secrecy throughput. Our numerical results
 213 and discussions are provided in Section V. Finally, Section VI
 214 presents our concluding remarks.

215 II. SYSTEM MODEL

216 A. System Description

217 Consider a cooperative relaying network consisting of a
 218 source S , a destination D , K_r relays R_k , $k = 1, \dots, K_r$, and
 219 an eavesdropper E , as shown in Fig. 1, where all nodes are
 220 equipped with a single transmit antenna (TA), except for the
 221 source, which has N_t TAs. The cooperative relay architecture
 222 in Fig. 1 is generally applicable to diverse practical wireless
 223 systems in the presence of an eavesdropper, including the
 224 family of wireless sensor networks (WSNs), mobile ad hoc
 225 networks (MANETs), and the long-term evolution advanced
 226 cellular systems [11].

227 To exploit the diversity potential of multiple relay nodes over
 228 independently fading channels, AF relay/jammer selection is
 229 employed. All relays operate in the half-duplex AF mode, and
 230 data transmission is performed in two phases. More particu-
 231 larly, during the broadcast phase, the source node transmits its
 232 signal to a selected relay with the aid of BF, which is invoked
 233 for forwarding the signal received from S to D . An inherent
 234 assumption is that the transmit BF weights are based on the
 235 CSI estimates quantified and fed back by the selected relay.
 236 During the cooperative phase, a pair of appropriately selected
 237 relays transmit toward D and E , respectively. A conventional

relay (denoted by R^*) forwards the source’s message to the
 238 destination. Another relay (denoted by J^*) operates in the
 239 “jammer mode” and imposes intentional interference upon E in
 240 order to confuse it. However, D is unable to mitigate the artificial
 241 interference emanating from the jammer node J^* due to its
 242 critical secrecy constraints [12]. It should be noted that both
 243 the process of RN/JN selection and the feedback of the transmit
 244 BF weights from R^* to S may impose a time lag between the
 245 data transmission and the channel estimation. These time delays
 246 are denoted by $T_{d_{SR}}$ and $T_{d_{RD}}$, respectively. Furthermore, we
 247 assume that the BF and RN/JN selection process is based
 248 on the perfectly estimated but outdated CSI. We employ the
 249 first-order autoregressive outdated CSI model of [20], while
 250 relying on the correlation coefficients of $\rho_{SR} = J_0(2\pi f_d T_{d_{SR}})$
 251 and $\rho_{RD} = J_0(2\pi f_d T_{d_{RD}})$ for the two hops, where $J_0(\cdot)$ is
 252 the zero-order Bessel function of the first kind, and f_d is the
 253 Doppler frequency.
 254

A slow flat block Rayleigh fading environment is assumed,
 255 where the channel remains static for the coherence interval (one
 256 slot) and changes independently in different coherence inter-
 257 vals, as denoted by $h_{i,j} \sim \mathcal{CN}(0, \sigma_{i,j}^2)$, $i, j \in \{S, R, J, D, E\}$.
 258 The direct communication links are assumed to be unavailable
 259 due to the presence of obstructions between S and D , as well
 260 as the eavesdropper.¹ This assumption follows the rationale of
 261 [12] and has been routinely exploited in previous literature (see
 262 [27] and [28] and the references therein), where the source
 263 and relays belong to the same cluster, whereas the destination
 264 and the eavesdropper are located in another. More specifically,
 265 this assumption is particularly valid in networks with broadcast
 266 and unicast transmission, where each terminal is a legitimate
 267 receiver for one signal and acts as an eavesdropper for some
 268 other signal. Therefore, the security concerns are only related
 269 to the cooperative relay-aided channel. Furthermore, additive
 270 white Gaussian noise (AWGN) is assumed with zero mean
 271 and unit variance N_0 . Let P_i be the transmit power of node
 272 i , and the instantaneous SNR of the $i \rightarrow j$ link is given by
 273 $\gamma_{i,j} = P_i |h_{i,j}|^2 / N_0$.
 274

We employ the constant-rate Wyner coding scheme for con-
 275 structing wiretap codes of [2] to meet the PLS requirements
 276 due to the fact that the accurate global CSI is not available.
 277 Let $\mathbb{C}(R_0, R_s, N)$ denote the set of all possible Wyner codes
 278 of length N , where R_0 is the codeword transmission rate, and
 279 R_s is the confidential information rate ($R_0 > R_s$). The positive
 280 rate difference $R_e = R_0 - R_s$ is the cost of providing secrecy
 281 against the eavesdropper. A confidential message is encoded
 282 into a codeword at S and then transmitted to D .
 283

284 B. Secure Transmission

In the broadcast phase, S transmits its BF signal $s(t)$ to the
 285 selected relay R^* , where the relay selection is performed
 286 before data transmission commences, and the selection cri-
 287 terion will be detailed later in the context of the cooper-
 288 ative phase. The transmit BF vector $\mathbf{w}(t|T_d)$ is calculated
 289 using the perfectly estimated but outdated CSI given by
 290

¹The case when the $S \rightarrow E$ link is introduced will be investigated separately in Section VI.

291 $\mathbf{w}(t|T_{d_{SR}}) = \mathbf{h}_{SR^*}^H(t - T_d)/|\mathbf{h}_{SR^*}(t - T_{d_{SR}})|$ [29], where we
 292 have $\mathbf{h}_{SR^*}(t) = [h_{SR^*,1}(t), \dots, h_{SR^*,N_t}(t)]^T$, and the signal
 293 received by the relay R^* can be written as

$$y_{R^*}(t) = \sqrt{P_s} \mathbf{w}(t|T_d) \mathbf{h}_{SR^*}(t) s(t) + n_{SR^*}(t) \quad (1)$$

294 where $n_{SR^*}(t)$ is the AWGN at the relay. Then, we can
 295 define the received SNR at the relay node as $\gamma_{SR} =$
 296 $P_S |\mathbf{w}(t|T_{d_{SR}}) \mathbf{h}_{SR^*}(t)|^2 / N_0$.

297 In the cooperative phase, we consider two RN/JN selection
 298 schemes performed by D : relay selection without jamming
 299 and JRJS.

300 1) *Traditional Best Relay Selection*: The first category of so-
 301 lutions does not involve a jamming process, and therefore, only
 302 a conventional relay accesses the channel during the second
 303 phase of the protocol. The relay selection process is performed
 304 based on the highest instantaneous SNR of the second hop,
 305 which is formulated as

$$R^* = \arg \max_{R_k \in \mathcal{R}} \left\{ \frac{\tilde{\gamma}_{R_k D}}{\mathbb{E}[\gamma_{R_k E}]} = \frac{P_R |\tilde{h}_{R_k D}(t - T_d)|^2}{N_0 \mathbb{E}[\gamma_{R_k E}]} \right\} \quad (2)$$

306 where $\tilde{\gamma}_{R_k D}$ is the instantaneous SNR in the relay selection
 307 process, and $\mathbb{E}[\gamma_{R_k E}]$ denotes the average SNR at E . We can
 308 model $\gamma_{R_k D}$ and $\tilde{\gamma}_{R_k D}$ as two gamma distributed random
 309 variables having the correlation factor of ρ_{RD}^2 .

310 During the second phase, the received signal $y_{R^*}(t)$
 311 is multiplied by a time-variant AF-relay gain G and
 312 retransmitted to D , where we have $G =$
 313 $\sqrt{P_R / (P_S |\mathbf{w}_{\text{opt}}(t|T_{d_{SR}}) \mathbf{h}_{SR^*}(t)|^2 + N_0)}$. After further math-
 314 ematical manipulations, the mutual information (MI) between
 315 S and D , as well as the eavesdropper, can be written as

$$I_D^{\text{TBRS}} = \frac{1}{2} \log(1 + \gamma_D^{\text{TBRS}}) = \frac{1}{2} \log \left(1 + \frac{\gamma_{SR} \gamma_{R^* D}}{\gamma_{SR} + \gamma_{R^* D} + 1} \right) \quad (3)$$

$$I_E^{\text{TBRS}} = \frac{1}{2} \log(1 + \gamma_E^{\text{TBRS}}) = \frac{1}{2} \log \left(1 + \frac{\gamma_{SR} \gamma_{R^* E}}{\gamma_{SR} + \gamma_{R^* E} + 1} \right). \quad (4)$$

316 2) *Joint Relay and Jammer Selection*: Similarly, consider-
 317 ing the unavailability of the instantaneous CSI regarding the
 318 eavesdropper, we adopt a suboptimal RN/JN selection metric
 319 conditioned on the outdated CSI as

$$R^* = \arg \max_{R_k \in \mathcal{R}} \left\{ \frac{\tilde{\gamma}_{R_k D}}{\mathbb{E}[\gamma_{R_k E}]} \right\} \quad (5)$$

$$J^* = \arg \min_{R_k \in \mathcal{R} - R^*} \left\{ \frac{\tilde{\gamma}_{R_k D}}{\mathbb{E}[\gamma_{R_k E}]} \right\}$$

320 where J^* is selected for minimizing the interference imposed
 321 on D .

322 It should be noted that, to have the same transmit power as
 323 that of the TBRS case, we assume that $P_{R^*} + P_{J^*} = P_R$ for
 324 our JRJS strategy and introduce $\lambda = P_{R^*} / (P_{R^*} + P_{J^*})$ as the

ratio of the relay's transmit power to the total power required
 by the active relay and jammer. 326

In the cooperative phase, R^* will also amplify the received
 signal $y_{R^*}(t)$ by G and forward it to D . At the same time, the
 jammer J^* will generate intentional interference to confuse E ,
 which will also cause interference at D . Consequently, the MI
 between the terminals is given by 331

$$I_D^{\text{JRJS}} = \frac{1}{2} \log(1 + \gamma_D^{\text{JRJS}}) = \frac{1}{2} \log \left(1 + \frac{\gamma_{SR} \frac{\gamma_{R^* D}}{\gamma_{J^* D} + 1}}{\gamma_{SR} + \frac{\gamma_{R^* D}}{\gamma_{J^* D} + 1} + 1} \right) \quad (6)$$

$$I_E^{\text{JRJS}} = \frac{1}{2} \log(1 + \gamma_E^{\text{JRJS}}) = \frac{1}{2} \log \left(1 + \frac{\gamma_{SR} \frac{\gamma_{RE}}{\gamma_{JE} + 1}}{\gamma_{SR} + \frac{\gamma_{RE}}{\gamma_{JE} + 1} + 1} \right). \quad (7)$$

Remark 1: Generally, the optimal RN/JN selection scheme
 should take into account the global SNR knowledge set
 $\{\gamma_{SR}, \gamma_{RD}, \gamma_{RE}\}$. However, given the potentially excessive
 implementational complexity overhead of the optimal selection
 schemes and the unavailability of the global CSI, we employ
 suboptimal selection schemes as in [12].² Furthermore, it is
 commonly assumed that the average SNR of the eavesdropper
 is available at the transmitter, which seems, somehow, not
 reasonable. However, as stated in most of the literature, such as
 [12]–[22], [24]–[28], and [30], provided that the eavesdropper
 belongs to the network, which is also the case in our paper,
 the related assumption might still be deemed reasonably. Addi-
 tionally, as in [8], [11], [12], and [24], for mathematical conve-
 nience, we assume that the relaying channels are independent
 and identically distributed and that we have $\mathbb{E}[\gamma_{SR_k}] = \bar{\gamma}_{SR}$,
 $\mathbb{E}[\gamma_{R_k D}] = \bar{\gamma}_{RD}$, and $\mathbb{E}[\gamma_{R_k E}] = \bar{\gamma}_{RE}$. The distances between
 the relays are assumed to be much smaller than the distances
 between relays and source/destination/eavesdropper; hence, the
 corresponding path losses among the different relays are ap-
 proximately the same. This assumption is reasonable both for
 WSNs and for MANETs associated with a symmetric clustered
 relay configuration, and it may be also satisfied as valid by
 classic cellular systems in a statistical sense [11]. 354

III. SECURE TRANSMISSION WITHOUT JAMMING 355

Here, we endeavor to characterize both the reliability and
 security performance comprehensively of the TBRS scheme.
 We first derive closed-form expressions for both the COP and
 the SOP. Then, the RSR is introduced through the asymptotic
 analysis of the COP and the SOP. Furthermore, we propose
 the novel definition of the RSCP and the effective secrecy
 throughput. 362

²To further alleviate the cooperation-related overhead, the selection criterion is based on the $R \rightarrow D$ link, since the second hop plays a dominant role in determining the received SNR, because the first hop corresponds to a multiple-input-single-output channel with the aid of multiple antennas, and hence, it is more likely to be better than the second hop. The optimal selection based on both hops is beyond the scope of this work.

363 A. COP and SOP

364 When the perfect instantaneous CSI of the eavesdropper's
 365 channel and even the legitimate users' channel is unavailable,
 366 alternative definitions of the outage probability may be adopted
 367 for the statistical characterization of the attainable secrecy
 368 performance, particularly for delay-limited applications. Based
 369 on [31, Def. 2], perfect secrecy cannot be achieved, when we
 370 have $R_e < I_E$, where I_E denotes the MI between the source
 371 and the eavesdropper. Encountering this event is termed as a
 372 secrecy outage. Furthermore, the destination is unable to flaw-
 373 lessly decode the received codewords when $R_0 > I_D$, which is
 374 termed as a connection outage. The grade of reliability and the
 375 grade of security maintained by a transmission scheme may be
 376 then quantified by the COP and the SOP, respectively.

377 We continue by presenting our preliminary results versus the
 378 point-to-point SNRs. Let us denote the cumulative distribution
 379 function (CDF) and the probability density function (PDF) of a
 380 random variable X by $F_X(x)$ and $f_X(x)$, respectively. On one
 381 hand, the PDF of γ_{SR} using [29, eq. (15)] is given by

$$f_{\gamma_{SR}}(x) = \sum_{n=0}^{N_t-1} \binom{N_t-1}{n} \frac{\rho_{SR}^{2(N_t-1-n)} (\bar{\gamma}_{SR} (1 - \rho_{SR}^2))^n}{\bar{\gamma}_{SR}^{N_t} (N_t - 1 - n)!} \times x^{N_t-1-n} e^{-\frac{x}{\bar{\gamma}_{SR}}} \quad (8)$$

382 whereas its CDF is given by

$$F_{\gamma_{SR}}(x) = 1 - \sum_{n=0}^{N_t-1} \sum_{m=0}^{N_t-1-n} \binom{N_t-1}{n} \times \frac{\rho_{SR}^{2(N_t-1-n)} (1 - \rho_{SR}^2)^n}{m! \bar{\gamma}_{SR}^m} x^m e^{-\frac{x}{\bar{\gamma}_{SR}}}. \quad (9)$$

383 On the other hand, for the instantaneous SNR of the $R \rightarrow$
 384 D hop, according to the principles of concomitants or induced
 385 order statistics, the CDF of γ_{R^*D} can be derived as in [32]

$$F_{\gamma_{R^*D}}(y) = K_r \sum_{k=0}^{K_r-1} (-1)^k \binom{K_r-1}{k} \frac{1 - e^{-\frac{-(k+1)y}{k(1-\rho_{RD}^2)+1} \bar{\gamma}_{RD}}}{k+1}. \quad (10)$$

386 Thus, the COP of the TBRS strategy is given by

$$P_{co}^{\text{TBRS}}(R_0) = \Pr [I_D^{\text{TBRS}} < R_0] = F_{\gamma_D^{\text{TBRS}}}(\gamma_{th}^D) \quad (11)$$

387 where we have $\gamma_{th}^D = 2^{2R_0} - 1$, and the CDF of γ_D^{TBRS} can be
 388 calculated as

$$F_{\gamma_D^{\text{TBRS}}}(x) = 1 - \int_0^\infty \left[1 - F_{\gamma_{R^*D}}\left(\frac{xz + x(x+1)}{z}\right) \right] f_{\gamma_{SR^*}}(z+x) dz. \quad (12)$$

389 Consequently, by substituting (8) and (10) into (12) and using
 390 [33, eq. (3.471.9)], we arrive at a closed-form expression for

$F_{\gamma_D^{\text{TBRS}}}(x)$ as

391

$$F_{\gamma_D^{\text{TBRS}}}(x) = 1 - 2 \sum_{n=0}^{N_t-1} \sum_{k=0}^{K_r-1} \sum_{m=0}^{N_t-1-n} (-1)^k K_r \binom{N_t-1}{n} \times \binom{K_r-1}{k} \binom{N_t-1-n}{m} \times \frac{\rho_{SR}^{2(N_t-1-n)} (1 - \rho_{SR}^2)^n x^{N_t-1-n-m}}{(N_t-1-n)! (k+1) \bar{\gamma}_{SR}^{N_t-n}} \times \left[\frac{\bar{\gamma}_{SR} x(x+1)}{\omega_k \bar{\gamma}_{RD}} \right]^{\frac{m+1}{2}} \times e^{-\left(\frac{\bar{\gamma}_{SR} + \omega_k \bar{\gamma}_{RD}}{\omega_k \bar{\gamma}_{SR} \bar{\gamma}_{RD}}\right) x} K_{m+1} \left(2 \sqrt{\frac{x(x+1)}{\omega_k \bar{\gamma}_{SR} \bar{\gamma}_{RD}}} \right) \quad (13)$$

where we have $\omega_k = (k(1 - \rho_{RD}^2) + 1)/(k+1)$. Then, by
 substituting $x = \gamma_{th}^D$ into (13), we obtain P_{co}^{TBRS} .

Furthermore, the SOP of the TBRS strategy may be expressed as

$$P_{so}^{\text{TBRS}}(R_0, R_s) = \Pr [I_E^{\text{TBRS}} > R_0 - R_s] = 1 - F_{\gamma_E^{\text{TBRS}}}(\gamma_{th}^E) \quad (14)$$

where we have $\gamma_{th}^E = 2^{2(R_0 - R_s)} - 1$. Similarly, we may calcu-
 late the CDF of γ_E^{TBRS} in (14) as

396

$$F_{\gamma_E^{\text{TBRS}}}(x) = 1 - 2 \sum_{n=0}^{N_t-1} \sum_{m=0}^{N_t-1-n} \binom{N_t-1}{n} \binom{N_t-1-n}{m} \times \frac{\rho_{SR}^{2(N_t-1-n)} (1 - \rho_{SR}^2)^n x^{N_t-1-n-m}}{(N_t-1-n)! \bar{\gamma}_{SR}^{N_t-n}} \times \left[\frac{\bar{\gamma}_{SR} x(x+1)}{\bar{\gamma}_{RE}} \right]^{\frac{m+1}{2}} \times e^{-\left(\frac{\bar{\gamma}_{SR} + \bar{\gamma}_{RE}}{\bar{\gamma}_{SR} \bar{\gamma}_{RE}}\right) x} K_{m+1} \left(2 \sqrt{\frac{x(x+1)}{\bar{\gamma}_{SR} \bar{\gamma}_{RE}}} \right). \quad (15)$$

Then, by substituting $x = \gamma_{th}^E$ into (15), we can derive P_{so}^{TBRS} .

The COP and the SOP in (11) and (14) characterize the at-
 tainable reliability and security performance, respectively, and
 can be regarded as the detailed requirements of accurate system
 design. From the definition of COP and SOP, it is clear that
 the reliability of the main link can be improved by increasing
 the transmit SNR (or decreasing its data rate) to reduce the
 COP, which unfortunately increases the risk of eavesdropping.
 Thus, a tradeoff between reliability and security may be struck,
 despite the fact that closed-form expressions cannot be obtained
 as in [11]. Furthermore, we denote the minimal reliability and
 security requirements by ν and δ , where the feasible range of
 the reliability constraint is $0 < \nu < 1$. Bearing in mind that
 the COP is a monotonously increasing function of R_0 , the
 corresponding threshold of the codeword transmission rate is
 $R_0^{th} = \arg\{P_{co}^{\text{TBRS}}(R_0) = \nu\}$, which leads to a lower bound of
 the SOP, when we have $(R_0 - R_s) \rightarrow R_0^{th}$. Thus, the feasible
 range of δ is $P_{so}^{\text{TBRS}}(R_0^{th}, 0) < \delta < 1$. The preceding analysis
 indicates that, given a reliability constraint ν , the lower bound
 of the security constraint is determined.

416

417 B. Reliability–Security Ratio

418 Here, we will focus our attention on the asymptotic analysis
419 of the COP and the SOP in the high-SNR regime. Then, inspired
420 by [25], we introduce the concept of the RSR for characterizing
421 the direct relationship between reliability and security.

422 *Proposition 1:* Based on the asymptotic probabilities of P_{co}
423 and P_{so} at high SNRs,³ the RSR is defined as

$$P_{co}(R_0) = \Lambda [1 - P_{so}(R_0, R_s)] \quad (16)$$

424 where $\Lambda = \lim_{\eta \rightarrow \infty} P_{co}/(1 - P_{so})$, which represents the im-
425 provement in COP upon decreasing the SOP. More specifically,
426 since the reduction of the SOP/COP must be followed by an
427 improvement of COP/SOP, a lower Λ implies that, when the
428 security is reduced, the reliability is improved, and *vice versa*.
429 Thus, for the TBRS scheme studied earlier, the RSR is derived
430 as (17), shown at the bottom of the page.

431 *Proof:* The proof is given in Appendix B.

432 *Remark 2:* It can be seen from the preceding expression
433 that the factor Λ is independent of the transmit SNR, but
434 directly depends on the channel gains, the rate pair (R_0, R_s) ,
435 and the number of TAs and relays. For a given R_s , reducing
436 R_0 to enhance the reliability may erode the security, because
437 $(R_0 - R_s)$ is also reduced. Conversely, increasing R_0 provides
438 more redundancy for protecting the security of the information,
439 but simultaneously, the reliability is reduced. Hence, the RSR
440 analysis underlines an important point of view concerning how
441 to balance the reliability versus security tradeoff by adjusting
442 (R_0, R_s) . Furthermore, as long as a CSI feedback delay exists,
443 the RSR has an intimate relationship with ρ_{SR} and ρ_{RD} . It is
444 clear that the value of Λ^{TBRS} decreases as ρ_{RD} increases, which
445 is due to the fact that the relay selection process only improves
446 the reliability of the legitimate user. On the other hand, since
447 we always have the conclusion that $\sum_{k=0}^{K_r-1} (-1)^k \binom{K_r-1}{k} (K_r/k$
448 $(k(1 - \rho_{RD}^2) + 1)) < 1$, when σ_{RD}^2 and σ_{RE}^2 are comparable,
449 Λ^{TBRS} will be reduced as ρ_{SR} increases. This observation
450 implies that, although both P_{co} and $(1 - P_{so})$ are reduced
451 when the first-hop CSI becomes better, the improvement of

the reliability is more substantial than the security loss, as ρ_{SR} 452
increases. 453

C. Effective Secrecy Throughput

454 It should be noted that the COP and SOP metrics ignore the 455
correlation between these two outage events. More specifically, 456
in contrast to the point-to-point transmission case, since the 457
 $S \rightarrow R$ link's SNR included in the MI expressions of (3) and 458
(4), the secrecy outage and the connection outage are definitely 459
not independent of each other. Therefore, it might be of limited 460
benefit in evaluating the reliability or the security separately. 461
We note furthermore that, although another metric referred to 462
as the secrecy throughput was introduced as the product of the 463
successful decoding probability and of the secrecy rate [21], 464
[22], this definition ignores the fact that a reliable transmission 465
may be insecure, and the SOP is not taken into consideration. 466
Hence, this metric is unable to holistically characterize the 467
efficiency of our scheme, while capable of achieving both re- 468
liable and secure transmission. Therefore, here, we redefine the 469
effective secrecy throughput as the probability of a successful 470
transmission (reliable and secure) multiplied by the secrecy 471
rate, namely, as $\varsigma = R_s P_{R\&S}$, where the RSCP is defined as 472

$$P_{R\&S} = \Pr\{I_D > R_0, I_E < R_0 - R_s\}. \quad (18)$$

473 Upon substituting the expressions of I_D and I_E in (3) and (4) 474
into (18), we can rewrite $P_{R\&S}$ for the TBRS strategy in (19), 475
shown at the bottom of the page.

476 Finally, using the corresponding CDFs and PDFs of (8)–(10) 477
from our previous analysis, we can obtain $P_{R\&S}^{\text{TBRS}}$ in (20), 478
shown at the bottom of the next page, as well as the secrecy 479
throughput.

480 Furthermore, considering the asymptotic result for RSCP at 481
high SNRs in (20) by applying the approximation $K_v(x) \approx$ 482
 $(v-1)!/2(x/2)^v$ and closing the highest terms of η after 483
invoking the McLaurin series representation for the exponential 484
function, the asymptotic effective secrecy throughput can be 485
approximated as

486 *Remark 3:* Given the definition of COP, SOP, and the secrecy 487
throughput result of (21), shown at the bottom of the next page, 488
it can be shown that, for a fixed R_s , if R_0 is too small, although 489

$$\Lambda^{\text{TBRS}} = \frac{\left[(1 - \rho_{SR}^2)^{N_t-1} + \sum_{k=0}^{K_r-1} (-1)^k \binom{K_r-1}{k} \frac{K_r \sigma_{SR}^2}{[k(1 - \rho_{RD}^2) + 1] \sigma_{RD}^2} \right] (2^{2R_0} - 1)}{\left[N_t (1 - \rho_{SR}^2)^{N_t-1} + \sigma_{SR}^2 / \sigma_{RE}^2 \right] (2^{2(R_0 - R_s)} - 1)} \quad (17)$$

$$\begin{aligned} P_{R\&S}^{\text{TBRS}} &= \Pr \left\{ \left\{ \gamma_{SR} > \gamma_{th}^D, \gamma_{R^*D} > \frac{\gamma_{th}^D \gamma_{SR} + \gamma_{SR}}{\gamma_{SR} - \gamma_{th}^D} \right\} \cap \left[\left\{ \gamma_{SR} > \gamma_{th}^E, \gamma_{R^*E} < \frac{\gamma_{th}^E \gamma_{SR} + \gamma_{SR}}{\gamma_{SR} - \gamma_{th}^E} \right\} \cup \left\{ \gamma_{SR} < \gamma_{th}^E \right\} \right] \right\} \\ &= \Pr \left\{ \gamma_{SR} > \gamma_{th}^D, \gamma_{R^*D} > \gamma_{th}^D + \frac{\gamma_{th}^D (\gamma_{th}^D + 1)}{\gamma_{SR} - \gamma_{th}^D}, \gamma_{R^*E} < \gamma_{th}^E + \frac{\gamma_{th}^E (\gamma_{th}^E + 1)}{\gamma_{SR} - \gamma_{th}^E} \right\} \end{aligned} \quad (19)$$

³Assume equal power allocation between S and the relay, yielding $P_S = P_R = P$, and define $\eta = P/N_0$ as the transmit SNR [24].

489 P_{RS} may be high (i.e., close to 1), the value of ς remains small.
 490 By contrast, if R_0 is too large, the value of P_{co} is close to 1,
 491 and therefore, ς will also become small. This observation is
 492 also suitable for R_s . Thus, as pointed out in the RSR analysis,
 493 it is elusive to improve both the reliability and the security
 494 simultaneously, but both of them are equally crucial in terms
 495 of the effective secrecy throughput, which depends on the rate
 496 pair (R_0, R_s) .

497 Additionally, (21) also reveals that increasing the SNR would
 498 drastically reduce the effective secrecy throughput. For high
 499 transmit SNRs, a high reliability can indeed be perfectly guar-
 500 anteed, but at the same time, the grade of the security is severely
 501 degraded. However, the probability of a reliable and simultane-
 502 ously secure transmission will tend toward zero. Hence, we may
 503 conclude that there exists an optimal SNR, which achieves the
 504 maximal secrecy throughput.

505 In conclusion, adopting the appropriate code rate pair and
 506 transmit SNR is crucial for achieving the maximum effective
 507 secrecy throughput, which can be formulated as

$$\begin{aligned} \max_{R_0, R_s, \eta} \quad & \varsigma(R_0, R_s) = R_s P_{R\&S}^{\text{TBRS}} \\ \text{s.t.} \quad & P_{co} \leq \nu, P_{so} \leq \delta, 0 < R_s < R_0 \end{aligned} \quad (22)$$

508 where ν and δ denote the system's reliability and security
 509 requirements. Unfortunately, it is quite a challenge to find
 510 the closed-form optimal solution to this problem due to the
 511 complexity of the expressions. Although suboptimal solutions
 512 can be found numerically (with the aid of gradient-based search
 513 techniques), the secrecy throughput optimization problem and
 514 the corresponding complexity analysis and performance com-
 515 parisons are beyond the scope of this work.

516 IV. SECURE TRANSMISSION WITH JAMMING

517 Here, we consider the extension of the aforementioned relay
 518 selection approaches to systems additionally invoking relay-

aided jamming. JRJS is based on the outdated but perfectly
 estimated CSI, and the details have been presented in Section II.
 We would also like to investigate the security performance
 from an outage-based perspective. The COP, SOP, RSCP, and
 effective secrecy throughput will be included.

A. COP and SOP

It is plausible that the main differences between the JRJS and
 TBRS schemes are determined by the instantaneous SNR of the
 $R \rightarrow D$ hop, where, now, a jammer is included. Based on our
 preliminary results detailed for the point-to-point SNRs in (8)
 and (10), we now focus our attention on the statistical analysis
 of the SNR, including J^* . As stated for the JRJS scheme in
 Section II, J^* corresponds to the lowest $\tilde{\gamma}_{R_k D}$ and is selected
 from the set $\{\mathcal{R} - R^*\}$. Recalling that R^* is the best relay
 of the second hop, we have $\tilde{\gamma}_{J^* D} = \min_{R_k \in \mathcal{R} - R^*} \{\tilde{\gamma}_{R_k D}\} \triangleq$
 $\min_{R_k \in \mathcal{R}} \{\tilde{\gamma}_{R_k D}\}$ for $K_r > 1$. Using the induced order statis-
 tics, the corresponding CDF of $\gamma_{R^* D}$ is presented in (10),
 whereas the PDF of $\gamma_{J^* D}$ can be formulated as

$$f_{\gamma_{J^* D}}(x) = \frac{K_r \exp\left(\frac{-K_r x}{[(K_r - 1)(1 - \rho_{RD}^2) + 1]\tilde{\gamma}_{JD}}\right)}{[(K_r - 1)(1 - \rho_{RD}^2) + 1]\tilde{\gamma}_{JD}}. \quad (23)$$

Although the relay and jammer selection processes are not
 entirely disjoint, we may exploit the assumption that $\gamma_{R^* D}$ and
 $\gamma_{J^* D}$ are independent of each other, which is valid when the
 number of relays is sufficiently high, as justified in [24]. Let us
 define the signal-to-interference-plus-noise ratio of the second
 hop as $\xi_D = \gamma_{R^* D} / (\gamma_{J^* D} + 1)$, using (10) and (23), whose
 CDF can be formulated as

$$F_{\xi_D}(x) = 1 - K_r \sum_{k=0}^{K_r - 1} (-1)^k \binom{K_r - 1}{k} \frac{\varphi_k e^{-\frac{x}{\tilde{\gamma}_{RD} \omega_k}}}{(k + 1)(x + \varphi_k)} \quad (24)$$

where we have $\varphi_k = \lambda K_r \omega_k / ((K_r - 1)(1 - \rho_{RD}^2) + 1)(1 - \lambda)$.

$$\begin{aligned} P_{R\&S}^{\text{TBRS}} &= \int_{\gamma_{th}^D}^{\infty} \left[1 - F_{\gamma_{R^* D}} \left(\gamma_{th}^D + \frac{\gamma_{th}^D (\gamma_{th}^D + 1)}{x - \gamma_{th}^D} \right) \right] F_{\gamma_{R^* E}} \left(\gamma_{th}^E + \frac{\gamma_{th}^E (\gamma_{th}^E + 1)}{x - \gamma_{th}^E} \right) f_{\gamma_{SR^*}}(x) dx \\ &\approx 2 \sum_{n=0}^{N_t - 1} \sum_{k=0}^{K_r - 1} \sum_{m=0}^{N_t - 1 - n} (-1)^k \binom{K_r - 1}{k} \binom{N_t - 1}{n} \binom{N_t - 1 - n}{m} \frac{K_r \rho_{SR}^{2(N_t - 1 - n)} (1 - \rho_{SR}^2)^n (\gamma_{th}^D)^{N_t - 1 - n - m}}{(N_t - 1 - n)! (k + 1) \tilde{\gamma}_{SR}^{N_t - n - (m + 1)/2}} \\ &\quad \times \exp \left[- \left(\frac{\gamma_{th}^D}{\tilde{\gamma}_{SR}} + \frac{\gamma_{th}^D}{\omega_k \tilde{\gamma}_{RD}} \right) \right] \left[\left(\frac{\gamma_{th}^D (\gamma_{th}^D + 1)}{\omega_k \tilde{\gamma}_{RD}} \right)^{\frac{m+1}{2}} K_{m+1} \left(2 \sqrt{\frac{\gamma_{th}^D (\gamma_{th}^D + 1)}{\omega_k \tilde{\gamma}_{SR} \tilde{\gamma}_{RD}}} \right) \right. \\ &\quad \left. - \exp \left(\frac{-\gamma_{th}^E}{\tilde{\gamma}_{RE}} \right) \left(\frac{\gamma_{th}^D (\gamma_{th}^D + 1)}{\omega_k \tilde{\gamma}_{RD}} + \frac{\gamma_{th}^E (\gamma_{th}^E + 1)}{\tilde{\gamma}_{RE} + \gamma_{th}^D - \gamma_{th}^E} \right)^{\frac{m+1}{2}} K_{m+1} \left(2 \sqrt{\frac{\gamma_{th}^D (\gamma_{th}^D + 1)}{\omega_k \tilde{\gamma}_{SR} \tilde{\gamma}_{RD}} + \frac{\gamma_{th}^E (\gamma_{th}^E + 1)}{\tilde{\gamma}_{SR} (\tilde{\gamma}_{RE} + \gamma_{th}^D - \gamma_{th}^E)}} \right) \right] \end{aligned} \quad (20)$$

$$\zeta^{\text{TBRS}}(R_0, R_s, \eta) = R_s \left\{ 1 - \left[\frac{N_t (1 - \rho_{SR}^2)^{N_t - 1}}{\sigma_{SR}^2} + \sum_{k=0}^{K_r - 1} \frac{K_r (-1)^k}{[k (1 - \rho_{RD}^2) + 1] \sigma_{RD}^2} \binom{K_r - 1}{k} \right] \times \frac{2^{2R_0} - 1}{\eta} \right\} \frac{2^{2(R_0 - R_s)} - 1}{\sigma_{RE}^2 \eta} \quad (21)$$

As far as the eavesdropper is concerned, γ_{R^*E} and γ_{J^*E} are independent and exponentially distributed. Furthermore, for $\xi_E = \gamma_{R^*E}/(\gamma_{J^*E} + 1)$, we have

$$F_{\xi_E}(x) = 1 - \frac{\phi}{x + \phi} e^{-\frac{x}{\bar{\gamma}_{RE}}} \quad (25)$$

where $\phi = \lambda/(1 - \lambda)$. According to the definition of COP and SOP in Section III-A, we can obtain the following closed-form approximations of the COP and the SOP.⁴

Lemma 1: The COP and the SOP of the JRJS strategy associated with feedback delays are approximated by

$$\begin{aligned} P_{\text{co}}^{\text{JRJS}}(R_0) &\approx 1 - \sum_{n=0}^{N_t-1} \sum_{k=0}^{K_r-1} \sum_{m=0}^{N_t-1-n} \binom{N_t-1}{n} \\ &\times \binom{K_r-1}{k} \binom{N_t-1-n}{m} \\ &\times \frac{(-1)^k (K_r+1) \rho_{SR}^{2(N_t-1-n)} (1 - \rho_{SR}^2)^n}{(N_t-1-n)!(k+1) \bar{\gamma}_{SR}^{N_t-n}} \\ &\times \frac{\Gamma(m+2) \hat{\phi}_k (\gamma_{th}^D)^{N_t-n} (\gamma_{th}^D + 1)^{m+1}}{(\gamma_{th}^D + \hat{\phi}_k)^{m+2}} \\ &\times \exp \left[-\frac{\gamma_{th}^D (\hat{\phi}_k - 1)}{\bar{\gamma}_{SR} (\gamma_{th}^D + \hat{\phi}_k)} \right] \\ &\times \Gamma \left(-m-1, \frac{\gamma_{th}^D (\gamma_{th}^D + 1)}{\bar{\gamma}_{SR} (\gamma_{th}^D + \hat{\phi}_k)} \right) \end{aligned} \quad (26)$$

where $\hat{\phi}_k = K_r \lambda \omega_k \eta \sigma_{RD}^2 / [(K_r - 1)(1 - \rho_{RD}^2) + 1](1 - \lambda) \eta \sigma_{RD}^2 + K_r$, and

$$\begin{aligned} P_{\text{so}}^{\text{JRJS}}(R_0, R_s) &\approx \sum_{n=0}^{N_t-1} \sum_{m=0}^{N_t-1-n} \binom{N_t-1}{n} \\ &\times \frac{\rho_{SR}^{2(N_t-1-n)} (1 - \rho_{SR}^2)^n}{m! \bar{\gamma}_{SR}^m} \\ &\times \frac{(2\gamma_{th}^E)^m \phi}{(2\gamma_{th}^E + \phi)} \exp \left[-\left(\frac{2\gamma_{th}^E}{\bar{\gamma}_{SR}} + \frac{2\gamma_{th}^E}{\bar{\gamma}_{RE}} \right) \right]. \end{aligned} \quad (27)$$

Proof: The proof is given in Appendix B. The feasible range of the reliability constraint is similar to that of the TBRS strategy, and hence, it is omitted here.

B. Reliability–Security Ratio

Lemma 2: Recalling the definition in Section III, the RSR for the JRJS strategy may be expressed in (28), shown at the bottom of the page.

⁴When we have $\lambda \rightarrow 1$, (24) will degenerate into the TBRS case seen in (10). The performance analysis of the JRJS will be presented separately in the following, since several approximations have to be included.

It can be seen from the previous expression that, in contrast to the analysis of the TBRS strategy operating without jamming, for a fixed SNR threshold, the CDF of the second-hop SNR will converge to a nonzero limit. We also find that this limit is determined by the power sharing ratio between the relay and the jammer. Furthermore, according to the analysis of the TBRS strategy, for $\eta \rightarrow \infty$, we have $F_{\gamma_{SR^*}}(x) \rightarrow 0$. Thus, by exploiting the tight upper bound that $\gamma_D^{\text{TBRS}} \leq \min\{\gamma_{SR}, \gamma_{R^*D}\}$ and $\gamma_E^{\text{TBRS}} \leq \min\{\gamma_{SR}, \gamma_{R^*E}\}$, we have $P_{\text{co}}^{\text{JRJS}, \infty} \rightarrow F_{\gamma_{\xi_D}}(\gamma_{th}^D)$ and $1 - P_{\text{so}}^{\text{JRJS}, \infty} \rightarrow F_{\gamma_{\xi_E}}(\gamma_{th}^E)$. Finally, substituting the corresponding results into (16), we arrive at the RSR of the JRJS strategy.

Remark 4: It can be seen from the RSR expression of (28) again that the rate-pair setting (R_0, R_s) has an inconsistent influence on the RSR, and hence, we have to carefully adjust R_0 and R_s to balance the reliability versus security performance. Let us now focus our attention on the differences between the JRJS scheme and the TBRS arrangement.

First, we may find that the power sharing ratio λ between the relay and the jammer plays a very important role. The optimization of λ will be investigated from an effective secrecy throughput optimization point of view in the following.

Second, it is plausible that, in contrast to the behavior of the TBRS strategy, Λ^{JRJS} of (28) is only related to the delay of the second hop, but it is still a monotonically decreasing function of ρ_{RD} . This implies that the improvement of the channel quality of the JRJS will achieve a more pronounced COP improvement than the associated SOP improvement. Furthermore, recalling that the RSR is considered in the high-SNR region, it has no dependence on the first hop quality. This is due to the fact that if the first-hop channel quality is sufficiently high for ensuring a successful transmission, the asymptotic CDFs of ξ_D and ξ_E in (29) and (30) associated with $\eta \rightarrow \infty$ will converge to a nonzero limit at high SNRs, which ultimately dominates the COP and the SOP.

C. Effective Secrecy Throughput

Before proceeding to the effective secrecy throughput analysis, we also have to investigate the RSCP.

Lemma 3: The RSCP of our JRJS strategy may be approximated as in (31), shown at the bottom of the next page, where we have $\theta_{1,k} = (\gamma_{th}^D (\gamma_{th}^D + 1)) / (\gamma_{th}^D + \hat{\phi}_k)$, $\theta_2 = \gamma_{th}^D - \gamma_{th}^E + (\gamma_{th}^E (\gamma_{th}^E + 1)) / (\gamma_{th}^E + \hat{\phi})$, and $\hat{\phi} = \lambda \eta \sigma_{RE}^2 / ((1 - \lambda) \eta \sigma_{RE}^2 + 1)$.

Proof: The proof is given in Appendix C.

Apart from the rate pair (R_0, R_s) , the aforementioned $P_{R\&S}^{\text{JRJS}}$ of (31) is also a function of the power sharing ratio λ between the selected relay and the jammer.

Given the complexity of the RSCP expression, it is quite a challenge to find a closed-form result for maximizing the

$$\Lambda^{\text{JRJS}} = \frac{(2^{2R_0} - 1)}{(2^{2(R_0 - R_s)} - 1)} \sum_{k=0}^{K_r-1} \binom{K_r-1}{k} \frac{(-1)^k K_r [(K_r - 1)(1 - \rho_{RD}^2) + 1] [(\lambda^{-1} - 1)(2^{2(R_0 - R_s)} - 1) + 1]}{[(K_r - 1)(1 - \rho_{RD}^2) + 1] (k+1)(\lambda^{-1} - 1)(2^{2R_0} - 1) + K_r [k(1 - \rho_{RD}^2) + 1]} \quad (28)$$

610 effective secrecy throughput that $\max_{0 < \lambda < 1} \varsigma = R_s P_{R\&S}^{\text{JRJS}}$. Al-
 611 ternatively, we can focus on the asymptotic analysis in the high-
 612 SNR region and try to find a general closed-form solution for λ .
 613 Specifically, when we have $\eta \rightarrow \infty$, $P_{R\&S}^{\text{JRJS}}$ will be dominated
 614 by the channel quality of the second hop; hence, we have

$$P_{R\&S}^{\text{JRJS},\infty}(R_0, R_s, \lambda) \approx \Pr \{ \xi_D > \gamma_{th}^D, \xi_E < \gamma_{th}^E \} \\ = [1 - F_{\xi_D}(\gamma_{th}^D)] F_{\xi_E}(\gamma_{th}^E) \quad (32)$$

615 where the approximation is based on the fact that, in contrast to
 616 both $F_{\xi_D}(\gamma_{th}^D)$ and $F_{\xi_E}(\gamma_{th}^E)$, which converge to a nonzero limit
 617 regardless of η , the first hop's $F_{\gamma_{SR}}(x)$ will tend to zero, and
 618 hence, it can be neglected. Substituting the asymptotic results
 619 of (29) and (30) into (33), we can obtain $P_{R\&S}^{\text{JRJS},\infty}$. In contrast to
 620 the TBRS case operating without jamming, as the SNR tends to
 621 ∞ , the RSCP will tend to a nonzero value and, upon increasing
 622 the transmit SNR beyond a certain limit, will no longer increase
 623 the effective secrecy throughput.

624 Then, based on (32), we arrive at the approximated optimal
 625 value λ_{opt} , which is the solution of the following equation:

$$\frac{\partial P_{R\&S}^{\text{JRJS},\infty}(R_0, R_s, \lambda)}{\partial \lambda} = 0. \quad (33)$$

626 Then, by exploiting the approximation of $[k(1 - \rho_{RD}^2) + 1]/$
 627 $(k + 1) \approx 1 - \rho_{RD}^2$ in (29) for a large ρ_{RD} (practically, the CSI
 628 delay is small, and $\rho_{RD} \rightarrow 1$), we have

$$\lambda_{\text{subopt}} = \frac{\sqrt{[(K_r - 1)(1 - \rho_{RD}^2) + 1] \gamma_{th}}}{\sqrt{[(K_r - 1)(1 - \rho_{RD}^2) + 1] \gamma_{th} + \sqrt{K_r(1 - \rho_{RD}^2)}}} \quad (34)$$

629 where $\gamma_{th} = (2^{2R_0} - 1)(2^{2(R_0 - R_s)} - 1)$. It is clear that this
 630 value is determined by the number of relays and (R_0, R_s) .

631 V. NUMERICAL RESULTS

632 Both our numerical and Monte Carlo simulation results are
 633 presented here for verifying the theoretical PLS performance
 634 analysis of the multiple-relay-aided network under CSI feed-

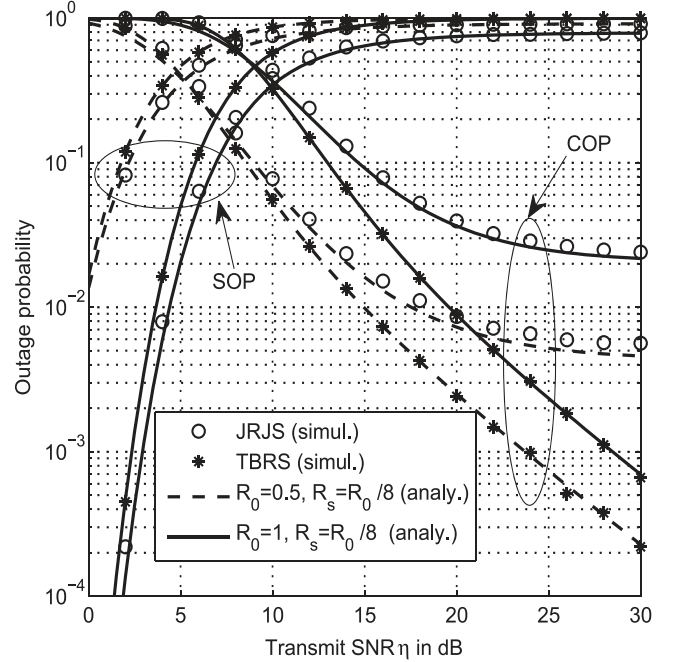


Fig. 2. COP and SOP versus transmit SNR for the TBRS and JRJS strategies in conjunction with different rate pairs, for $N_t = K_r = 3$, $f_d T_d = 0.1$, and $\lambda = 1/10$.

back delays. Explicitly, the COP, SOP, RSCP, and RSR are
 635 validated for both the TBRS and JRJS strategies. Furthermore,
 636 the effects of feedback delays and system parameters (including
 637 the transmission rate pair (R_0, R_s) and the power sharing ratio
 638 λ between the relay and the jammer) on the achievable effective
 639 secrecy throughput are evaluated. The Rayleigh fading model
 640 is employed for characterizing all communication links in our
 641 system. Additionally, we set the total power to $P = 1$ and
 642 $\sigma_{SR}^2 = \sigma_{RD}^2 = \sigma_{RE}^2 = 1$, and used $T_{dSR} = T_{dRD} = T_d$.
 643

644 Fig. 2 plots the COP and the SOP versus the transmit SNR for
 645 both the TBRS and JRJS strategies in conjunction with different
 646 rate pairs. The analytical lines are plotted by using (11) and (14)
 647 for the TBRS strategy and by using (26) and (27) for the JRJS

$$P_{R\&S}^{\text{JRJS}}(R_0, R_s, \lambda) \approx \sum_{n=0}^{N_t-1} \sum_{k=0}^{K_r-1} \sum_{m=0}^{N_t-1-n} (-1)^k \binom{N_t-1}{n} \binom{K_r-1}{k} \binom{N_t-1-n}{m} \\ \times \frac{K_r \rho_{SR}^{2(N_t-1-n)} (1 - \rho_{SR}^2)^n \hat{\varphi}_k (\gamma_{th}^D)^{N_t-1-n-m}}{(N_t-1-n)! (k+1) \bar{\gamma}_{SR}^{N_t-n} (\gamma_{th}^D + \hat{\varphi}_k) e^{\frac{\gamma_{th}^D}{\bar{\gamma}_{SR}} + \frac{\gamma_{th}^D}{\bar{\gamma}_{RD} \omega_k}}} \\ \times \left\{ \theta_{1,k}^{m+1} e^{\frac{\theta_1}{\bar{\gamma}_{SR}}} \Gamma(m+2) \Gamma\left(-m-1, \frac{\theta_{1,k}}{\bar{\gamma}_{SR}}\right) - \frac{\hat{\varphi} e^{-\gamma_{th}^E / \bar{\gamma}_{RE}}}{(\gamma_{th}^E + \phi) (\theta_{1,k} - \theta_2)} \Gamma(m+3) \right. \\ \times \left[\theta_2^{m+2} e^{\frac{\theta_2}{\bar{\gamma}_{SR}}} \Gamma\left(-m-2, \frac{\theta_2}{\bar{\gamma}_{SR}}\right) - \theta_{1,k}^{m+2} e^{\frac{\theta_1}{\bar{\gamma}_{SR}}} \Gamma\left(-m-2, \frac{\theta_{1,k}}{\bar{\gamma}_{SR}}\right) \right] + \Gamma(m+2) (\gamma_{th}^D - \gamma_{th}^E) \\ \left. \times \left[\theta_2^{m+1} e^{\frac{\theta_2}{\bar{\gamma}_{SR}}} \Gamma\left(-m-1, \frac{\theta_2}{\bar{\gamma}_{SR}}\right) - \theta_{1,k}^{m+1} e^{\frac{\theta_1}{\bar{\gamma}_{SR}}} \Gamma\left(-m-1, \frac{\theta_{1,k}}{\bar{\gamma}_{SR}}\right) \right] \right\} \quad (31)$$

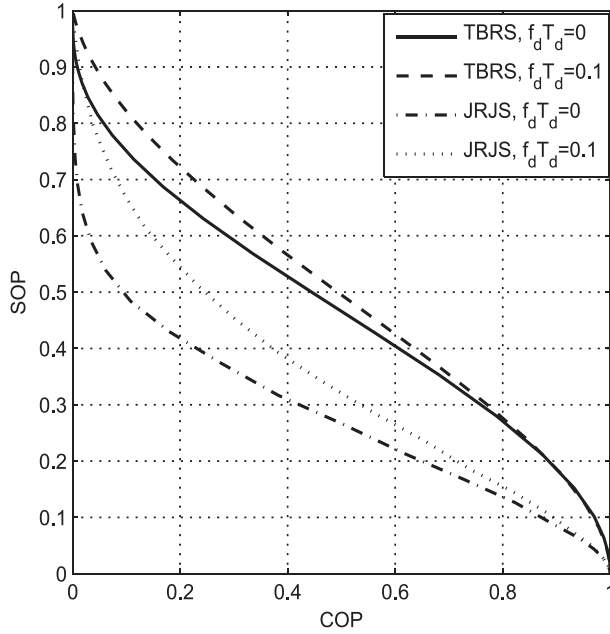


Fig. 3. SOP versus COP for the TBRS and JRJS strategies with different feedback delays for $N_t = K_r = 3$, $R_s = R_0/8$, and $\lambda = 1/10$.

648 case, respectively. It can be clearly seen from the figure that the
 649 analytical and simulated outage probability curves match well,
 650 which confirms the accuracy of the mathematical analysis. As
 651 expected, compared with the TBRS strategy, the SOP of the
 652 JRJS strategy is much better, whereas the COP is worse. We
 653 can also find that both the COP and the SOP will converge to an
 654 outage floor at high SNRs for the JRJS strategy. The reason for
 655 this is that the jammer also imposes interference on the destina-
 656 tion and the interference inflicted increases with the SNR. Thus,
 657 the designers have to take into account the tradeoff between
 658 the reliability and the security and the interference imposed on
 659 D , particularly when considering the JRJS strategy. Moreover,
 660 we can observe in Fig. 2 that increasing the transmission rate
 661 decreases the COP and increases the SOP.

662 Fig. 3 further characterizes the SOP versus COP for both the
 663 TBRS and JRJS strategies based on the numerical results in
 664 Fig. 2, which shows the tradeoff between the reliability and the
 665 security. It can be seen from the figure that the SOP decreases as
 666 the COP increases, and for a specific COP, the SOP of the JRJS
 667 scheme is strictly lower than that of TBRS. This confirms that
 668 the JRJS scheme performs better than the conventional TBRS
 669 scheme. Furthermore, the CSI feedback delay will also degrade
 670 the system tradeoff performance.

671 Fig. 4 illustrates the RSCP versus transmit SNR for the
 672 TBRS strategy in the context of different network configura-
 673 tions, including different rate pairs, different number of relays,
 674 and both perfect and outdated CSI feedback scenarios. The
 675 analytical lines are plotted by using the approximation in (20).
 676 We may conclude from the figure that the rate-pair setting
 677 (R_0, R_s) determines both the reliability and security transmis-
 678 sion performance. These curves also show that the RSCP is a
 679 concave function of the transmit SNR, whereas the continued
 680 boosting of the SNR would only decrease the probability of
 681 a successful transmission. We can observe from Fig. 4 that,

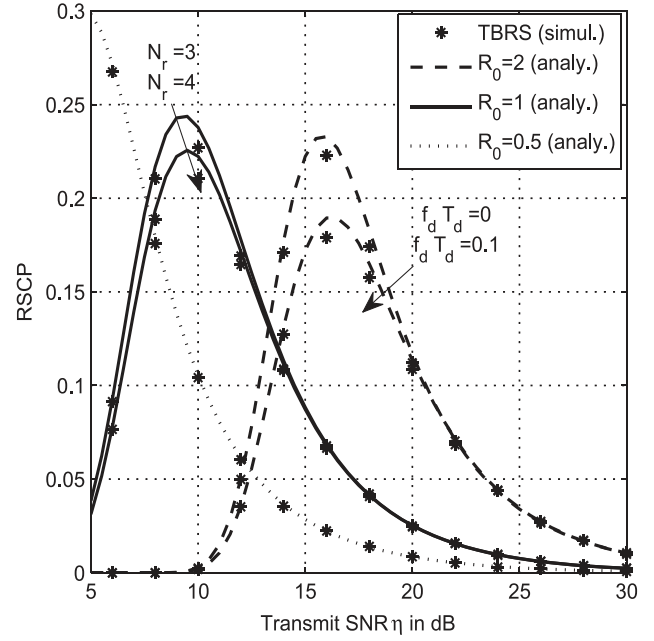


Fig. 4. RSCP versus transmit SNR for the TBRS strategy with different rate pairs for $N_t = K_r = 3$, $f_d T_d = 0.1$.

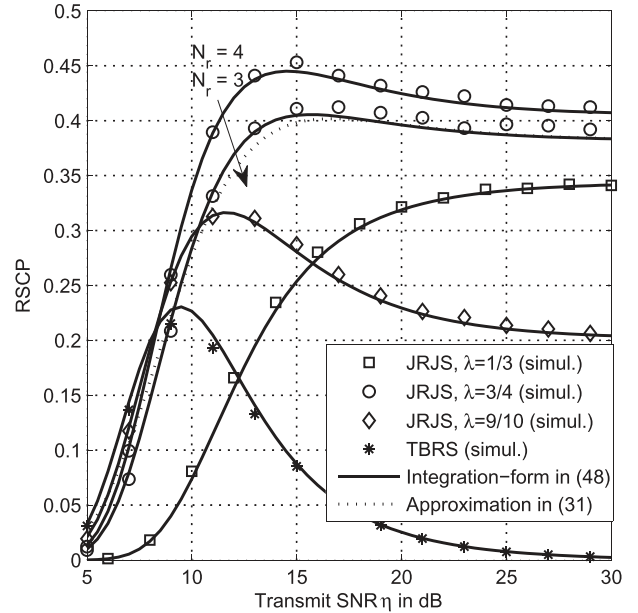


Fig. 5. RSCP versus transmit SNR for the JRJS strategy for different power sharing ratios λ and for $N_t = K_r = 3$, $f_d T_d = 0.1$, and $R_0 = 1$, $R_s = R_0/8$.

for a high transmit SNR, total reliability can be guaranteed,
 682 whereas the associated grade of security is severely eroded.
 683 Furthermore, increasing the number of relays and decreasing
 684 the feedback delay will improve both the reliability and security
 685 performance. 686

The RSCP of the JRJS strategy is presented in Fig. 5 for
 687 different power sharing ratios between relaying and jamming.
 688 Both the integration form (45) and the approximated closed
 689 form in (31) match well with the Monte Carlo simulations.
 690 The performance of the TBRS strategy is also included for
 691 comparison. The JRJS scheme outperforms the TBRS operating
 692

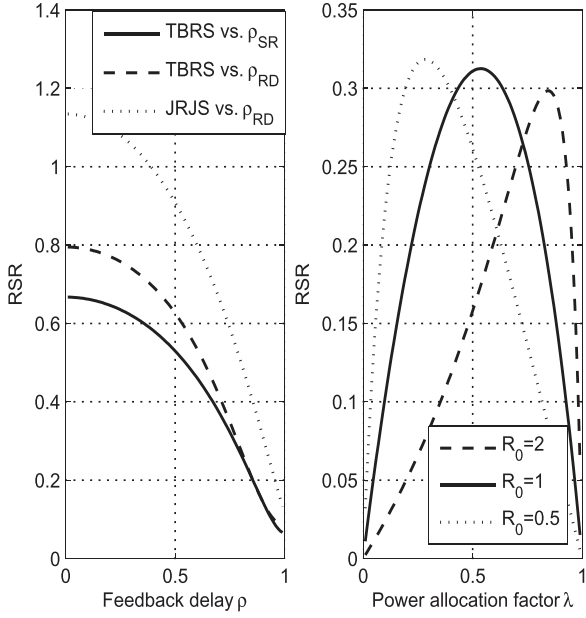


Fig. 6. RSR versus feedback delay coefficient ($R_0 = 1$, $R_s = R_0/8$, $\lambda = 3/4$) and power sharing ratio λ ($R_s = R_0/8$, $\rho_{SR} = \rho_{RD} = 0.9$) for the TBRS and JRJS strategies, with $N_t = K_r = 3$.

693 without jamming under the scenario considered when encoun-
 694 tering comparable relay–destination and relay–eavesdropper
 695 channels. For some extreme configurations (when the relay–
 696 eavesdropper links are comparatively weak), this statement
 697 may not hold, but this scenario is beyond the scope of this
 698 paper. The maximum RSCP appears at about $\eta = 15$ dB
 699 for the JRJS strategy using $\lambda = 3/4$, whereas it is $\eta = 10$ dB
 700 for the TBRS strategy. Furthermore, as expected, increasing the
 701 number of available relays and jamming nodes will always be
 702 able to improve the reliability and security performance. How-
 703 ever, the continued boosting of the jammer’s power (decreasing
 704 λ) will not always improve the overall performance, because
 705 the interference improves initially the security, but then, it starts
 706 to reduce the reliability as λ decreases. This further motivates
 707 the designer to carefully take into account the power sharing
 708 between relaying and jamming. The effect of the rate-pair
 709 setting on the security and reliability of the JRJS strategy is
 710 neglected here, which follows a similar trend to that of the
 711 TBRS strategy.

712 Fig. 6 characterizes the RSR versus feedback delay and
 713 power sharing ratio for both TBRS and JRJS, in which the
 714 RSR curves are plotted by using (17) and (28), respectively.
 715 The first illustration shows that the RSR decreases as the delay
 716 coefficients (ρ_{SR} and ρ_{RD}), which confirms that the im-
 717 provement of reliability becomes more pronounced than the
 718 reduction of the security as the feedback delay decreases.
 719 This observation implies an improvement in terms of the
 720 security–reliability tradeoff. In addition, the RSR versus ρ_{RD}
 721 is larger than that of ρ_{SR} , which indicates that the impact of the
 722 second-hop CSI feedback delay is more prominent. The other
 723 illustration in the right demonstrates that the RSR is a concave
 724 function of the power sharing ratio, which reflects the tradeoff
 725 between the reliability and the security struck by adjusting λ .

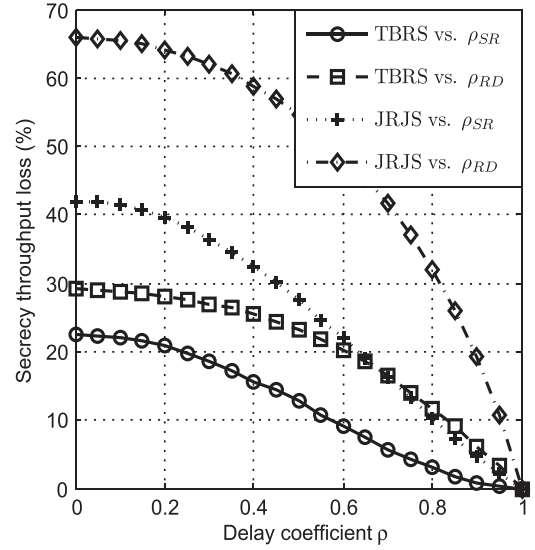


Fig. 7. Percentage secrecy throughput loss versus delay coefficients with $N_t = K_r = 3$, $R_0 = 1$, $R_s = R_0/8$, $\lambda = 3/4$, and $\eta = 10$ dB.

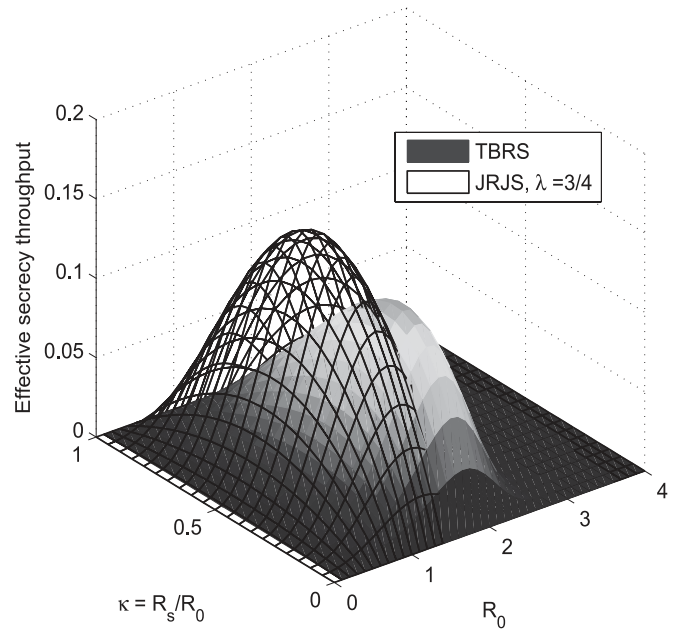


Fig. 8. Secrecy throughput versus R_0 and $\kappa = R_s/R_0$ for both the TBRS and JRJS strategies with $N_t = K_r = 3$, $f_d T_d = 0.1$, and $\eta = 15$ dB.

To further evaluate the effect of feedback delays on the
 726 secrecy performance, Fig. 7 plots the resultant percentage of 727
 728 secrecy throughput loss versus the delay, which is defined as

$$\text{S}_{\text{loss}} = \frac{S_{\text{no-delay}} - S_{\text{delay}}}{S_{\text{no-delay}}}. \quad (35)$$

It can be seen from the figure that, compared with the TBRS
 729 scheme, JRJS is more sensitive to the feedback delays. Further-
 730 more, recalling that increasing the delay coefficient ρ_{SR} of the
 731 first hop improves the reliability, but at the same time also helps
 732 the eavesdropper, it is not surprising that the secrecy throughput
 733 loss due to the second-hop feedback delay is more pronounced. 734

Fig. 8 illustrates the achievable effective secrecy throughput
 735 for both the TBRS and JRJS strategies versus the codeword 736

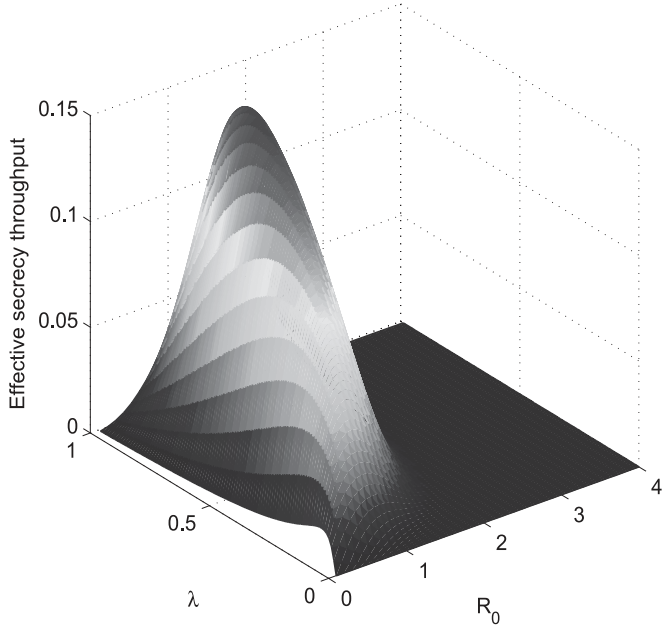


Fig. 9. Secrecy throughput versus R_0 and λ for the JRJS strategy with $N_t = K_r = 3$, $f_d T_d = 0.1$, $\eta = 15$ dB, and $R_s/R_0 = 1/8$.

737 transmission rate R_0 and the secrecy code ratio $\kappa = R_s/R_0$
 738 with no outage constraints ($v = \delta = 1$). The values of the
 739 effective secrecy throughput are plotted by using $\zeta = R_s P_{R\&S}$.
 740 We can observe in Fig. 8 that, subject to a fixed code rate
 741 ratio κ , the effective secrecy throughput increases to a peak
 742 value as R_0 reaches its optimal value and then decreases. This
 743 phenomenon can be explained as follows. At a low transmission
 744 rate, although the COP increases with R_0 , which has a negative
 745 effect on the effective secrecy throughput, both the secrecy
 746 rate and the SOP performance will benefit. However, after
 747 reaching the optimal R_0 , the effective secrecy throughput drops
 748 since the main link cannot afford a reliable transmission, and
 749 the resultant COP increase becomes dominant. On the other
 750 hand, subject to a fixed R_0 (which results in a constant COP),
 751 the effective secrecy throughput is also a concave function
 752 of κ , and increasing the code rate ratio ultimately results
 753 in an increased secrecy information rate at the cost of an
 754 increased SOP.

755 The achievable effective secrecy throughput for the JRJS
 756 strategy is also presented in Fig. 8, and similar conclusions and
 757 trends can be observed to that of the TBRS case. Additionally,
 758 the comparison of the two strategies indicates that the JRJS
 759 scheme attains a higher effective secrecy throughput than the
 760 TBRS scheme operating without jamming, even if no power
 761 sharing optimization has been employed.

762 Fig. 9 further illustrates the impact of power sharing between
 763 the relay and the jammer on the achievable effective secrecy
 764 throughput of the JRJS strategy versus R_0 in the absence of
 765 outage constraints. Given a fixed code rate pair (R_0, R_s) , the
 766 effective secrecy throughput follows the trend of the RSCP,
 767 which is a concave function of λ , as shown in Fig. 6. The
 768 interference introduced by the jammer initially improves both
 769 the reliability and the security as λ increases, but this trend is
 770 reversed beyond a certain point.

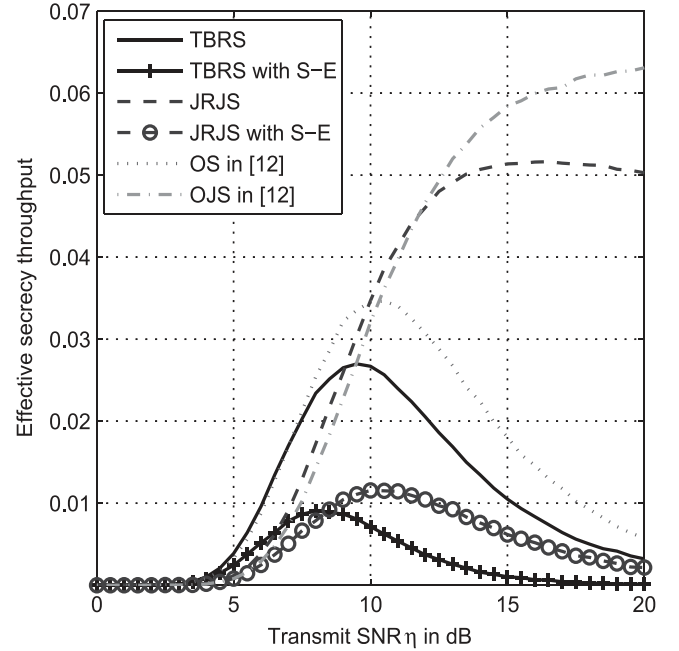


Fig. 10. Comparisons for different strategies with and without the S-E link, for $N_t = K_r = 3$, $R_0 = 1$, $R_s = R_0/8$, $f_d T_d = 0.1$, and $\lambda = 3/4$.

VI. DISCUSSION

771

A. Impact of the S-E Link

772

We note that the introduction of the S-E link, i.e., the
 773 information leakage in the first phase, is very critical to the
 774 security. There are also some research studies focusing on
 775 the corresponding secure transmission design and performance
 776 evaluation for cooperative networks with the S-E link, such
 777 as [15] and [16]. Here, we assume that the eavesdropper can
 778 receive information directly from the source in the first phase.
 779 Thus, following the steps in the prior sections, for the TBRS
 780 and JRJS schemes, it is clear that the SNR experienced at the
 781 eavesdropper should be rewritten as

$$\tilde{\gamma}_E^T = \gamma_{SE} + \gamma_E^T \quad (36)$$

where $\gamma_{SE} = P_s |\mathbf{w}_{\text{opt}}(t|T_{dSR}) \mathbf{h}_{SE}(t)|^2 / N_0$ follows the ex-
 783 ponential distribution with the average value $\bar{\gamma}_{SE}$, $\tau =$
 784 $\{\text{TBRS, JRJS}\}$, and γ_E^T has been defined in (4) and (7).
 785

Then, the corresponding SOP, RSCP, and effective secrecy
 786 throughput have to be reconsidered. Unfortunately, to the best
 787 of our knowledge, it is a mathematically intractable problem
 788 to obtain closed-form results for the related performance eval-
 789 uations. Therefore, we resorted to numerical simulations for
 790 further investigating the impact of the S-E link. Fig. 10 com-
 791 pares the effective secrecy throughput of the TBRS and JRJS
 792 schemes both with and without considering the direct S-E
 793 link. It becomes clear that the information leakage in the first
 794 phase will lead to a severe security performance degradation,
 795 particularly for the JRJS scheme, which will no longer be
 796 capable of maintaining a steady throughput at high SNRs. The
 797 reason for this trend is that increasing the transmit SNR will
 798 help the eavesdropper in the presence of the direct S-E link.
 799

800 B. Comparisons

801 Here, based on the outdated CSI assumption, we provide per-
802 formance comparisons with a range of other schemes advocated
803 in [12] with the aid of the proposed outage-based characteriza-
804 tion. Fig. 10 also incorporates our effective secrecy throughput
805 performance comparison, where the optimal selection (OS)
806 regime and the optimal selection combined with jamming (OSJ)
807 were proposed in [12]. They are formulated as

$$808 \text{ OS : } R^* = \arg \max_{R_k \in \mathcal{R}} \left\{ \frac{\tilde{\gamma}_{R_k D}}{\tilde{\gamma}_{R_k E}} \right\} \quad (37)$$

$$809 \text{ OSJ : } \begin{cases} R^* = \arg \max_{R_k \in \mathcal{R}} \left\{ \frac{\tilde{\gamma}_{R_k D}}{\tilde{\gamma}_{R_k E}} \right\} \\ J^* = \arg \min_{R_k \in \mathcal{R} - R^*} \left\{ \frac{\tilde{\gamma}_{R_k D}}{\tilde{\gamma}_{R_k E}} \right\} \end{cases} \quad (38)$$

810 where $\tilde{\gamma}_{R_k E}$ is the delayed version of the instantaneous CSI of
811 the R–E link. It should be noted that this constitutes an entirely
812 new performance characterization of these schemes from the
813 perspective of the effective secrecy throughput. It is shown in
814 Fig. 1 that the selection combined with jamming outperforms
815 the corresponding nonjamming techniques at high SNRs, albeit
816 this trend may no longer prevail at low SNRs. In comparison,
817 compared with those selections relying on the average SNRs of
818 the R–E link, the optimal selections relying on the idealized
819 simplifying assumptions of having global CSI (OS and OSJ
820 schemes) knowledge can only achieve throughput gains at high
821 SNRs due to the inevitable feedback delay.

822 VII. CONCLUSION

823 An outage-based characterization of cooperative relay net-
824 works has been provided in the face of CSI feedback delays.
825 Two types of relaying strategies were considered, namely, the
826 TBRS strategy and the JRJS strategy. Closed-form expressions
827 of the COP, the SOP, and the RSCP, as well as of the RSR,
828 were derived. The RSR results demonstrated that the reliability
829 is improved more substantially than the security performance
830 when the CSI feedback delays are reduced. Furthermore, we
831 presented a modified effective secrecy throughput definition
832 and demonstrated that the JRJS strategy achieves a significant
833 effective secrecy throughput gain over the TBRS strategy. The
834 transmit SNR, the secrecy codeword rate setting, and the power
835 sharing ratio between the relay and jammer nodes play impor-
836 tant roles in striking a balance between the reliability and the
837 security in terms of the secrecy throughput. The impact of the
838 direct S–E link and the performance comparisons with other
839 selection schemes were also included. Additionally, our results
840 demonstrate that JRJS is more sensitive to the feedback delays
841 and that the secrecy throughput loss due to the second-hop
842 feedback delay is more pronounced than that due to the first-
843 hop one.

844 APPENDIX A

845 PROOF OF PROPOSITION 1

846 To simplify the asymptotic performance analysis, (3) can be
847 expressed in a more mathematically tractable form by the com-
848 monly used tight upper bound of $\gamma_D^{\text{TBRS}} \leq \min\{\gamma_{SR}, \gamma_{R^*D}\}$

849 and $\gamma_E^{\text{TBRS}} \leq \min\{\gamma_{SR}, \gamma_{R^*E}\}$. When we have $\eta \rightarrow \infty$, based
850 on the CDFs in (9) and (10) and closing the smallest order terms
851 of x/η , we have

$$852 F_{\gamma_{SR}}(x) \rightarrow 1 - \left[\sum_{n=0}^{N_t-1} \binom{N_t-1}{n} \rho_{SR}^{2(N_t-1-n)} (1 - \rho_{SR}^2)^n \right. \\ 853 + \sum_{n=0}^{N_t-2} \binom{N_t-1}{n} \times \rho_{SR}^{2(N_t-1-n)} \\ 854 \left. \times (1 - \rho_{SR}^2)^n \frac{x}{\tilde{\gamma}_{SR}} + \mathcal{O}\left(\frac{x}{\tilde{\gamma}_{SR}}\right) \right] \\ 855 \times \left[1 - \frac{x}{\tilde{\gamma}_{SR}} + \mathcal{O}\left(\frac{x}{\tilde{\gamma}_{SR}}\right) \right] \\ 856 = 1 - \left[1 + (1 - (1 - \rho_{SR}^2)^{N_t-1}) \frac{x}{\tilde{\gamma}_{SR}} + \mathcal{O}\left(\frac{x}{\tilde{\gamma}_{SR}}\right) \right] \\ 857 \times \left[1 - \frac{x}{\tilde{\gamma}_{SR}} + \mathcal{O}\left(\frac{x}{\tilde{\gamma}_{SR}}\right) \right] \\ 858 = (1 - \rho_{SR}^2)^{N_t-1} \frac{x}{\tilde{\gamma}_{SR}} + \mathcal{O}\left(\frac{x}{\tilde{\gamma}_{SR}}\right) \quad (39)$$

859 where $\mathcal{O}(x)$ denotes the high-order infinitely small contribu-
860 tions as a function of x , and

$$861 F_{\gamma_{R^*D}}(x) \rightarrow 1 - \sum_{k=0}^{K_r-1} (-1)^k \frac{K_r}{k+1} \binom{K_r-1}{k} \\ 862 \times \left[1 - \frac{k+1}{k(1 - \rho_{RD}^2) + 1} \frac{x}{\tilde{\gamma}_{RD}} + \mathcal{O}\left(\frac{x}{\tilde{\gamma}_{RD}}\right) \right] \\ 863 = \sum_{k=0}^{K_r-1} (-1)^k \binom{K_r-1}{k} \frac{K_r}{k(1 - \rho_{RD}^2) + 1} \\ 864 \times \frac{x}{\tilde{\gamma}_{RD}} + \mathcal{O}\left(\frac{x}{\tilde{\gamma}_{RD}}\right). \quad (40)$$

865 Then, applying the upper bound of the receiver SNR, we may
866 rewrite the COP and the SOP of the TBRS strategy at high
867 SNRs as

$$868 P_{\text{co}}^{\text{TBRS}, \infty} = 1 - (1 - F_{\gamma_{SR^*}}(\gamma_{th}^D)) (1 - F_{\gamma_{R^*D}}(\gamma_{th}^D)) \\ 869 = \left[\frac{(1 - \rho_{SR}^2)^{N_t-1}}{\sigma_{SR}^2} + \sum_{k=0}^{K_r-1} (-1)^k \right. \\ 870 \left. \times \binom{K_r-1}{k} \frac{K_r}{[k(1 - \rho_{RD}^2) + 1] \sigma_{RD}^2} \right] \frac{2^{2R_0} - 1}{\eta} \quad (41)$$

871 and according to the fact that γ_{R^*E} is exponentially distributed,
872 we have

$$873 1 - P_{\text{so}}^{\text{TBRS}, \infty} = 1 - (1 - F_{\gamma_{SR^*}}(\gamma_{th}^E)) (1 - F_{\gamma_{R^*E}}(\gamma_{th}^E)) \\ 874 = \left[\frac{(1 - \rho_{SR}^2)^{N_t-1}}{\sigma_{SR}^2} + \frac{1}{\sigma_{RE}^2} \right] \frac{2^{2(R_0 - R_s)} - 1}{\eta}. \quad (42)$$

875 Finally, substituting (41) and (42) into the definition of RSR
876 in (16), we can obtain (17).

859 APPENDIX B
860 PROOF OF LEMMA 1

861 According to the description of COP and SOP, replacing
862 $F_{\gamma_{R^*D}}(x)$ and $F_{\gamma_{R^*E}}(x)$ by $F_{\xi_D}(x)$ and $F_{\xi_E}(x)$ in (12) and (14)
863 will involve a mathematically intractable integration of the form

$$\Upsilon(a, b, \mu, \nu) = \int_0^{\infty} \frac{z^a}{z+b} \exp\left(-\mu z - \frac{\nu}{z}\right) dz \quad (43)$$

864 which, to the best of our knowledge, does not have a closed-
865 form solution. Alternatively, bearing in mind that the preceding
866 integration has a great matter with ξ_D , we now focus our
867 attention on the approximation of ξ_D . Based on the PDF
868 results in (23), it may be seen that γ_{J^*D} obeys an exponential
869 distribution. Then, we can approximate $\hat{\gamma}_{J^*D} = \gamma_{J^*D} + 1$ by
870 the exponential distribution as well, with an average value
871 of $\mathbb{E}\{\hat{\gamma}_{J^*D}\} = ((K_r - 1)(1 - \rho_{RD}^2) + 1)\bar{\gamma}_{RD} + K_r)/K_r$ by
872 assuming that the AWGN term "1" is part of the stochastic
873 mean terms. The approximation based on this method provides
874 a very accurate analysis, and the accuracy of this method is
875 verified by the numerical results of [34]. Thus, the CDF of
876 $\hat{\xi}_D = \gamma_{R^*D}/\hat{\gamma}_{J^*D}$ can be derived as

$$F_{\hat{\xi}_D}(x) = \sum_{k=0}^{K_r-1} (-1)^k \binom{K_r-1}{k} \frac{K_r}{k+1} \frac{x}{x + \hat{\varphi}_k} \quad (44)$$

877 where $\hat{\varphi}_k = \mathbb{E}\{\gamma_{R^*D}\}\mathbb{E}\{\hat{\gamma}_{J^*D}\}$.

878 Then, substituting (44) into (11), we have

$$\begin{aligned} & F_{\gamma_{D}^{\text{JRJS}}}(x) \\ & \approx \sum_{n=0}^{N_t-1} \sum_{k=0}^{K_r-1} \sum_{m=0}^{N_t-1-n} \binom{N_t-1}{n} \binom{K_r-1}{k} \binom{N_t-1-n}{m} \\ & \times \frac{(-1)^k K_r \rho_{SR}^{2(N_t-1-n)} (1 - \rho_{SR}^2)^n \varphi_k x^{N_t-1-n-m} e^{-\frac{x}{\bar{\gamma}_{SR}}}}{(N_t-1-n)!(k+1)\bar{\gamma}_{SR}^{N_t-n} (x + \varphi_k)} \\ & \times \int_0^{\infty} \frac{z^{m+1}}{z + \frac{x(x+1)}{x+\varphi_k}} \exp\left(-\frac{z}{\bar{\gamma}_{SR}}\right) dz. \end{aligned} \quad (45)$$

879 Using [33, eq. (3.383.10)], we can obtain the CDF of γ_D^{JRJS} as

$$\begin{aligned} F_{\gamma_D^{\text{JRJS}}}(x) & \approx 1 - \sum_{n=0}^{N_t-1} \sum_{k=0}^{K_r-1} \sum_{m=0}^{N_t-1-n} \binom{N_t-1}{n} \\ & \times \binom{K_r-1}{k} \binom{N_t-1-n}{m} \\ & \times \frac{(-1)^k (K_r+1) \rho_{SR}^{2(N_t-1-n)} (1 - \rho_{SR}^2)^n}{(N_t-1-n)!(k+1)\bar{\gamma}_{SR}^{N_t-n}} \\ & \times \frac{\Gamma(m+2) \hat{\varphi}_k x^{N_t-n} (x+1)^{m+1}}{(x + \hat{\varphi}_k)^{m+2}} \\ & \times \exp\left[-\frac{x(\hat{\varphi}_k - 1)}{\bar{\gamma}_{SR}(x + \hat{\varphi}_k)}\right] \\ & \times \Gamma\left(-m-1, \frac{x(x+1)}{\bar{\gamma}_{SR}(x + \hat{\varphi}_k)}\right). \end{aligned} \quad (46)$$

880 Finally, substituting $x = \gamma_{th}^D$ into (46), we obtain $P_{\text{co}}^{\text{JRJS}}$.

As far as the SOP is considered, we exploit the commonly 881
used tight upper bound of $\gamma_E^{\text{JRJS}} \geq (1/2) \min\{\gamma_{SR}, \xi_E\}$ to 882
calculate it, which may be rewritten as 883

$$\begin{aligned} P_{\text{so}}^{\text{JRJS}} & \approx \Pr\left\{\frac{1}{2} \min\{\gamma_{SR}, \xi_E\} > \gamma_{th}^E\right\} \\ & = [1 - F_{\gamma_{SR}}(2\gamma_{th}^E)] [1 - F_{\xi_E}(2\gamma_{th}^E)]. \end{aligned} \quad (47)$$

Substituting (9) and (25) into (47), we obtain $P_{\text{so}}^{\text{JRJS}}$. 884

APPENDIX C 885
PROOF OF LEMMA 3 886

According to the definition of the RSCP in (18), we can 887
calculate it by 888

$$\begin{aligned} P_{RS}^{\text{JRJS}} & = \int_0^{\infty} \left[1 - F_{\xi_D}\left(\gamma_{th}^D + \frac{\gamma_{th}^D(\gamma_{th}^D + 1)}{z}\right)\right] \\ & \times F_{\xi_E}\left(\gamma_{th}^E + \frac{\gamma_{th}^E(\gamma_{th}^E + 1)}{z + \gamma_{th}^D - \gamma_{th}^E}\right) f_{\gamma_{SR^*}}(z + \gamma_{th}^D) dz. \end{aligned} \quad (48)$$

To make the integration mathematically tractable, we invoke 889
a simple approximation for $F_{\xi_E}(x)$ by treating the AWGN term 890
"1" in $\xi_E = \gamma_{R^*E}/(\gamma_{J^*E} + 1)$ as part of the stochastic mean 891
terms. Hence, we have 892

$$F_{\xi_E}(x) = \frac{x}{x + \hat{\phi}} \quad (49)$$

where $\hat{\phi} = \lambda\eta\sigma_{RE}^2/((1-\lambda)\eta\sigma_{RE}^2 + 1)$. 893

Then, replacing the corresponding CDFs of the second hop 894
with $F_{\hat{\xi}_D}(x)$ and $F_{\hat{\xi}_E}(x)$ in (26), the integration can be derived as 895

$$\begin{aligned} P_{RS}^{\text{JRJS}} & \approx 1 - \sum_{n=0}^{N_t-1} \sum_{k=0}^{K_r-1} \sum_{m=0}^{N_t-1-n} (-1)^k \binom{N_t-1}{n} \\ & \times \binom{K_r-1}{k} \binom{N_t-1-n}{m} \\ & \times \frac{(K_r+1) \rho_{SR}^{2(N_t-1-n)} (1 - \rho_{SR}^2)^n}{(N_t-1-n)!(k+1)\bar{\gamma}_{SR}^{N_t-n}} \\ & \times \frac{\hat{\varphi}_k (\gamma_{th}^D)^{N_t-1-n-m}}{\gamma_{th}^D + \hat{\varphi}_k} \exp\left(-\frac{\gamma_{th}^D}{\bar{\gamma}_{SR}} - \frac{\gamma_{th}^D}{\omega_k \bar{\gamma}_{RD}}\right) \\ & \times \int_0^{\infty} e^{-\frac{z}{\bar{\gamma}_{SR}}} z^{m+1} \left[\frac{1}{z + \theta_{1,k}} - \frac{\hat{\phi} (z + \gamma_{th}^D - \gamma_{th}^E) e^{-\frac{\gamma_{th}^E}{\bar{\gamma}_{RE}}}}{(\gamma_{th}^E + \hat{\phi})(\theta_{1,k} - \theta_2)} \right] \\ & \times \left(\frac{1}{z + \theta_2} - \frac{1}{z + \theta_{1,k}} \right) dz \end{aligned} \quad (50)$$

where $\hat{\varphi}_k$ and $\hat{\phi}$ are introduced by relying on the similar approx- 896
imation as in Appendix B. Then, using [33, eq. (3.383.10)], we 897
obtain $P_{R\&S}^{\text{JRJS}}$. 898

899

REFERENCES

900 [1] B. Schneier, "Cryptographic design vulnerabilities," *Computer*, vol. 31,
901 no. 9, pp. 29–33, Sep. 1998.

902 [2] A. D. Wyner, "The wire-tap channel," *Bell Syst. Techn. J.*, vol. 54, no. 8,
903 pp. 1355–1387, Oct. 1975.

904 [3] I. Csiszar and J. Korner, "Broadcast channels with confidential messages,"
905 *IEEE Trans. Inf. Theory*, vol. IT-24, no. 3, pp. 339–348, May 1978.

906 [4] W. K. Harrison, J. Almeida, M. R. Bloch, S. W. McLaughlin, and
907 J. Barros, "Coding for secrecy: An overview of error-control coding tech-
908 niques for physical-layer security," *IEEE Signal Process. Mag.*, vol. 30,
909 no. 5, pp. 41–50, Sep. 2013.

910 [5] P. K. Gopala, L. Lai, and H. E. Gamal, "On the secrecy capacity of
911 fading channels," *IEEE Trans. Inf. Theory*, vol. 54, no. 10, pp. 4687–4698,
912 Oct. 2008.

913 [6] Y. W. P. Hong, P. C. Lan, and C. C. J. Kuo, "Enhancing physical-layer
914 secrecy in multi-antenna wireless systems: An overview of signal process-
915 ing approaches," *IEEE Signal Process. Mag.*, vol. 30, no. 5, pp. 29–40,
916 Sep. 2013.

917 [7] R. Bassily *et al.*, "Cooperative security at the physical layer: A summary
918 of recent advances," *IEEE Signal Process. Mag.*, vol. 30, no. 5, pp. 16–28,
919 Sep. 2013.

920 [8] L. Dong, Z. Han, A. P. Petropulu, and H. V. Poor, "Improving wire-
921 less physical layer security via cooperating relays," *IEEE Trans. Signal
922 Process.*, vol. 58, no. 3, pp. 1875–1888, Mar. 2010.

923 [9] J. Huang and A. L. Swindlehurst, "Cooperative jamming for secure com-
924 munications in MIMO relay networks," *IEEE Trans. Signal Process.*,
925 vol. 59, no. 10, pp. 4871–4884, Oct. 2011.

926 [10] Y. Zou, X. Wang, and W. Shen, "Optimal relay selection for physical-layer
927 security in cooperative wireless networks," *IEEE J. Sel. Areas Commun.*,
928 vol. 31, no. 10, pp. 2099–2111, Oct. 2013.

929 [11] Y. Zou, X. Wang, W. Shen, and L. Hanzo, "Security versus reliability
930 analysis of opportunistic relaying," *IEEE Trans. Veh. Technol.*, vol. 63,
931 no. 6, pp. 2653–2661, Jul. 2014.

932 [12] I. Krikidis, J. S. Thompson, and S. McLaughlin, "Relay selection
933 for secure cooperative networks with jamming," *IEEE Trans. Wireless
934 Commun.*, vol. 8, no. 10, pp. 5003–5011, Oct. 2009.

935 [13] J. Chen, R. Zhang, L. Song, Z. Han, and B. Jiao, "Joint relay and jammer
936 selection for secure two-way relay networks," *IEEE Trans. Inf. Forensic
937 Security*, vol. 7, no. 1, pp. 310–320, Feb. 2012.

938 [14] Z. Ding, M. Xu, J. Lu, and F. Liu, "Improving wireless security
939 for bidirectional communication scenarios," *IEEE Trans. Veh. Technol.*,
940 vol. 61, no. 6, pp. 2842–2848, Jul. 2012.

941 [15] C. Wang, H. M. Wang, and X. G. Xia, "Hybrid opportunistic relay-
942 ing and jamming with power allocation for secure cooperative net-
943 works," *IEEE Trans. Wireless Commun.*, vol. 14, no. 2, pp. 589–605,
944 Feb. 2015.

945 [16] H. Deng, H. M. Wang, W. Guo, and W. Wang, "Secrecy transmission with
946 a helper: To relay or to jam," *IEEE Trans. Inf. Forensic Security*, vol. 10,
947 no. 2, pp. 293–307, Feb. 2015.

948 [17] B. He, X. Zhou, and T. D. Abhayapala, "Wireless physical layer secu-
949 rity with imperfect channel state information: A survey," *ZTE Commun.*,
950 vol. 11, no. 3, pp. 11–19, Sep. 2013.

951 [18] A. Mukherjee and A. L. Swindlehurst, "Robust beamforming for security
952 in MIMO wiretap channels with imperfect CSI," *IEEE Trans. Signal
953 Process.*, vol. 59, no. 1, pp. 351–361, Jan. 2011.

954 [19] J. Zhang and M. C. Gursoy, "Relay beamforming strategies for physical-
955 layer security," in *Proc. CISS*, Princeton, NJ, USA, Mar. 2010, pp. 1–6.

956 [20] M. Bloch, J. Barros, M. R. D. Rodrigues, and S. W. McLaughlin, "Wire-
957 less information-theoretic security," *IEEE Trans. Inf. Theory*, vol. 54,
958 no. 6, pp. 2515–2534, Jun. 2008.

959 [21] X. Zhou, M. R. McKay, B. Maham, and A. Hjørungnes, "Rethink-
960 ing the secrecy outage formulation: A secure transmission design
961 perspective," *IEEE Commun. Lett.*, vol. 15, no. 3, pp. 302–304,
962 Mar. 2011.

963 [22] J. Hu, Y. Cai, N. Yang, and W. Yang, "A new secure transmission scheme
964 with outdated antenna selection," *IEEE Trans. Inf. Forensics Security*,
965 to be published.

966 [23] J. Hu, W. Yang, N. Yang, X. Zhou, and Y. Cai, "On-off-based secure trans-
967 mission design with outdated channel state information," *IEEE Trans.
968 Veh. Technol.*, to be published.

969 [24] N. E. Wu and H. J. Li, "Effect of feedback delay on secure cooperative
970 networks with joint relay and jammer selection," *IEEE Wireless Commun.
971 Lett.*, vol. 2, no. 4, pp. 415–418, Aug. 2013.

972 [25] X. Guan, Y. Cai, and Y. Yang, "Secure transmission design and perfor-
973 mance analysis for cooperation exploring outdated CSI," *IEEE Commun.
974 Lett.*, vol. 18, no. 9, pp. 1637–1640, Sep. 2014.

[26] L. Wang, S. Xu, W. Yang, W. Yang, and Y. Cai, "Security performance
975 of multiple antennas multiple relaying networks with outdated relay
976 selection," in *Proc. WCSP*, Hefei, China, Oct. 2014, pp. 1–6. 977

[27] J. Huang and A. L. Swindlehurst, "Buffer-aided relaying for two-hop
978 secure communication," *IEEE Trans. Wireless Commun.*, vol. 14, no. 1,
979 pp. 152–164, Jan. 2015.

[28] S. I. Kim, I. M. Kim, and J. Heo, "Secure transmission for multiuser relay
980 networks," *IEEE Trans. Wireless Commun.*, vol. 14, no. 7, pp. 3724–3737,
981 Jul. 2015. 982

[29] Y. Ma, D. Zhang, A. Leith, and Z. Wang, "Error performance of transmit
983 beamforming with delayed and limited feedback," *IEEE Trans. Wireless
984 Commun.*, vol. 8, no. 3, pp. 1164–1170, Mar. 2009. 985

[30] Z. Rezki, A. Khisti, and M. S. Alouini, "Ergodic secret message capac-
986 ity of the wirechannel with finite-rate feedback," *IEEE Trans. Wireless
987 Commun.*, vol. 13, no. 6, pp. 3364–3379, Jun. 2014. 988

[31] X. Tang, R. Liu, P. Spasojevic, and H. V. Poor, "On the throughput of
989 secure hybrid-ARQ protocols for Gaussian block-fading channels," *IEEE
990 Trans. Inf. Theory*, vol. 55, no. 4, pp. 1575–1591, Apr. 2009. 991

[32] H. A. Suraweera, M. Soysa, C. Tellambura, and H. K. Garg, "Performance
992 analysis of partial relay selection with feedback delay," *IEEE Signal
993 Process. Lett.*, vol. 17, no. 6, pp. 531–534, Jun. 2010. 994

[33] I. S. Gradshteyn and I. M. Ryzhik, *Table of Integrals, Series and Products*,
995 6th ed. San Diego, CA, USA: Academic, 2000. 996

[34] S. Kim and J. Heo, "Outage probability of interference-limited amplify-
997 and-forward relaying with partial relay selection," in *Proc. IEEE VTC*,
998 Yokohama, Japan, May 2011, pp. 1–5. 999



Lei Wang (S'11) received the B.S. degree in elec- 1001
tronics and information engineering from Central 1002
South University, Changsha, China, in 2004 and 1003
the M.S. degree in communications and informa- 1004
tion systems from PLA University of Science and 1005
Technology, Nanjing, China, in 2011. He is currently 1006
working toward the Ph.D. degree in communications 1007
and information systems with PLA University of 1008
Science and Technology. 1009

His current research interests include cooperative 1010
communications, signal processing in communi- 1011
cations, and physical layer security. 1012



Yueming Cai (M'05–SM'12) received the B.S. 1013
degree in physics from Xiamen University, 1014
Xiamen, China, in 1982 and the M.S. degree in 1015
microelectronics engineering and the Ph.D. degree in 1016
communications and information systems from 1017
Southeast University, Nanjing, China, in 1988 and 1018
1996, respectively. 1019

He is currently with the College of Communica- 1020
tions Engineering, PLA University of Science and 1021
Technology, Nanjing, China. His current research 1022
interests include multiple-input–multiple-output sys- 1023
tems, orthogonal frequency-division multiplexing systems, signal processing in 1024
communications, cooperative communications, and wireless sensor networks. 1025

1026
1027
1028
AQ6 1029
1030
1031
1032
1033
1034
1035
1036



Yulong Zou (SM'13) received the B.Eng. degree in information engineering from Nanjing University of Posts and Telecommunications (NUPT), Nanjing, China, in July 2006; the Ph.D. degree in electrical engineering from Stevens Institute of Technology, Hoboken, NJ, USA, in May 2012; and the Ph.D. degree in signal and information processing from NUPT in July 2012.

He is currently a Professor with NUPT. His research interests span a wide range of topics in wireless communications and signal processing, including cooperative communications, cognitive radio, wireless security, and energy-efficient communications.

Dr. Zou has been a symposium chair, a session chair, and a technical program committee member for several IEEE-sponsored conferences, including the IEEE Wireless Communications and Networking Conference, the IEEE Global Communications Conference, the IEEE International Conference on Communications, the IEEE Vehicular Technology Conference, and the International Conference on Communications in China. He serves on the editorial board of *IEEE Communications Surveys and Tutorials*, *IEEE Communications Letters*, *IET Communications*, and the *EURASIP Journal on Advances in Signal Processing*. He was a received the 2014 IEEE Communications Society Asia-Pacific Best Young Researcher award.

1049
1050
1051
1052
AQ7 1053
1054
1055
1056
1057
1058



Weiwei Yang (S'08–M'12) received the B.S., M.S., and Ph.D. degrees from PLA University of Science and Technology, Nanjing, China, in 2003, 2006, and 2011, respectively.

He is currently with the College of Communications Engineering, PLA University of Science and Technology. His research interests are orthogonal frequency-domain multiplexing systems, signal processing in communications, cooperative communications, cognitive networks, and network security.



Lajos Hanzo (M'91–SM'92–F'04) received the 1059 M.S. degree in electronics and the Ph.D. de- 1060 gree from the Technical University of Budapest, 1061 Budapest, Hungary, in 1976 and 1983, respectively; 1062 the D.Sc. degree from the University of Southampton, 1063 Southampton, U.K., in 2004; and the "Doctor Honoris 1064 Causa" degree from the Technical University of 1065 Budapest in 2009. 1066

During his 38-year career in telecommunications, 1067 he has held various research and academic posts in 1068 Hungary, Germany, and the U.K. Since 1986, he has 1069

been with the School of Electronics and Computer Science, University of 1070 Southampton, where he holds the Chair in Telecommunications. He is currently 1071 directing an academic research team, working on a range of research projects 1072 in the field of wireless multimedia communications sponsored by industry, the 1073 Engineering and Physical Sciences Research Council (EPSRC), the European 1074 Research Council's Advanced Fellow Grant, and the Royal Society's Wolfson 1075 Research Merit Award. During 2008–2012, he was a Chaired Professor with 1076 Tsinghua University, Beijing, China. He is an enthusiastic supporter of ind- 1077 dustrial and academic liaison and offers a range of industrial courses. He 1078 has successfully supervised about 100 Ph.D. students, coauthored 20 John 1079 Wiley/IEEE Press books on mobile radio communications totaling in excess of 1080 10 000 pages, and published more than 1400 research entries on IEEE Xplore. 1081

Dr. Hanzo is a Fellow of the Royal Academy of Engineering, the Institution 1082 of Engineering and Technology, and the European Association for Signal 1083 Processing. He is also a Governor of the IEEE Vehicular Technology Society. 1084 During 2008–2012, he was the Editor-in-Chief of IEEE Press. He has served 1085 as the Technical Program Committee Chair and the General Chair of IEEE 1086 conferences, has presented keynote lectures, and has received a number of 1087 distinctions. His published work has more than 20 000 citations. Further in- 1088 formation on research in progress and associated publications is available at 1089 <http://www-mobile.ecs.soton.ac.uk>. 1090

AUTHOR QUERIES

AUTHOR PLEASE ANSWER ALL QUERIES

AQ1 = RV was expanded as “random variable.” Please check if appropriate. Otherwise, please make the necessary changes.

AQ2 = Equations (29) and (30) are missing in the document. Please check.

AQ3 = Please provide publication update in Ref [22].

AQ4 = Please provide publication update in Ref [23].

AQ5 = Current affiliation of author Yueming Cai was provided as captured from the first footnote. Please check if appropriate. Otherwise, please make the necessary changes.

AQ6 = Please confirm that Dr. Zou has received two Ph.D. degrees.

AQ7 = Current affiliation of author Weiwei Yang was provided as captured from the first footnote. Please check if appropriate. Otherwise, please make the necessary changes.

END OF ALL QUERIES